A LOW COST 2-AXIS PLC CONTROLLED FILAMENT WINDING MACHINE WITH SIMPLIFIED FIBER WINDING ANGLE AND TENSION CONTROL SYSTEM

by

Trinankur Hazra

Submitted in partial fulfillment of the requirements
for the degree of Master of Applied Science

at

Dalhousie University
Halifax, Nova Scotia
March 2011

DALHOUSIE UNIVERSITY
DEPARTMENT OF ELECTRICAL AND COMPUTER ENGINEERING

The undersigned hereby certify that they have read and recommend to the Faculty of Graduate Studies for acceptance a thesis entitled "A LOW COST 2 AXIS PLC CONTROLLED FILAMENT WINDING MACHINE WITH SIMPLIFIED FIBER WINDING ANGLE AND TENSION CONTROL SYSTEM" by Trinankur Hazra in partial fulfillment of the requirements for the degree of Master of Applied Science.

Dated: March, 17th 2011

Supervisor: _____

Co-Supervisor: _____

Readers: _____

_____

DALHOUSIE UNIVERSITY

DATE: March, 17th 2011

AUTHOR: Trinankur Hazra

TITLE: A LOW COST 2 AXIS PLC CONTROLLED FILAMENT WINDING MACHINE WITH SIMPLIFIED FIBER WINDING ANGLE AND TENSION CONTROL SYSTEM

DEPARTMENT OR SCHOOL: Department of Electrical and Computer Engineering

DEGREE: MASc CONVOCATION: May YEAR: 2011

_____

Signature of Author

Table of Contents

List of Tables

List of Figures

List of Abbreviations

FRP:	Fiber Reinforced Plastic
RTM:	Resin Transfer Molding
VARTM:	Vacuum Assisted Resin Transfer Molding
SMC:	Sheet Molding Compound
BMC:	Bulk Molding Compound.
RPM:	Rotations per Minute
CNC:	Computer Numerical Control
PLC:	Programmable Logic Controller
VFD:	Variable Frequency Drive
CTRIO:	High Speed Counter Input Output Card
AC:	Alternating Current
DC:	Direct Current
PID:	Proportional Integral Derivative
PI:	Proportional Integral
RMS:	Root Mean Square
PV:	Process Variable
SV:	Set Variable
FLC:	Fuzzy Logic Controller
FIS:	Fuzzy Inference System
PWM:	Pulse Width Modulation
BCD:	Binary Coded Decimal
TTL:	Transistor Transistor Logic
NEMA:	National Electrical Manufacturers Association

Acknowledgement

The author would like to express his gratitude to, Dr. Jason Gu of the Department of Electrical and Computer Engineering at Dalhousie University for his motivation and guidance throughout the dissertation work.

The author is indebted to, Dr. Farid Taheri of the Department of Civil Engineering at Dalhousie University, for his supervision, guidance and motivation throughout this dissertation and for providing in-depth understanding on laminate composites and their manufacturing processes.

The author would like to acknowledge the readers of this thesis, Dr. M. El Hawary of the Department of Electrical and Computer Engineering at Dalhousie University and Dr. Guy Kember of the Department of Engineering Mathematics at Dalhousie University.

The author would like to thank electrical Technologists, Christopher Hill, Alex Pudsey, Mark LeBlanc, civil technologist Brian Kennedy and instrumentation technologist Jesse Keane for their support and help rendered in developing the prototype machine.

Author would like to thank the technical support groups of Automation Direct.com, Baldor Electric Inc. DigiKey Corp and Marathon Electric for sharing their technical know how about different systems used in the prototype in this dissertation. Author is thankful to Selina Cajolais and Nicole Smith, who have made his stay in Dalhousie University a pleasant and memorable one. Author would also like to thank all his colleagues and friends in Dalhousie University for supporting him in his work.

Author is ever grateful to his father, Dr U S Hazra of School of Technology, Department of Electrical Engineering at Pandit Deendayal Petroleum University, for his unfathomable help and support for this dissertation work. Last but not the least the author thanks his wife and mother for their support and confidence in him.

Abstract

Designing a filament winding machine involves two major components. First component is the designing of the mechanism which delivers appropriate winding pattern as specified by the user (i.e. the winding angle). The second component is the realization of an effective fiber tensioning system for ensuring consistent overall consolidation.

Today, there exist a variety of sophisticated methods to achieve both these parameters; however the implementation of these techniques increases the price of a winding machine, making its acquisition very difficult for small scale applications. Sophisticated winding machine includes higher number of degrees of freedom, and high end CNC controlled algorithms. However for creating axi-symetric products with constant diameter, only a 2-axis winding is sufficient. On this note a novel cost effective method for fiber winding angle control and fiber winding tension control is designed, simulated, implemented into a low cost prototype 2-axis filament winding machine, and the scope for its' further improvement has also been discussed.

The system designed, uses a cost effective PLC as the centralized controller of the system for implementing both fiber winding control and tension control through PID control. A novel actuator for tension control is designed and implemented.

Also a comparison between the conventional PI controller and a Mamdani type Fuzzy inference based control system for controlling the fiber tension is made. In this process a novel technique for making PI controller capable of handling known nonlinearities in the system is introduced. Experimental system responses of the designed prototype are analyzed.

Chapter 1

INTRODUCTION

The distinct advantage of using Fiber reinforced polymer (FRP) composite materials in various and especially harsh environmental conditions has resulted in the development of many sophisticated process of its manufacturing, aiming at higher strength/weight ratio of the product.

The involvement of complicated control applications in the manufacturing process have led to the increase in hardware cost. Therefore, small scale manufacturing of the composites became costly and could not become a popular practice.

The present dissertation work aims at development of a cost effective controls of a 2-axis filament winding machine by using novel control techniques and thereby reducing the hardware cost.

The most challenging task involved in producing a low cost filament winding machine is ensuring effective winding angle and tension control mechanism, which would be adequate to manufacture the composites in a small scale, with desired quality.

To have a firsthand appraisal on the process of composite manufacturing, the subject has been studied along with the historical backgrounds. To arrive at the best and optimum control mechanism, a detailed literature survey has been done to understand the state of the art in filament winding machine.

Fiber winding angle determines the winding pattern. It is a key parameter in filament winding process. The winding pattern governs the stress handling capability of the composite wound tubes [1].

The other factor that is critical for a winding process is the fiber tension. Adequate fiber tension ensures reduction of voids in the winding and has impact on the volume fraction

of the composite. Increase in winding tension reduces the residual stresses on the composite making it more suitable for high pressure application [2]. Maintaining tension in a filament winding machine is a very complex nonlinear process. The tension in fiber is dependent on number of factors viz. friction, elastic characteristics of the fiber and the winding angle.

A novel actuator is utilized for tension control; it is therefore modeled and simulated. In accordance to the actuator, the control system is mathematically modeled. The control algorithms for both, winding angle and tension control are derived from first principles. A prototype Filament Winding machine has been developed. The controls have been instituted as conceived. The real time operating results have been captured. Furthermore, the results have been found to be in line with the simulated off line responses.

Then to explore the scope for future work a comparison between the conventional PI controller and a Mamdani type Fuzzy inference based control system for tension control were analyzed through offline simulations. In this process a novel technique for making PI controller capable of handling known nonlinearities in the system is introduced.

1.1 Thesis Outline

A detailed subject review has been conducted to understand the process of composite manufacturing process; the findings are discussed in chapter 2 and 3.

The winding of the filament is the key process in manufacture of FRP. The brief description of the process of winding and various control elements along with their associated mathematical elaboration have been dealt in chapter 4. The research motivation and the project concept have been presented in chapter 5.

Chapter 6 describes the hardware with particular reference to mandrel, motor along with drives, encoder, horizontal positioner and the tension actuator. The chapter also presents the concept of actuator design by using a general purpose solenoid. The PLC along with

its hardware has also been briefed. The cost analysis of the prototype is also discussed in this chapter

Chapter 7 describes the Control Algorithms for both Angle control and tension control along with simulated outputs. PLC Logic and the flowcharts have been presented in chapter 8.

The result of experimental prototype have been presented in chapter 9, which establishes the fact that with the application of the conceived control concept it is possible to develop a low cost filament winding machine.

Chapter 10 brings forward the concept of fuzzy winding tension control to overcome some shortcomings of the PID tension control modeled in the system.

In chapter 11, the results of this thesis are analyzed and conclusions are drawn. Based on the conclusions, the current status of the prototype setup and the authors understanding of the subject, recommendations for future work, that could be under taken to further improve the system integrity, at the same time keeping the cost of the filament winding machine low, are outlined.

Chapter 2

FIBER-REINFORCED POLYMER (FRP) COMPOSITES

Composite material is a combination of a reinforcement fiber in a thermoset polymer resin matrix, where the reinforcement has an aspect ratio that facilitates the transfer of loads among fibers, and the fibers are bonded to the resin matrix. In other words, a composite is produced by bonding of two or more materials that result in a new material that is usually stronger than the individual ingredients. Compared to metallic materials, composites have better flexibility, can handle highly corrosive environment and they are comparatively lighter in weight.

North America is the largest producer of FRP composite materials and Figure 2.1 shows that. United States alone with approximately 2000 composite manufacturing units produces about 1.4 billion Kilograms of composite products each year [3].

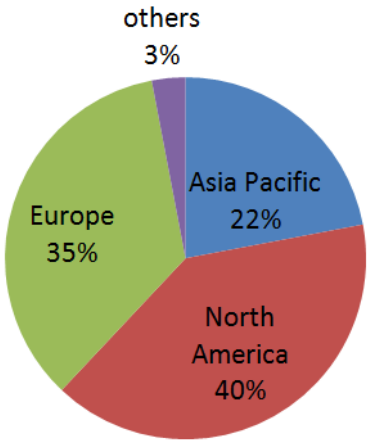

Figure 2.1: Distribution of composite manufacturing – continent wise [4]

2.1 History of Composite Materials

History of composite pipes dates back to 1500 BC. As quoted by Margaret Gowen [5], the owner of "Margaret Gowen and Co. Ltd" an archeological consultant firm, "there is a suggestion of an early Chinese composite instrument like pan pipes with a gourd that is

the wind chamber going back to about 1500 BC". The first modern composite was discovered in the 1930s, when a US company Owens Corning Fiberglass, started marketing fiberglass in 1937 [6]. Fiberglass was initially used as insulation; it was soon discovered that its light weight and durability could benefit the aircraft industry, and Douglas Aircraft Company was the first to use fiberglass reinforced composites in aviation [7].

The first composites were made with Phenolic resin, but later many high performance resins were created over the years. The applicative value of composite materials grew from time to time, ranging from aircraft ducts, boats, automobiles and rocket engines.

Concentrating on composite pipes, in the present day scenario, they find a major consumer market in petrochemicals, oil and natural gas sectors. The United States alone has hundreds of manufacturers of fiberglass composite pipe and polyethylene pipe. The key areas of application of composite pipes today are oil and gas pipelines, petrochemical and other chemical industrial piping [8].

Chapter 3

COMPOSITE MANUFACTURING PROCESSES

There are many ways of making composite goods. Even though each technique is different, but they all have the following goals [9]:

- Arrange fibers in the desired orientation and stacking sequence--This ensures the appropriate fiber orientation. This specifies the amount of fiber in each layer of the composite, so it governs the strength and stiffness of the composite.
- Ensure adequate wetting of fibers--Adequate wetting of the fiber is important to allow the right amount of resin in between the fibers so as to have an appropriate fiber/resin ratio. This is also crucial to the strength and stiffness of the composite.
- Curing of resin--Curing enables the bonding of each layer of the composite to each other, thus unifying the product.
- Minimization of the amount of voids--One of the most important factors in composite manufacturing is the removal of voids or air gaps between two successive layers of fiber. The voids reduce the stress bearing capacity of the fiber.

The earliest method of making composites was by manual layup, where each layer of the composites is manually put one above the other to produce the final layout. This is very time consuming and needs a lot of skilled manpower. This method was made easier through the use of prepregs, which are fibers pre-impregnated with resin. Major advantages of the manual set up are that it has high versatility; but accuracy is dependent on the skill of the worker and can yield goods with high volume fractions. Its major disadvantages are that it is slow, yields low production rates and there are health and safety issues, such as physical contact with the resin and its fumes [10].

3.1 Pultrusion

Pultrusion is an automated continuous composite manufacturing process, where materials of constant cross section are produced by pulling of fibers through resin over a heated die. The process was developed by Goldsworthy [11]. The major application of the pultrusion process is in the fabrication of composite parts that have a prismatic cross-section profile. The manufacturing process of pultrusion is suited ideally for mass scale production.

In the pultrusion process, fibers are pulled through a resin bath, to coat the reinforcement with the resin. Then excess resin is removed, as fibers are passed through heated die. Die completes the curing of the resin and controls the shape of the section. Figure 3.1 shows the schematic of pultrusion process. The major advantages of the pultrusion process are its capability to produce in high volume and being a very highly automated process. Its major disadvantages are the expensive die costs and its inability to produce products non prismatic geometries.

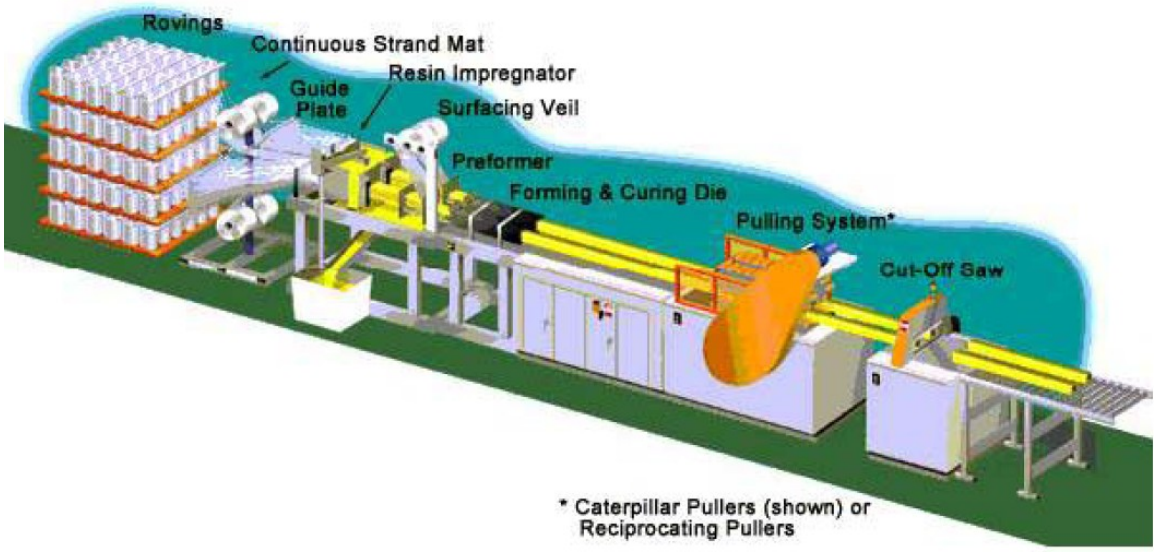

Figure 3.1: Pultrusion schematic [12]

3.2 Resin Transfer Molding (RTM)

In this process the layers of fibers or a fiber prepreg are placed between male and female molds, pressurized and injected with resin. The resin is injected to fill all voids within the mold and thus penetrates and wets all surfaces of the reinforcing materials.

A wide variety of reinforcement materials can be used. This process offers low wastage and reduced machining cost of the finished product. The process can be automated. The major limitations of this process are that the manufacturing of complex shapes requires lot of trial and error to ensure proper wetting; also the mold designing is complex. Figure 3.2 shows the schematic of the process.

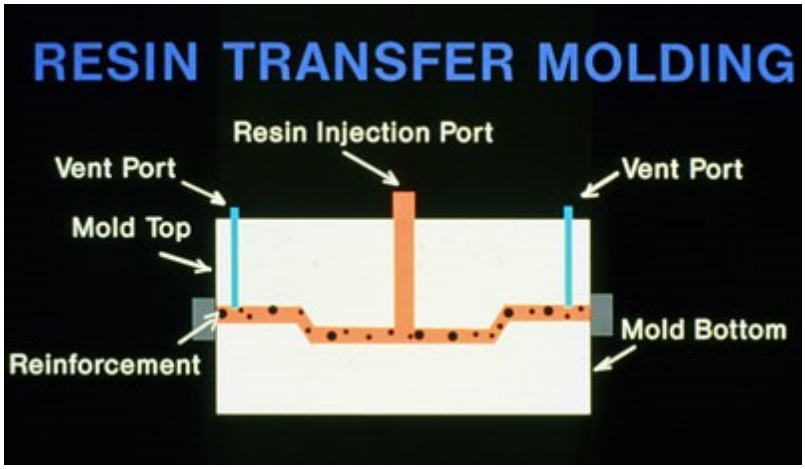

Figure 3.2: Schematic of RTM process [13]

3.3 Vacuum Assisted Resin Transfer Molding (VARTM)

Conceptually, this process is similar to RTM, but it is different on many accounts. First of all the VARTM is a single side process under a sealed enclosure and instead of the positive pressure used in RTM, vacuum is applied to the mold and sucked into the fabric/fiber.

In this process, wetting of the fiber is dependent on the permeability of the preformed laminate and architecture of the fiber. Viscosity of the resin has to be low. This process is very safe from health hazard point of view as the entire system is under vacuum and can yield very high quality products. Figure 3.3 shows the schematic of VARTM process.

Typical applications of VARTM include production of train seats, marine, complex aircraft and automotive parts.

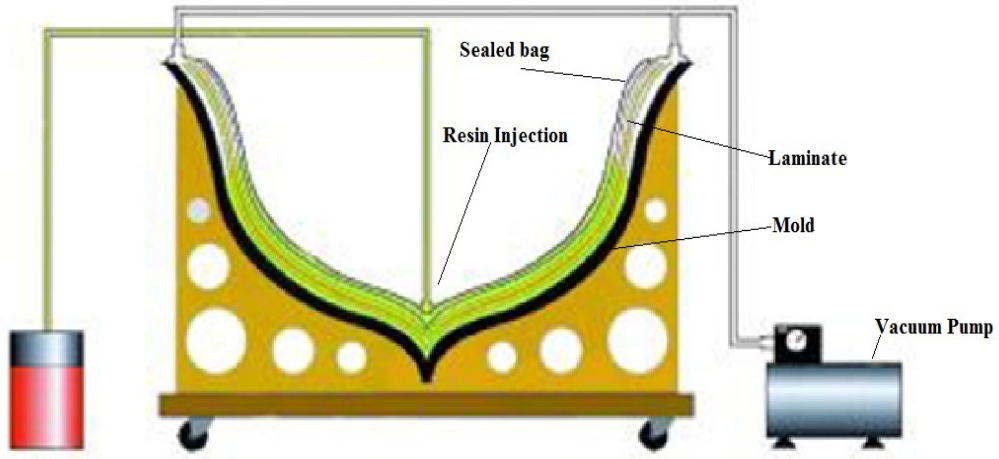

Figure 3.3: Schematic of VARTM [14].

3.4 Compression Molding

Compression Molding is used in manufacturing sheet molding compound (SMC) composites and bulk molding compound (BMC). This process consists of three stages, namely charging, compressing and ejecting. The material to be molded is preheated and placed in a mold in the charging stage. Then pressure and additional heat is applied in the compression stage. Finally the finished product is removed from the mold after sufficient curing time. Figure 3.4 shows the schematic of the entire compression molding process.

Major applications of the compression moldings are automotive components such as fenders, bumpers, and leaf springs. The major disadvantages of this process are that it cannot produce long fiber composite parts and mold costs cannot be justified for low production volumes. Also, resins with high shrinkage rates can cause waviness, ripples, sink marks and rough surfaces on the product.

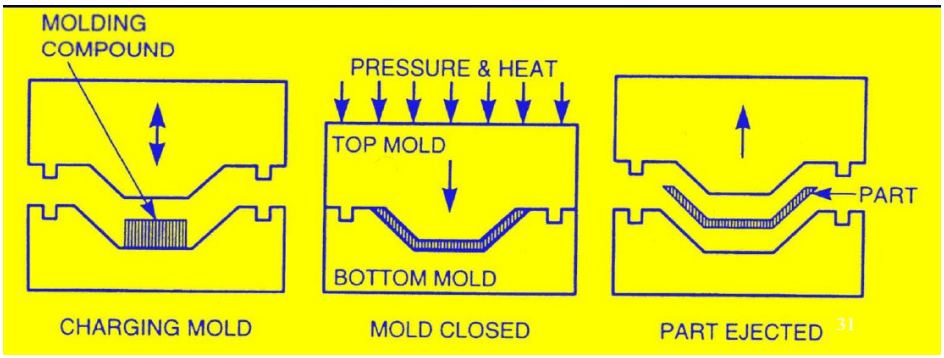

Figure 3.4: Schematic of compression molding

3.5 Filament Winding

Filament winding is an automated process for manufacturing advanced reinforced composite structural components. It entails the winding of resin impregnated fibers around a mandrel and then curing them so that the wound fiber can take the shape of the mandrel. The fibers are placed on the rotating mandrel by a horizontal carrier. The fiber orientation is controlled by controlling the speed of the horizontal carrier. Subsequently curing is done for an appropriate time and temperature. After curing, the wound composite is removed from the mandrel if the mandrel is not sacrificial; but, sometimes the mandrel can be a part of the design. It is used to manufacture pipes, tanks, gas cylinders, etc. the major advantages of the winding process are that it is highly automated, and capable of producing accurate repetitive fiber orientation. It does have some limitations however, which include difficulty in placing fibers parallel to the axis of the mandrel, high mandrel cost, and special treatment on the external mandrel surface needed to ensure evenness. Figure 3.5 illustrates a schematic of a 2-axis filament winding.

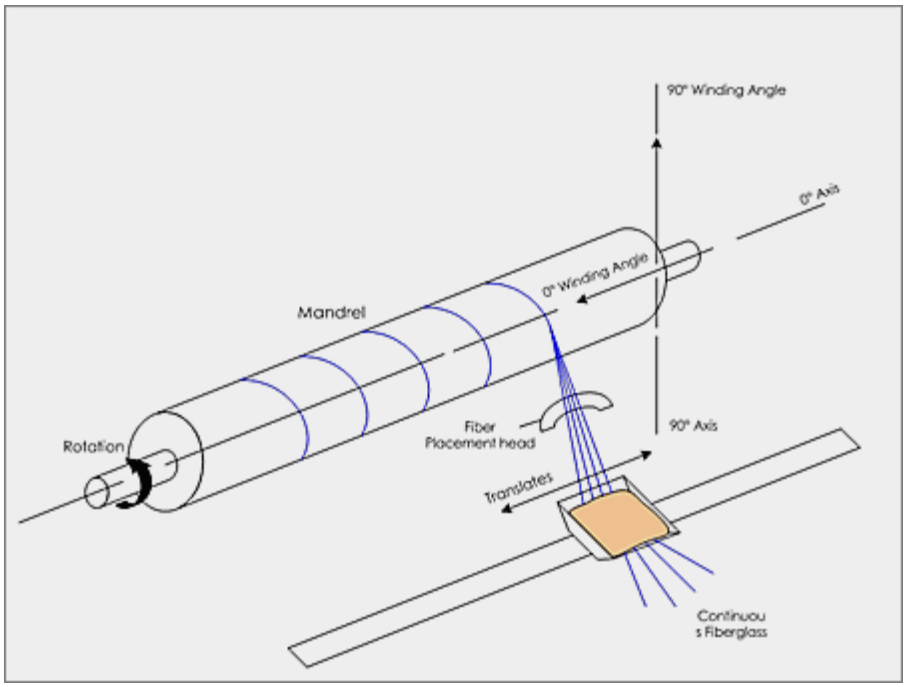

Figure 3.5: Schematic of filament winding [15]

3.6 Selection Basis of Various Processes

Considering the three major regions as in Figure 2.1 of composite manufacturing filament winding is the second largest process for manufacturing composites as illustrated by the statistics in Figure 3.6

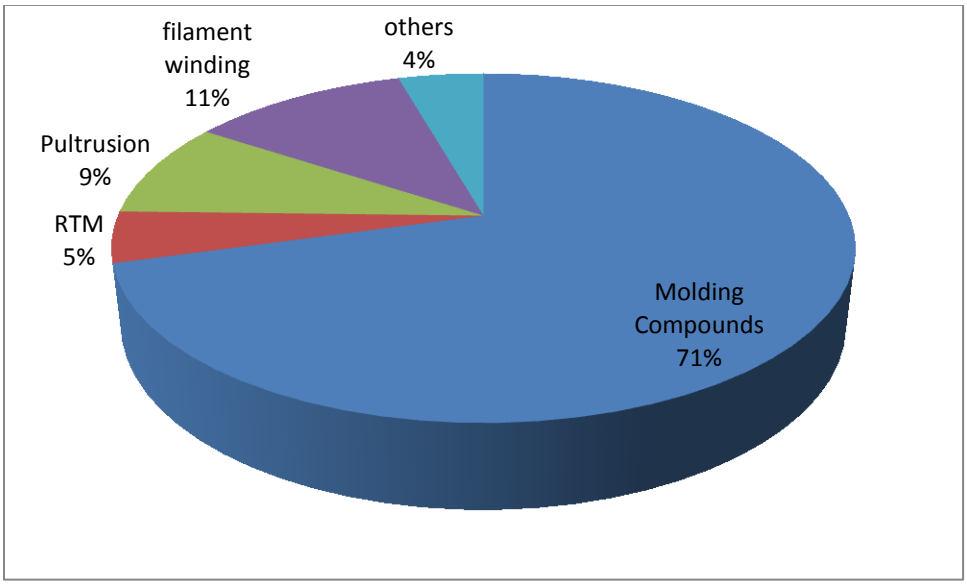

Figure 3.6: Distribution of composite manufacturing process wise [3], [16]

Cost of composite production is also a leading factor in choosing the equipment. Figure 3.7 below gives the comparative analysis of equipment cost for different winding processes.

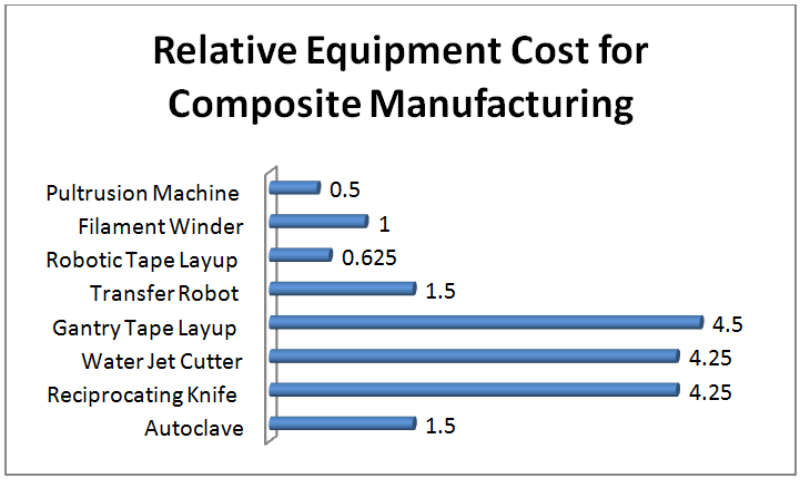

Figure 3.7: Cost incurred by different processes to manufacture composite [10]

Chapter 4

FILAMENT WINDING

Filament Winding is one of the most widely used processes for manufacturing axis-symmetric objects. Despite all its limitation as stated earlier in section 3.5 of chapter 3, the easier and most accurate way of producing axis-symmetric parts, is filament winding. Moreover, since it can be highly automated; it is quite economical in mass production. The applications of filament winding range are very wide; it includes pressure vessels, chemical tanks, aircraft fuselages, rocket motor cases, helicopter rotor shafts, high-pressure pipelines, sporting goods, wind turbine blades and other structural applications. This chapter deals with the composite manufacturing process of filament winding and outlines the key control aspects in a filament winding process.

4.1 Process Description

Filament winding is a process, where fibers after being wetted in a resin, are positioned on rotating mandrel under controlled tension, by a carrier following on a specific pattern which establishes winding angle. The winding angle is achieved by controlling the carrier velocity with respect to the mandrel rotation. The winding angle is the angle between fibers and mandrel axis of rotation. In a winding process, the angles can vary from perpendicular to the longitudal axis of the mandrel to any angle other than being parallel to the axis. The layers which are perpendicular to the axis are called hoop layers and the layers at an angle to the axis are called the helical layers.

According to Hoa [17], the filament winding process is a “reverse mechanism of a lathe” operation. The way a lathe removes material from the rotating mandrel at a required rate and quantity, the filament winding machine adds material to a rotating mandrel. As the mandrel rotates, the carriage travels along the mandrel length and delivers fiber on the mandrel with a controlled position and tension. Mandrel rotation, the carriage velocity

and carriage position are controlled by the winder controller and these parameters define the winding pattern.

Filament winding machines are categorized by their degrees of freedom. The minimum degrees of freedom possible are two, first the rotation of mandrel and second the horizontal movement of the carriage. For a two axis winder the delivery eye can be integral part of the horizontal carrier. Other possible degrees of freedom can be additional movement of the delivery eye, like vertical movement, rotational movement and forward and backward motions. To date, the maximum number of axis available on a filament winder are seven. Figure 4.1 below shows all probable degrees of freedom that are possible in filament winding machine. The degrees of freedom, other than the two obvious two degrees of freedom, are indicated by red arrows and the later part of the Figure shows all the seven possible degrees of freedom.

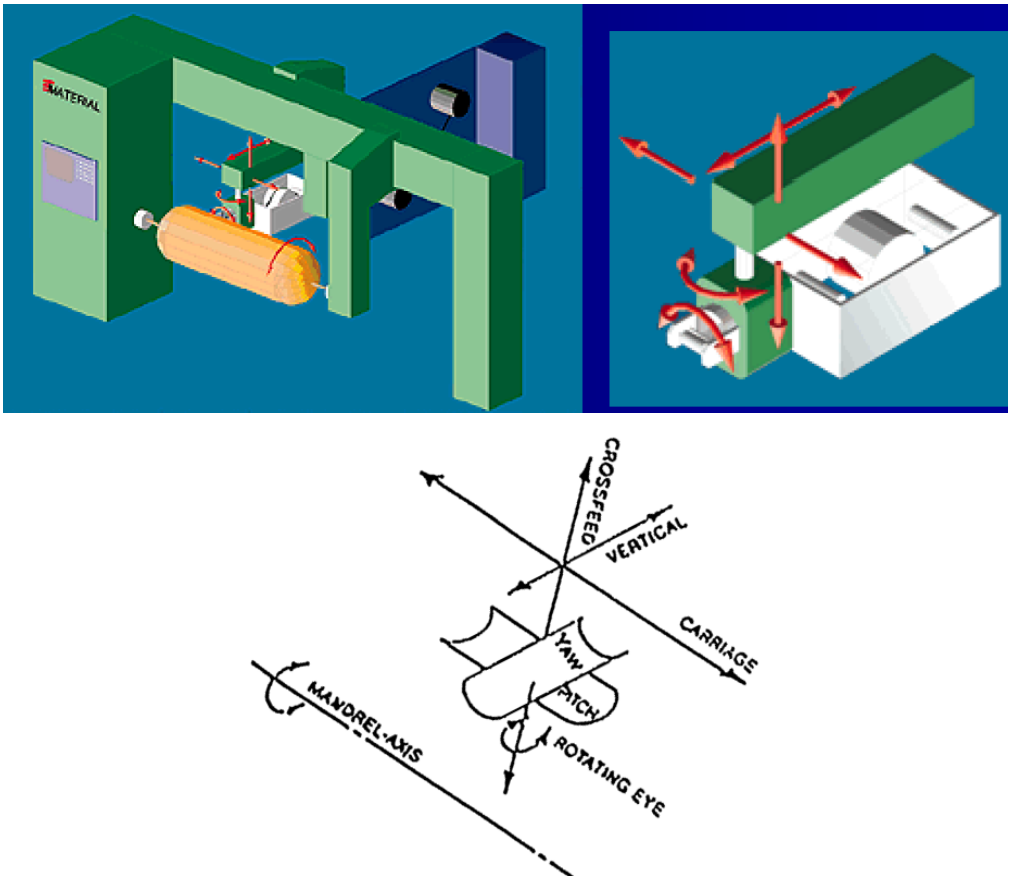

Figure 4.1: Different possible axis of rotation for filament winding process [18]

Other than the pattern of the winding, the winding tension is also a critical parameter of the winding process. Adding tension to fibers in winding process increases the volume fraction of composite and reduces the residual stresses in it. Inadequate winding tension can result in voids or air gap in the winding, which would in turn decrease the mechanical properties of the pipe to a great extent. Also inconsistent winding tension is to be avoided as it changes the friction between fiber and the mandrel and can result in slippage of the fiber [19].

The wetting of the fiber is done in a resin bath. Non rotating parts are used to guide the fiber in and out of the bath, so as to reduce the breakage of the fiber at the rotating surface. Wetting is not required when a prepreg fiber is used [19].

Filament winding is an effective way to produce high strength tubes of various sizes, capable of handling high internal pressure. In order to optimize the design for several usage purposes winding angles can also be arranged. It is possible to use filament winding for reinforcement. Typical filament winding applications include tubes, pipes, vessels thick pressure vessels, rocket motor cases and reinforce concrete columns.

Considering the basic winding principle, a simple two axis filament winder is capable of producing fiber reinforced pipes of consistent diameters. But it would require additional axis to produce other shapes. Complex geometries demand complex machines with higher degrees of freedom. Cost of the machine increases drastically with the complexity.

4.2 Control Elements in Filament Winding

The major control parameters in a filament winding as discussed above are winding angle and winding tension, which contribute primarily to the strength of the produced composites.

4.2.1 Winding Angle

As discussed above the winding machine in general consists of at least two major moving parts; first, the rotating system on which the mandrel rotates, and second, the fiber

delivery system or the carrier which is linear in motion. The composite manufacturing as discussed earlier is produced by layers of reinforcement bonding together by a resin matrix. The formation of every layer in a composite manufacturing process is critical. Orientation of the fibers in each layer contributes to the characteristics and strength of the composite. In filament winding the orientation of the fiber layout is governed by the winding angle of the machine. Soden et al [20] analyzed the effect of winding angle on the tensile strengths of the composite. They summarized that with the increase in winding angle, the circumferential tensile strength increases and the axial strength decreases.

When the fiber is wound and completes one full cycle through entire length of a mandrel, then one circuit is formed. In practice, due to continuous and complete motion, the fiber may not reach the starting point after its complete cycle. In fact, due to an offset reach of a different point it might take more than one cycle of the entire length for the fiber to reach the start point; when the winding reaches that point, it is referred to as pattern. Finally, a layer is the number of patterns required to cover the entire mandrel surface with fiber. The mathematical calculations below formulate the winding angle and then demonstrate how the winding angle is related to circuit, pattern and finally to the layer.

Considering a helical winding pattern; Figure 4.2, below shows the path followed by the fiber in a winding operation.

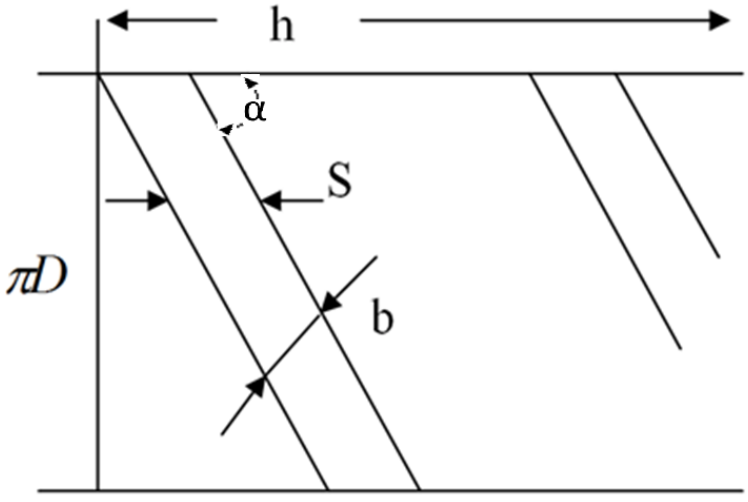

Figure 4.2: Schematic of the fiber path in a winding process

Let α = winding angle (radians)

We get;

$$\tan\alpha = \frac{N_m \pi D}{60 V_c} \tag{4.1}$$

where;

V_c = Carrier Velocity (m/s)

N_m = Mandrel Velocity (RPM)

D = Diameter of mandrel (m)

The length covered by a single bandwidth of fiber in one mandrel revolution can be established by:

$$L = \frac{\pi D}{\tan\alpha} \tag{4.2}$$

If h, is the total mandrel length, then the number of revolutions required to cover the whole mandrel can be established by.

$$n = \frac{h}{L} = \frac{h\tan\alpha}{\pi D} \tag{4.3}$$

$$n = h\frac{N_m \pi D}{60 V_c} \tag{4.4}$$

If S is the circumferential coverage with fiber of bandwidth, b and winding angle, α then S, can represented by

$$S = \frac{b}{\cos\alpha} \tag{4.5}$$

So number of circuits per layer, C can be calculated as:

$$C = \frac{\pi D}{S} \tag{4.6}$$

$$C = \frac{\pi D 60 V_C}{b\sqrt{(60V_c)^2 + (\pi D N_m)^2}} \tag{4.7}$$

4.2.2 Tension Control

The tension in the fiber is one of the major factors which accounts for 70% of product's stiffness and tensile strength [21]. Fiber tension contributes for volume fraction, which is a measure of the compactness of the fiber and is dependent on the winding tension [22]. This confirms the relationship of the fiber stress and the tolerance of the internal pressure by the composite. Also, it can be seen that the longitudal and horizontal stresses are a function of the winding angle α. The relationship is explained mathematically below.

The stress in fiber, σ_f, in a fiber can be broken into components σ_x stress σ_y (i.e. longitudal and circumferential stresses respectively) [17].

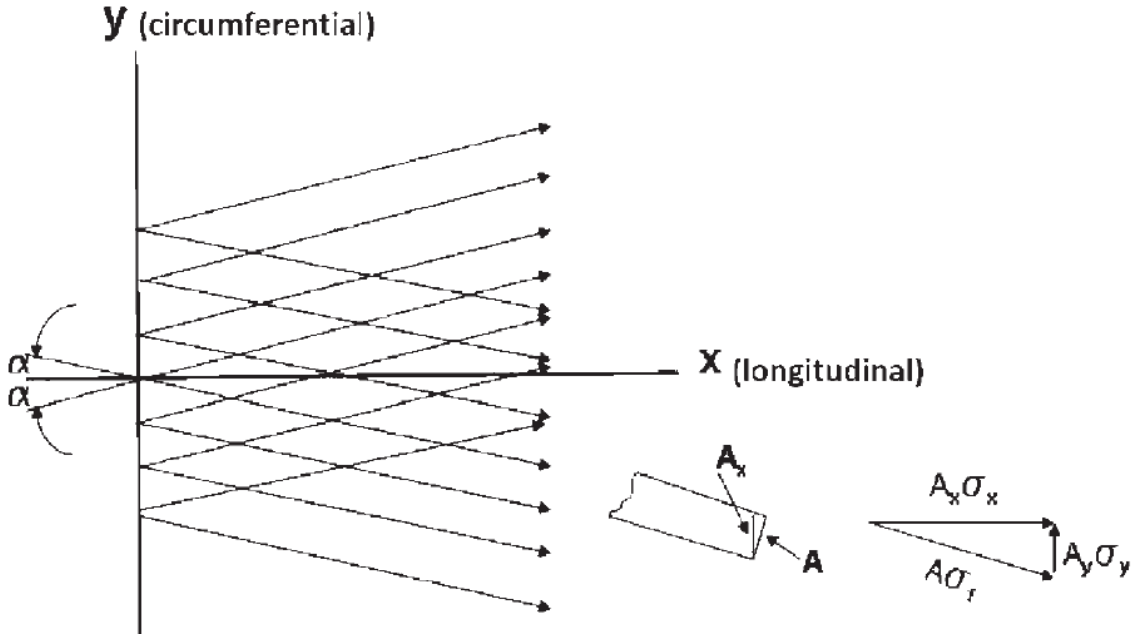

Figure 4.3: Stress analysis of fiber in filament winding [17]

$$\sigma_y = \frac{Pr}{2t} \tag{4.8}$$

$$\sigma_x = \frac{Pr}{t} \tag{4.9}$$

where:

P = Internal Pressure (N/m^2)

r = Radius of Cylinder (m)

t = Thickness (m)

A = Fiber-band Cross Section Area, which includes resin. (m^2)

σ_x; σ_y =Longitudal and Hoop Stress Respectively (N/m^2)

σ_f= Resultant fiber stress in the direction of the winding angle (N/m^2).

Summing up the stress components in equations 4.8 and 4.9

$$\sigma_f = \frac{\sqrt{5}Pr}{2t} \tag{4.10}$$

Equation 4.10, shows how the internal pressure tolerance can be controlled by the stress of fiber. If T, is the instantaneous fiber tension then;

$$\sigma_f = \frac{T}{AV_f} \tag{4.11}$$

where V_f is the fiber volume fraction.

Equation 4.11 shows that tension in the fiber contributes to fiber stress [17]. Also adding of adequate tension in the fiber eliminates voids in the winding increasing the tension, decreasing the viscosity and winding speed can reduce the void content to 1% [7]. The presence of a void air gap reduces σ, the stress handling capacity of the fiber, considerably. This makes the tension control a very important parameter of the filament winding process. In other words, the pressure handling capability of a wound composite is governed by the number of layers, the winding angle [23] and fiber tension [24]. Improper or inconsistent fiber tension disturbs the winding angle as well [19].

Chapter 5

BACKGROUND AND SCOPE OF DISSERTATION

This chapter presents an insight to the development of filament winding technology over the years and the current state of the technology. The research motivations derived out of the limitations on availability of low cost filament winding machines. The scope of the dissertation is then presented.

5.1 Current State of the Technology

The history of modern winding technology has three important stages [25]. The first patent in 1963 [26], the invention of NOL ring sample for testing the tensile strength of the wound composite [27] and the first monograph exclusively pertaining to filament winding published in 1964 [28] .

Over the last two decades the filament winding industry has undergone a renaissance in terms of automation, advanced and innovative fibers and resins [29]. The technology of winding has also given birth to newer automated filament placement technology in 1990 [30]. Moreover the filament winding itself, by the virtue of it applicative value, has given rise to newer improved techniques with respect to its production speed, volume, size and the shapes of products. Entec, the company to produced the first computer controlled filament winding machine, has built the largest five axis filament winder in the world, which is capable of producing turbine blades up to 54.54 (m) long, 8.23 (m) in diameter and weighing over 136.363 (kgs) [31]. In 2006 Brigham Young University researchers patented a new filament winding machine technology called LOTUS, capable of winding materials in the shape of L, O, T, U, S. [32]. In 2009 San Diego composites successfully fabricated a toroidal shaped composite tank by filament winding [33]. Michael et al [34] indicated the production rates could vary from few feet per minutes to 60 meters per minute.

Control system for winding machines have evolved from simpler mechanical chain machine, open loop control using hydraulic stepper motors controlled punched paper tapes, servo analog control [35] to sophisticated programmable computer control, CNC and advanced robotic control. Stewart and Middleton et.al [36], [37], used CADFIL software to establish control for CNC machines. Seng [38] used an industrial robot to establish accuracy speed relationship of a robotic filament winding.

5.2 High Cost Winding Machine

As discussed above, filament winding is one of the most preferred methods of manufacturing composite pipes. Industrial developments in recent times have lead to high sophistication of winding machine and as a result the prices of the winding machines have increased. The price range of 5 to 7 axis, filament winding machines ranges from $300,000 to $700,000 [39]. There is no data on price range of 2 axis winding machines. According to the market survey, through various price quotations, today the smallest filament winding machines range from $35,000 to $100,000, making it unaffordable for small scale or research applications. Moreover, there is no commercial availability of 2 axis winding machines which are sufficient for winding pipes. Keeping cost reduction in mind, a small scale winding machine was designed. The winding machine in general consists of a minimum of two rotating parts, which in general are controlled by CNC machines [40] [41]. The CNC machines are very expensive, especially the control software; software licenses like CADFIL are in the range of $4,000 to $20,000 which leads to higher machine prices [42].

5.3 Scope of the Study

The use of PLC is a better alternative for machine control from the cost prospective. There are PLCs available with programming tools in the range of $1,000, reducing the overall cost by at least 75%. The next important challenge in this design is the incorporation of closed loop tension control. Since tension is a nonlinear and complex parameter, it needs sophisticated control algorithms like the neural [43] and the fuzzy [44], [45], [44] techniques to control the tension, implementation of which is very difficult through a PLC. The direct implementation of tension control by PID logic is also

difficult; it requires constant tuning of the PID parameters to deal with the nonlinearity of the tension. Use of PID control with conventional PID leads to overshoot [46] and when dealing with filament winding, overshoots in the winding tension are very dangerous for it may seriously damage the fiber. Moreover inconsistent tension would lead to undesired alteration in fiber path on the mandrel. In this context a PID controller is designed with a concept of virtual linearization. The next step was to design the feedback for the system.

The first method that can be used as a feedback for tension control is by direct implementation of a tension sensor in the path of the fiber. Most of the literatures on winding tension control have used this technique [43], [47], [46] such as using a potentiometer or a roller nip. Invariably, the tension is maintained in this type of system by two motors, one drives the fiber source creel and the other drives the mandrel. In the above scenario the source spindle is an inherent part of the system. The system that is discussed here does not include an inherent source creel. It is designed as such to wind from any creel giving more flexibility to the operation.

The other method is by considering the fiber as an elastic string, with a start point that is the point where the actuator is placed and the end point being the point where the fiber comes in contact with the mandrel. When a tension or a force is exerted on the fiber parallel to its motion but in the opposite direction between these two points then the velocities in the fiber line at these two points would be different initially and the tension in the fiber can be measured as a function of these two velocities. The tension changes until the velocities are equal. Once the velocities are equal, the tension has reached its steady state. This implies that the maximum change in the length has been achieved due to the change in tension. Once this state is reached the tension is constant. Ren et al [48] used this system by using a swinging bar.

Using Hooke's law the tension, T in the system can be formulated as

$$T = \frac{SE}{l_0} \int (v_1 - v_2) dt \tag{5.1}$$

where;

S = Cross section area (m^2);

E = Modulus of Elasticity (N/m^2);

lo = Original Length (m);

v_1 = Velocity of the fiber at the actuator (m/s);

v_2 = velocity of fiber at the mandrel (m/s)

Hooke's law states that the elongation in any elastic element is the function of force; so, the above equation 5.1 is rearranged to give force in an elastic element. But using this system in the model under discussion it would be required to measure the velocity of the of the fiber line at the point of the actuators contact with the fiber. To avoid this task a third approach has been adopted to model the feedback of the system, which incorporates the change in the mandrel angular velocity to give an indication of the tension.

5.4 Development of a Prototype

A commonly used wood lathe framework is used to facilitate the mandrel rotation. The Lathe driving mechanism is modified by addition of an induction motor, driven by a VFD, whose mandrel is fitted in yolk of the lathe. The rotating side of the lathe is driven by the VFD the speed reference is given manually by the user. A horizontal slide is designed based on a screw mechanism. The screw, on which the resin carrying tank and the tension actuating system are mounted on, is driven by a servo motor. The movement of the horizontal carrier is controlled by a servo drive. The controller gives the speed command to the servo drive via a signal conditioning card. The speed feedback of the carrier is input to the PLC (Automation Direct.com, Cumming GA, USA) through a high speed counter CTRIO card (Automation Direct.com, Cumming GA, USA). The output going to the servo motor drive is based on the winding angle specified by the user and is calculated by the PLC. The actuator is designed to impart a controlled variable tension to the fiber. The input to the actuator is fed from the output card of the PLC via a signal conditioner, which is a power operational amplifier. The winding angle is controlled by

the speed control feature of the VFD (Baldor Electric Company, Fort Smith, AR, USA) with respect to the ratio of the servo motor's speed to mandrel's angular velocity. An encoder is fitted at the rotating end of the mandrel. The encoder output serves as tension feedback for the system. The control system of the winding machine is done by a PLC.

Figure 5.1: Developed prototype filament winding machine

Chapter 6

HARDWARE DESCRIPTION

Figure 6.1 illustrates a schematic of the prototype filament winding machine setup. The setup includes a lathe, a speed encoder on mandrel, an induction motor with gear box, a horizontal slide, a servomotor, a fiber delivery head with fixed guides and a tension actuator. Induction motor is connected to the mandrel with a belt and the servo motor drive the horizontal slide screw coupled with its shaft.

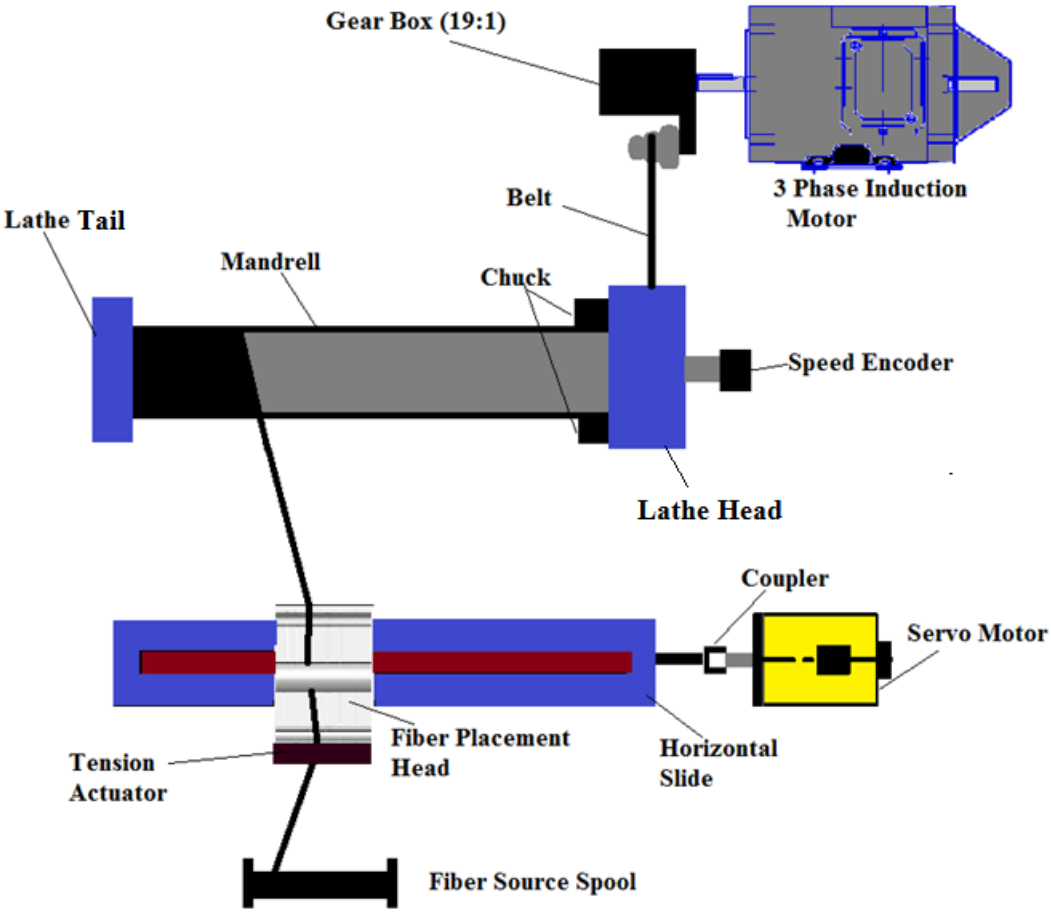

Figure 6.1: Schematic of the hardware setup

6.1 Mandrel

The mandrel is fixed to the head of the lathe by a chuck and is capped on the other side retained by a screw operated support at the tail side. It is driven by a three phase induction motor. The head spindle of lathe, as mentioned in the previous section, is connected to the motor by a belt through a gear box. In addition, there are two pulleys at lathe head spindle and motor gear box with 3 different diameter slots. The gear ratio of the gear box is 19:1 and with the pulley slots five different gear ratios is possible viz. 6.33:1, 12.67:1, 19:1, 28.5:1 and 57:1. Motor is controlled by a VFD. Figure 6.2, shows the gear box with the pulley.

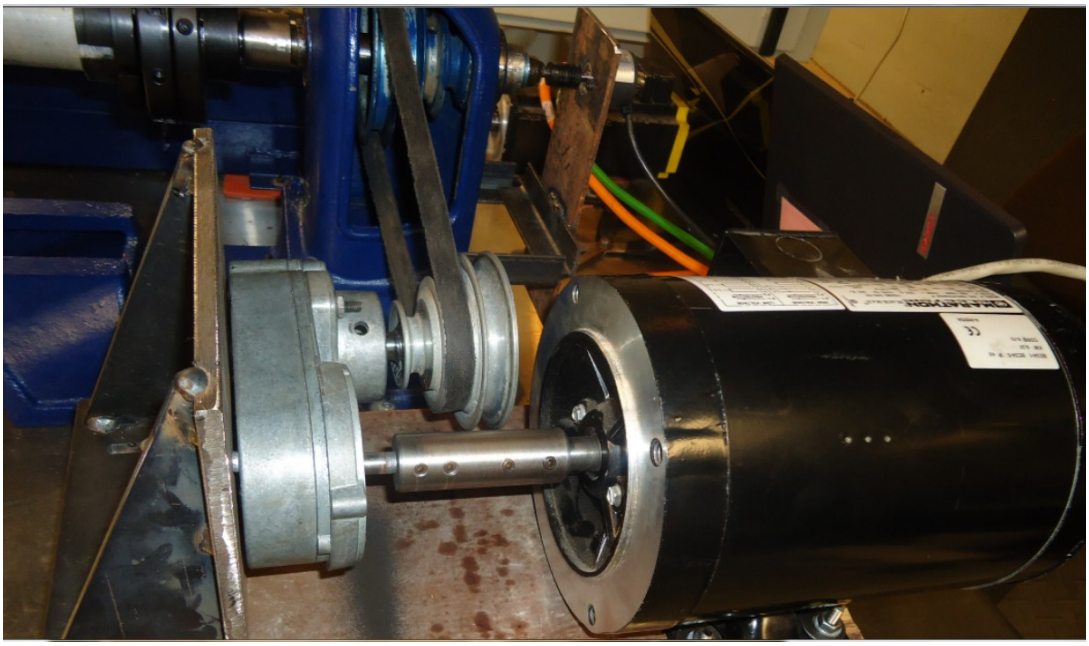

Figure 6.2: Gear box pulley and belt used in the prototype

6.1.1 Induction Motor

A three phase induction motor drives the mandrel. The motor is Marathon Motor (Marathon Electric Motors, Wausau, WI, USA) made; model no: 56H17T5301 B. Frame NEMA 56 C. It is a 0.5 Hp, 3 phase, 230 V, four pole machine with Full load speed of 1735 RPM. The graphs below in Figures 6.3 and 6.4, gives an idea of motor performance in varying load condition as prepared from the data received from manufacturing load test, curtsey: Marathon Motors.

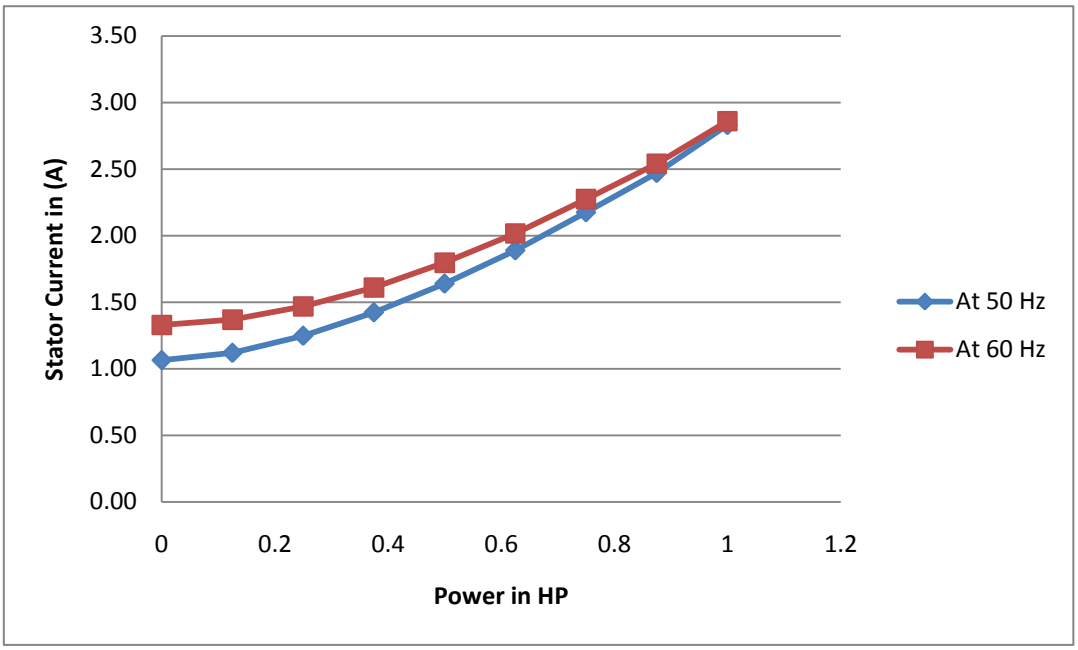

Figure 6.3: Change in input current due to change in load

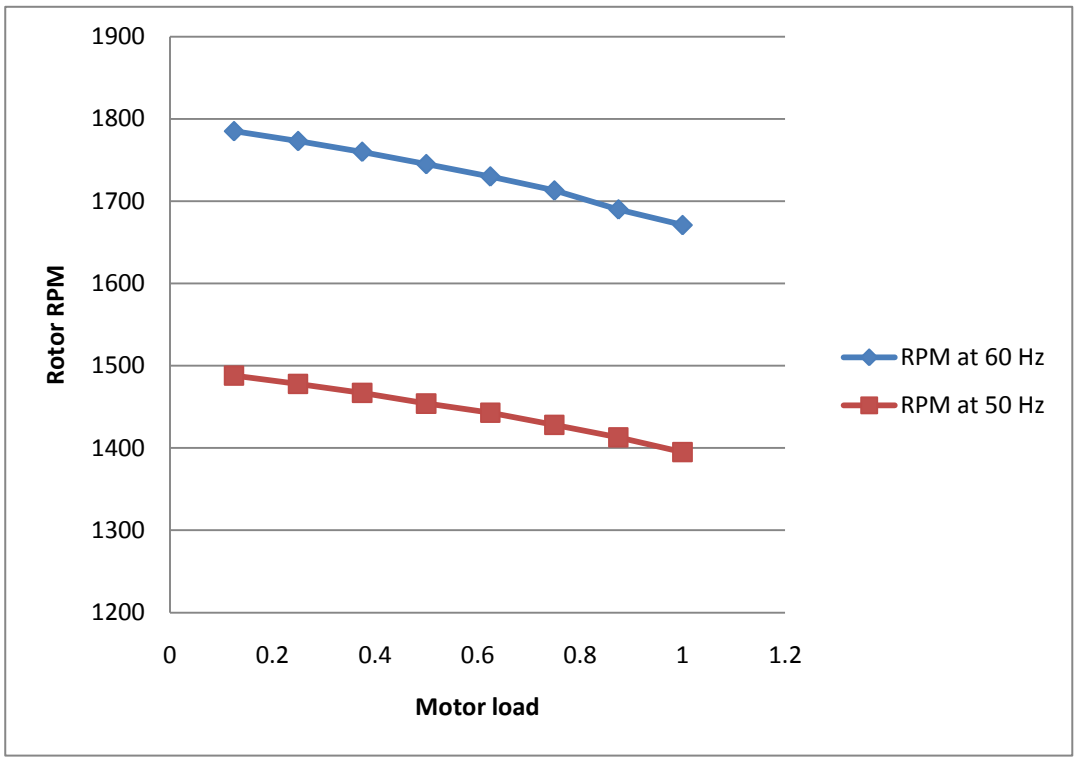

Figure 6.4: Change in rotor angular velocity due to change in load

The graphs in Figures 6.3 and 6.4 show the motor behavior under changing load at different input frequencies. The load test data from the factory was available for only 50 and 60 Hz, which is more than twice the operating speed. Load characteristics for low speed range were not available for this particular motor.

6.1.2 Motor Drive-Variable Frequency Drive

The induction motor is controlled by Baldor Electric Motor manufactured variable frequency drive (VFD), which is an adjustable frequency PWM drive operating in constant Volts per Hertz, sensor-less vector mode. The drive Model no is VS1ST AC micro-drive. The application of the drive is to maintain the motor at the input frequency speed.

The drive has a single phase 110V input and 230V, 3 phase output. The carrier frequency of the PWM converter is adjustable to 8, 16 or 32 kHz. The 0 to rated speed, acceleration and deceleration can be adjusted from 0 to 300 sec. The Volts per hertz ratio is 3.83.An adjustable voltage boost option is available which would give additional voltage at start up, to overcome the starting torque. A max of 10% of the rated voltage (23V) boost is allowed for the motor. The drive has a 0 to 10 V analog output and 30 Vdc Relay output.

The constant V/F operation is in three stages; first, the input AC signal is converted to a constant DC signal subsequently in the second stage a PWM convertor is used to create a switching circuit to invert the DC signal to a changing AC output. The frequency of the AC output is controlled by a switching circuit. Then in the third stage a constant voltage is maintained in accordance to the required frequency.

For example, if the V/Hz ratio is 3.83 as in the prototype system, the frequency at 50% of the rated speed would be 30Hz and the corresponding Voltage would 3.83 times 30, which is 115V. The Volts per Hz in the initial stage (less than 50% of the rated speed) can be boosted by a voltage boost through VFD to overcome high load inertia, if required. In the prototype the voltage boost is 7V. Also a change in the carrier frequency

of the PWM of the drive can boost the voltage permanently as with increase in the frequency the resultant voltage decreases [49]. Figure 6.5 shows how voltage boost is implemented in the VFD used in the prototype.

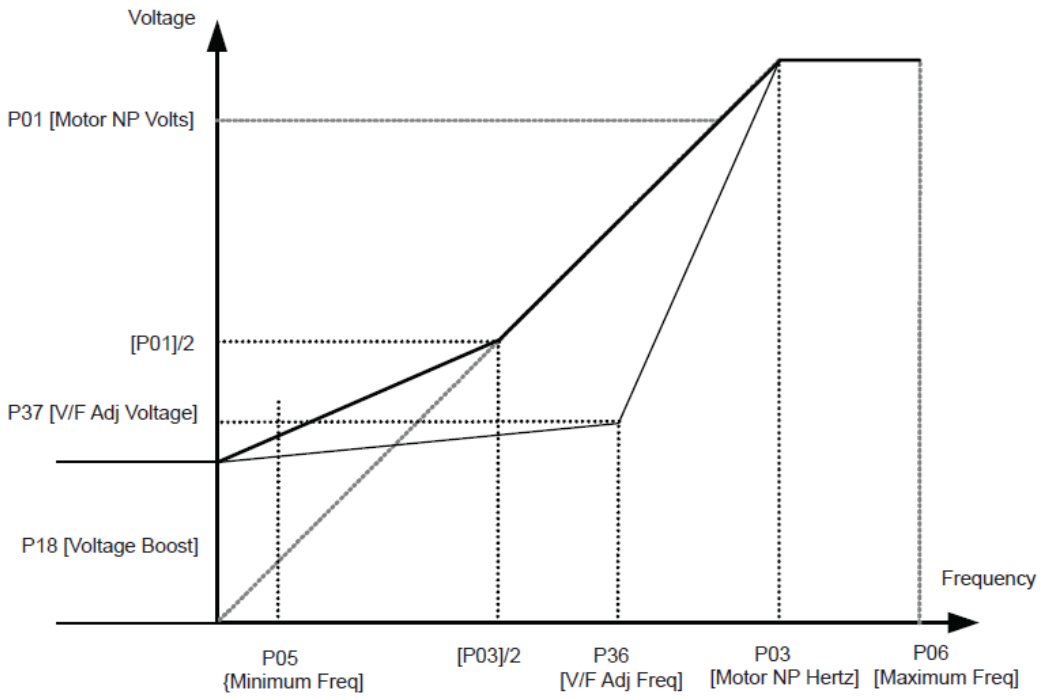

Figure 6.5: Adjusting Volts/Hz characteristics- through voltage boost in VS1ST (courtesy Baldor VS1ST manual).

Figures 6.6 a, b, c, shows the wiring of the VFD.

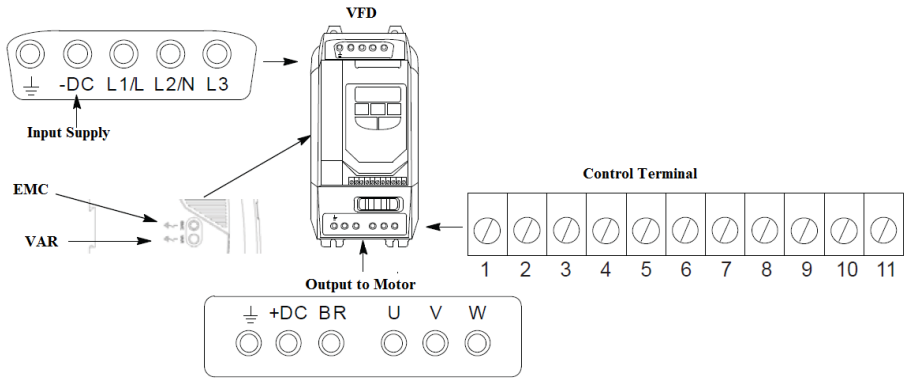

(a)

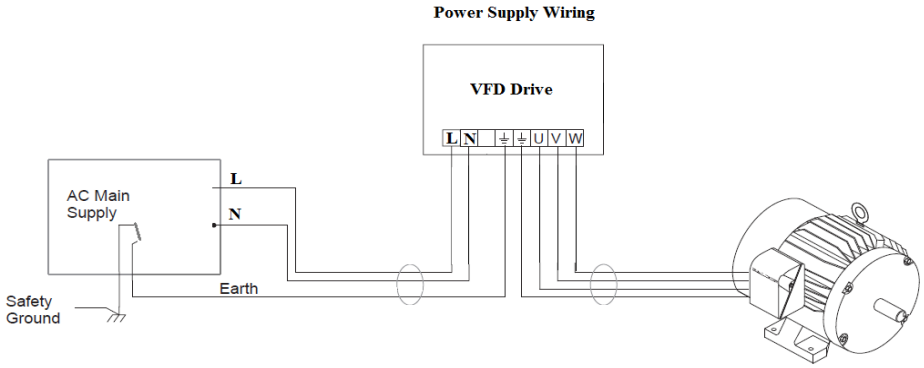

(b)

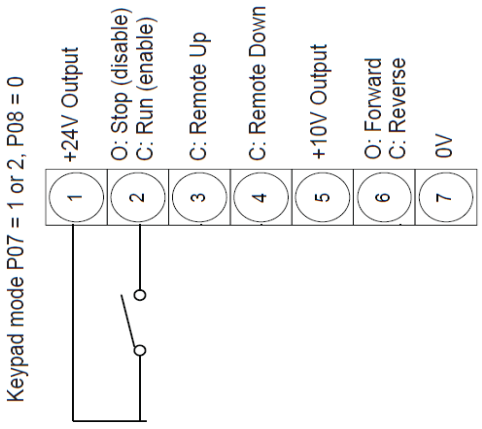

(c)

Figure 6.6: (a): Schematic of the drives terminal. (b): Drive input power supply and output wiring. (c): Drive control terminal.

6.1.3 Encoder

An encoder is used at the lathe head to facilitate accurate measurement of the mandrel angular speed. The Encoder is an NPN open collector quadrature counter with a resolution of 1000 counts per second, Model no: TRD-S1000-BD, manufactured by Automation Direct.com; (Cumming GA, USA). Figure 6.7 shows the encoder.

Figure 6.7: TRD-S1000-BD encoder (courtesy Automation Direct Manual)

The encoder counts two pulses A and B that are out of phase by 90 degrees. It is called quadrature counter, because it creates four logic states based on the rising and falling edges namely a, b, c and d as illustrated in Figure 6.8 by the timing cycle of the encoder. Channel Z denotes one full cycle used for home position reference. When the encoder completes one full cycle, then Z gives one pulse.

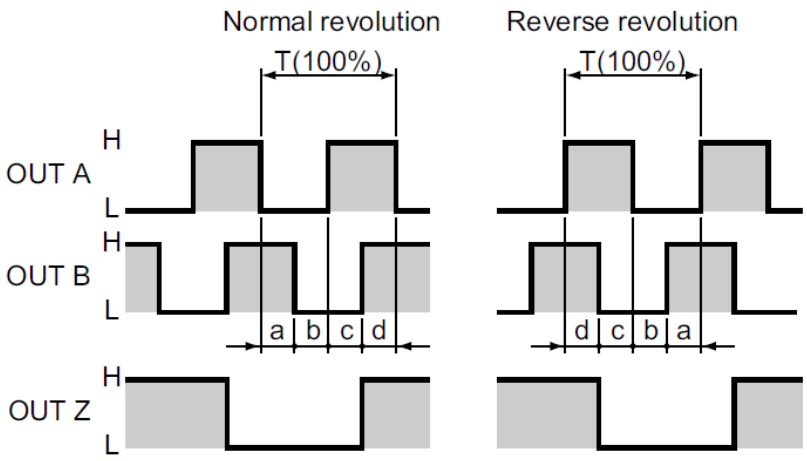

Figure 6.8: Timing cycle of the encoder. (Courtesy: Automation Direct Manual)

Figure 6.9: Actual setup of the encoder at the head of the lathe.

6.2 Horizontal slide

Horizontal slide is connected to a long worm screw driven by the servo motor. The length of the slider is 40 inches. The setup is capable of winding up to 1 meter of the mandrel.

The screw has a diameter of 1 inch and a pitch of 16 turns per inch. Figure 6.10 shows the 3D modeling schematic of the horizontal slider.

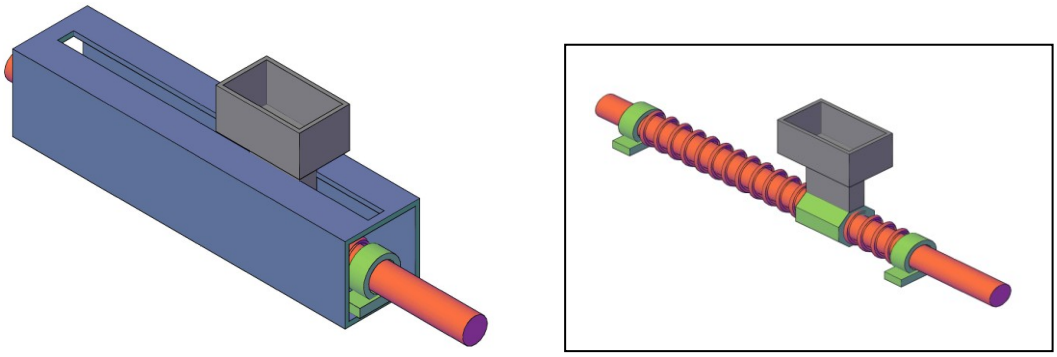

Figure 6.10: Schematic 3D modeling of the horizontal slide

6.2.1 Servo Motor

Figure 6.11: Baldor servomotor model BSM80B-233AF

The horizontal slide is driven by a four pole servo motor manufactured by Baldor Electric Company, model BSM80B-233AF. The motor has continuous stall torque of 2.2 (Nm)

and max torque rating of 7.7 (Nm). The rated voltage is 200 and the rated speed is 6000 RPM. The motor has a voltage constant of $23V_{RMS}$ / kRPM and a torque constant of 0.384 (Nm/amp).

6.2.2 Servomotor Drive

Figure 6.12: MicroFlex servo drive.

The servo motor is driven by a Baldor MicroFlex Servo drive. It is a single axis AC brushless AC servo drive. It controls the speed of the servo motor based on the input signal from the PLC. The drive has user interface but it is not used as the total control of the slide positioning, which has been done by the PLC through the servo drive. The MicroFlex is a single axis AC brushless drive. The drive supports single phase 115V or 230 V or 3 phase 230V input supply. It has an incremental encoder for feedback, two optically isolated digital inputs and one optically isolated output for fault indication. It has an -10V to +10 V analog input for speed reference or position reference.

In the prototype the PLC give the drive speed signal. The raw pulses form the encoder in the drive is fed to PLC through a signal conditioner. The scaling and calculation of position and velocity are done in the PLC.

6.3 Actuator

This section illustrates a novel actuating system to facilitate the tension control system.

6.3.1 Design concept

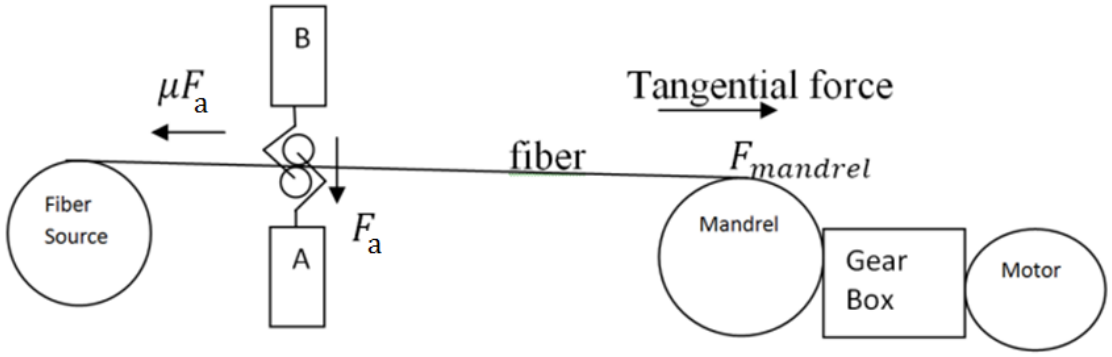

Figure 6.13: The tension control concept.

Based on the system described above, an actuator is designed to generate the required tension in the fibers for fabricating a part as specified by an operator. In the system illustrated in Figure 6.13, "A" represents a solenoid and "B" is fixed. Attached to these two entities are two rollers. When the current in the system is varied, the "A" block presses the fiber against the "B" block with a force (F_a). The actuation force can be calculated using equation 6.1.

$$F_a = -\mu_0 \frac{N^2 I^2 A}{2g^2} \tag{6.1}$$

where μ_0 is the permittivity of air ($4\pi X10^{-7}(\mathrm{NA}^{-2})$), N is the number of turns, I is the current in the coil (A), A is the cross section area of the core and g is the air gap between the shaft and the coil (m). Figure below shows the 3d model and the front view of the designed actuator.

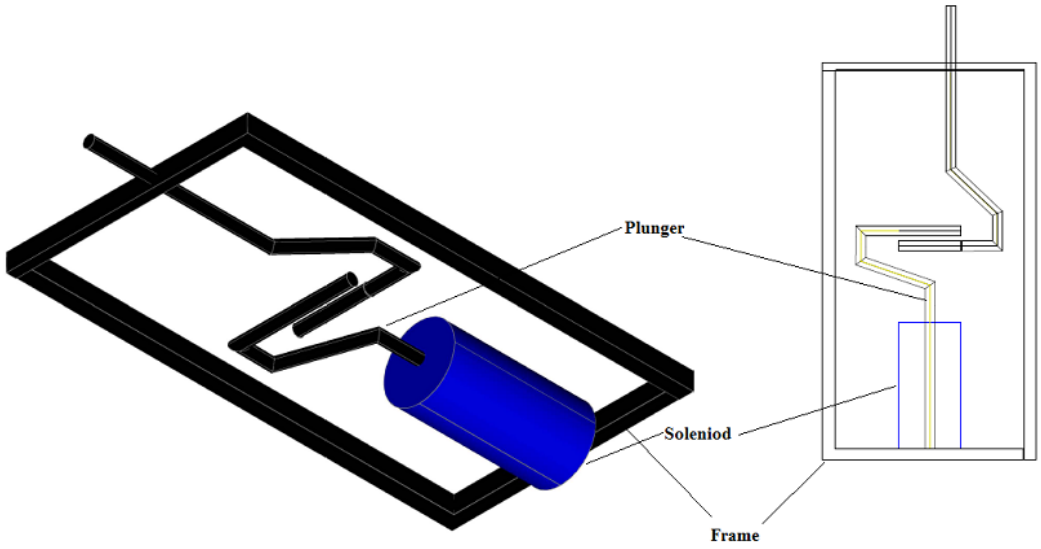

Figure 6.14: 3D modeling of the actuator.

Since the solenoid generates the force F_a onto the fibers, it will result in a horizontal force against the force delivered by the mandrel motor, in proportion toμF_a, which would be opposite to fibers' direction of movement, where μ is the coefficient of friction between the fiber and actuator surface. The terms μ_0, N, A, g in the equation 6.1 are constant. So F_a can be simply expressed by:

$$F_a = \alpha I^2 \tag{6.2}$$

where, α is a constant, which can be determined through solenoid's manufacturer supplied datasheet. In terms of stroke length, the force equation can be written as:

$$F_a = \frac{aI^2}{b+ax} \tag{6.3}$$

When movement of the solenoid is zero, x=0, coefficient of I in equation 6.3 $becomes \frac{a}{b}$, a constant, which is computed from datasheet as in equation(6.4):

$$Force_{sealed} = \alpha \left(\frac{Rated\ Voltage}{coil\ Resistance}\right)^2 \tag{6.4}$$

In this paper value of const, α, is taken as 49.57 N/A^2 and coil resistance, per the datasheet is 11Ω, leading to $Force_{sealed}$ of 58.94 N for a rated voltage of 12V DC. Therefore the force F_a, in terms of input Voltage V can be represented by:

$$F_a = 0.41V^2 \tag{6.5}$$

6.3.2 Solenoid

Figure 6.15, shows the open frame pull type solenoid used as the actuator

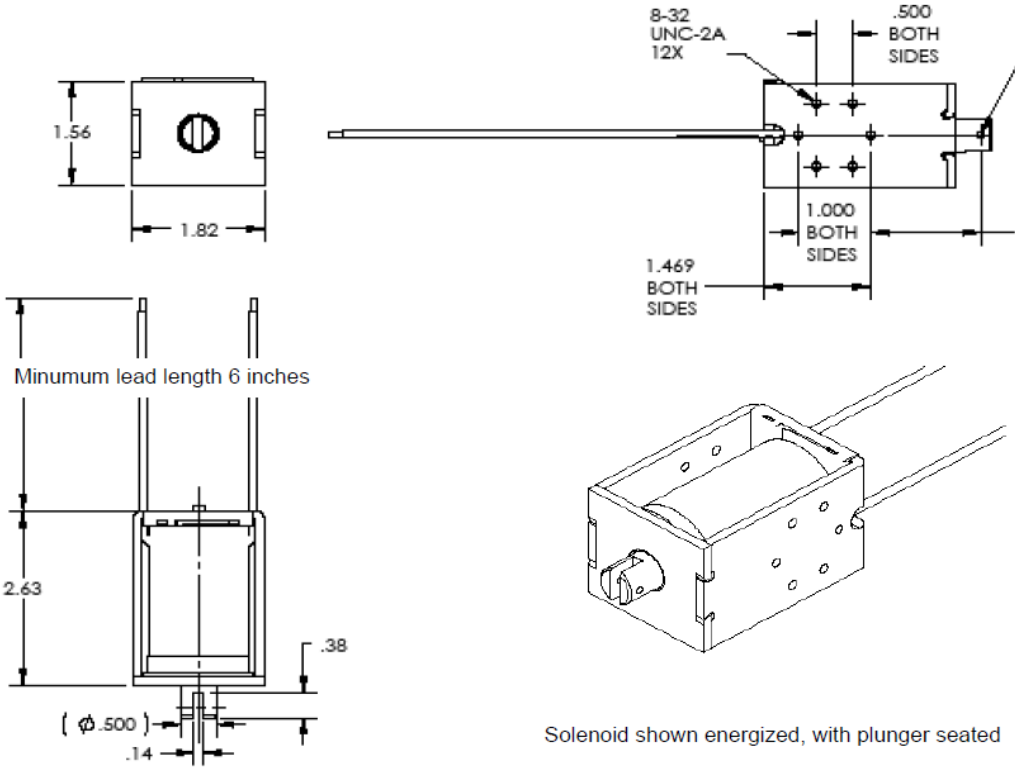

Figure 6.15: Layout of the solenoid used in the actuation system.

6.3.3 Simulation

Figure 6.16, below gives the schematics of the simulation in Matlab Simulink:

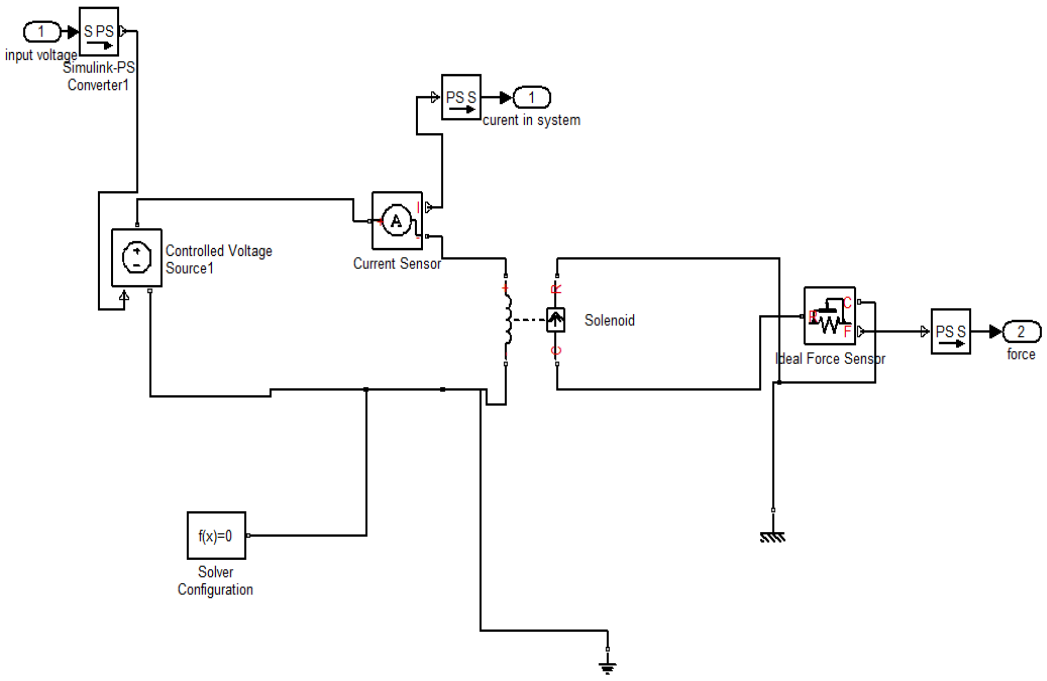

Figure 6.16: Actuator simulation model.

The force stroke curve data is input as matrices in the solenoid block of the model. With rated voltage and current, pulling force is calculated in negative direction of the R to C of the solenoid block. Figure 6.17, shows the simulated response of the actuator force, with varying 0 to 12V DC input. There is a step change of 1 volt in every one second and Figure 6.18, shows the response of the actuator to a ramping input.

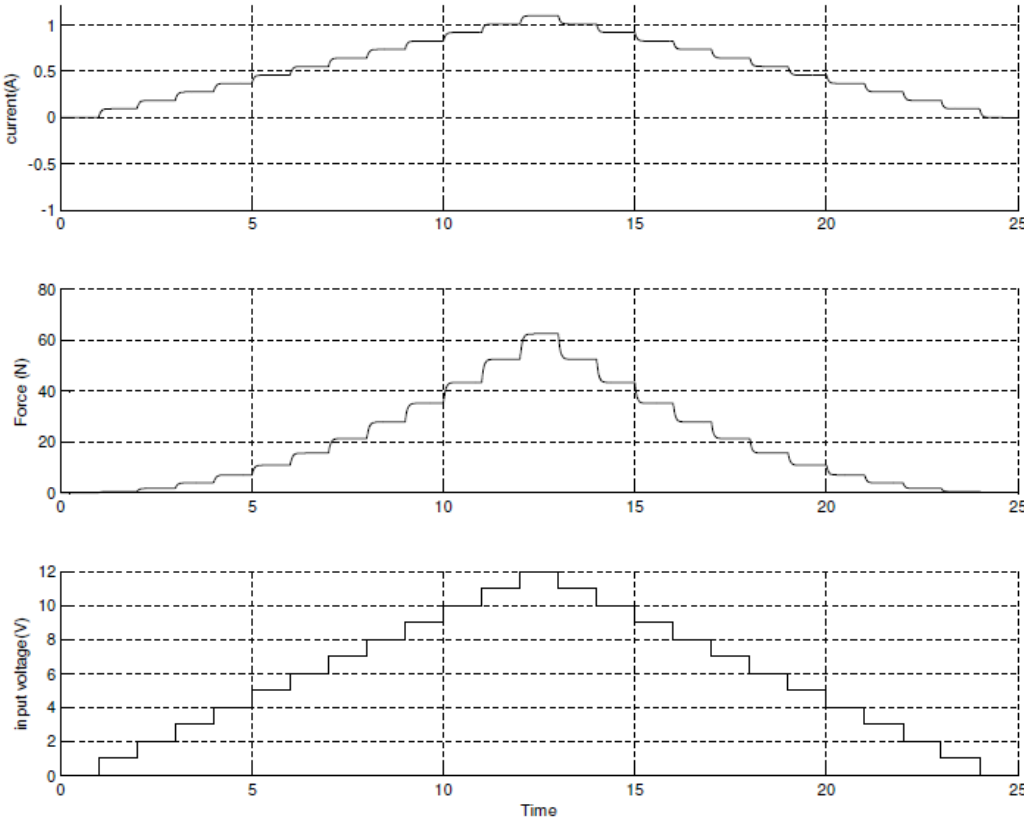

Figure 6.17: Actuator response to step increases in voltage

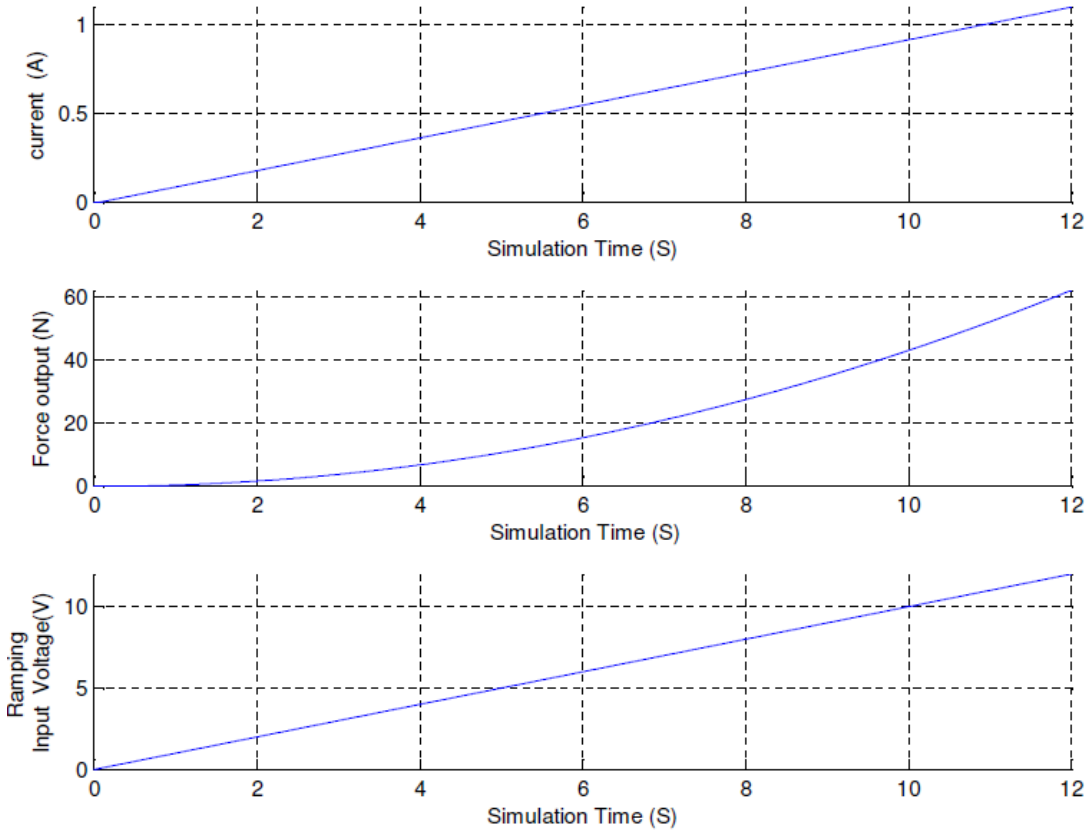

Figure 6.18: Actuator response to ramping input voltage

6.4 PLC

Figure 6.19, shows the PLC used in the prototype.

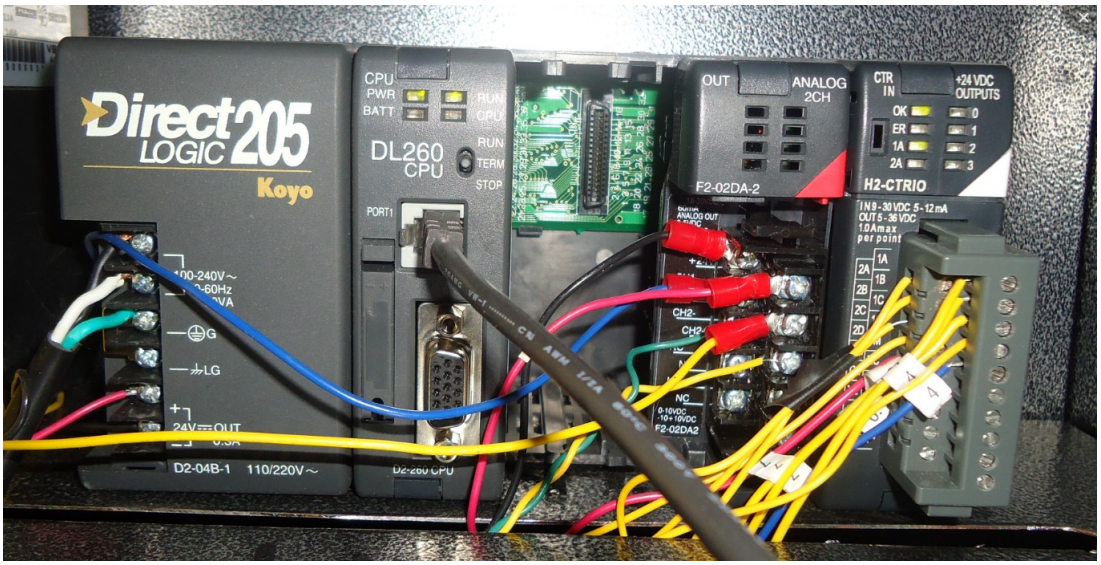

Figure 6.19: PLC used in prototype

6.4.1 Controller

Automation Direct, Direct logic DL205 series, D2 260 PLC is used as the master controller for the prototype. The D2-260 has a total memory of 30000 words. It has flash enable ladder memory of 15872 words and V reference memory of 14592. The typical scan cycle of the controller is 1.9 ms, and it has Boolean execution time of 0.61µs. D2-260 supports RLL Ladder Style, and RLL_{PLUS}/Flowchart Style (Stages) programming. It also supports run time editing of the program and overrides. It has options for fixed and variable scan in a program. It additional to the conventional ladder instruction supports: Subroutines, For/Next loops, Timed Interrupt, Integer Math, Floating-point Math, Trigonometric functions, Table Instructions, PID and Drum Sequencers.

6.4.2 Analog Output Card

An Automation Direct, F2-02DA-2; 2-Channel Voltage Analog Output card is used for giving output to the Tension actuator solenoid and the speed reference signal to the MicroFlex drive. The channels can be configured for 0 to 5V, 0 to 10V, -5 to 5V and -10 to 10V individually. For the MicroFlex drive it is configured as -10 to 10 V in channel one of the card. For the actuator the channel 2 is configured as 0 to 5 volts output. The output card needs a minimum load impedance of 2KΩ and it can deliver a maximum

current of 70mA. Since impedance of the actuator is 11 Ω and the required current is 1.1A for max force, a signal conditioner is designed to limit the output current and increase the output impedance of the controller and at the same time to amplify the input to the actuator. The entire range is divided into 0 to 4095 counts in PLC**.** The section 6.4.2.1, gives a brief idea about the signal conditioner.

6.4.2.1 Analog Output Signal Amplifier and Isolator

LM 675T a monolithic power op.amp is used to amplify and isolate the load from the analog output card. The amplifier is capable of handling current flow up to 3A. The maximum gain bandwidth of the amplifier is 5MHz. and the power bandwidth is 70 KHz. The amplifier is having short circuit protection to ensure huge output current doesn't flow back to the card. Input power supply is in the range of 16V to 60V. It has a 90dB ripple rejection and maximum of 1 mV offset in voltage. The amplifier is provided with internal output protection diodes and has a wide common mode range. Figure 6.20, shows the circuit diagram as used.

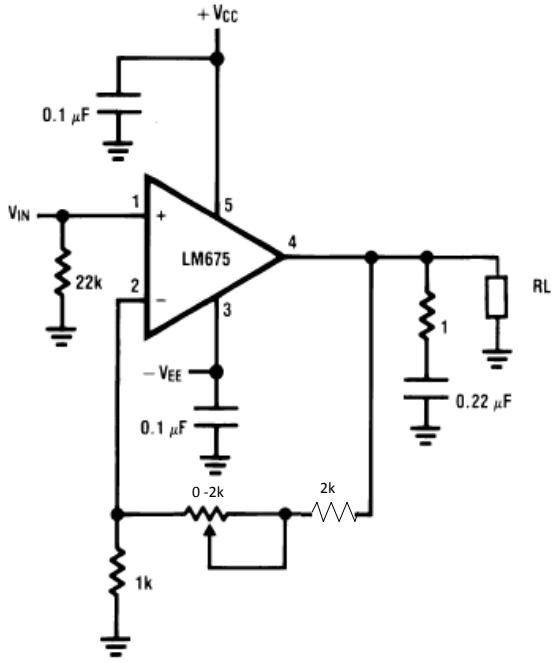

Figure 6.20: Circuit of the power amplifier as used.

The LM675 is used as a non inverting amplifier with a gain of 2.4 and a heat sink of 2deg/V is provided. This amplifies the 0-5V analog card output at 22KΩ input resistance to 0-12V output with a load resistance of 11Ω. The output current varies from 0 to 1.1A.

6.4.3 CTRIO Card

A high speed counter card is used for inputting the angular speed of mandrel and the position of the horizontal slide. The card has a microprocessor of its own which is synchronous to the PLC processing. The response time of on-board outputs is based on the CTRIO scan time, not the CPU's scan time. In the prototype H2- CTRIO is used which has two channels and can accept two Counters, Quad Counters, Pulse Catches, Edge Timers, and Dual Edge Timers. The card has four input slots in each channel. The above mentioned inputs use two input slots. Remaining input slots can be used as secondary input as Reset, Capture, and Inhibit functions or as a general purpose digital inputs or switches. In the prototype two Quad counters are used and remaining inputs are used as digital inputs for limit switches and manual switches.

The card stores it values in the controller V Memory locations address as configured by the user. There is also a user interface, CTRIO workbench for scaling the input pulses and configuring the inputs and outputs in the card. More information about CTRIO work bench is given in Appendix A.2.1. In the Prototype the channel 1 for horizontal slide is scaled from 0 to 1041 mm as position and the channel 2 is scaled as velocity for the mandrel angular speed Figure 6.21, shows the display of scaled value and raw counts through the CTRIO workbench. Resolutions up to 2 decimal points are available in the scaling in the BCD format. Other formats are also available, but use of BCD formats makes it easy to use the value in PLC programming.

.

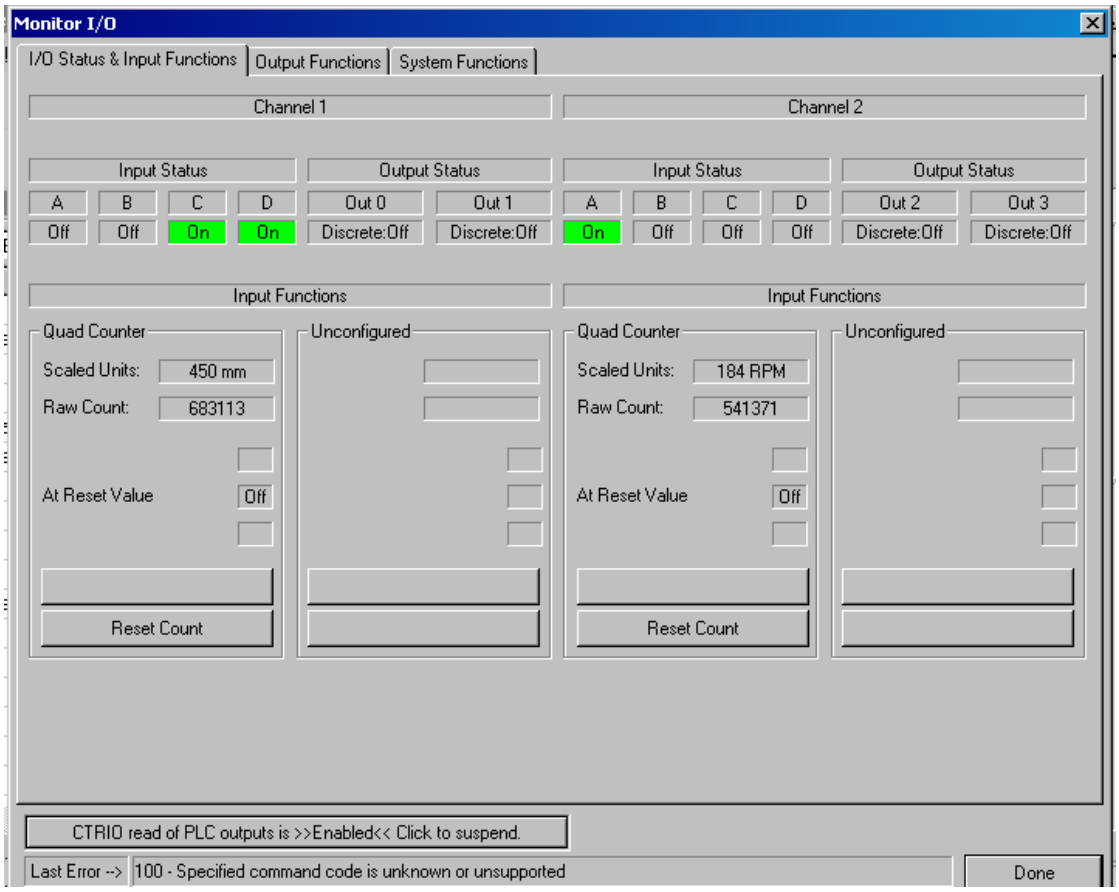

Figure 6.21: Scaled and raw values of mandrel angular speed and horizontal slide speed

6.4.3.1 TTL to NPN signal conditioning

The CTRIO card accepts open collector inputs directly but using a Line-Driver TTL encoder output requires signal conditioning as the card can only recognize voltage pulses in the range of 9 -36Vdc, and the Line-Driver TTL outputs 5Vdc pulses. So a counter comparator circuit was designed a signal conditioner to pull up each pulse over 9 Vdc.

6.5 Cost Analysis

Table 6.1, tabulates the cost incurred to make the prototype.

Table 6.1: Prototype manufacturing cost

Used Products	Price
BALDOR BSM80B-233AF	$1,117
BALDOR FMH2A06TR-EN23 MICRO FLEX DRIVE	$1,077
Motor ion Motor 56H17T5301	$437
VFD Baldor VST1ST	$500
Tension Actuator solenoid LM90	$35
Controller PLC D260 205	$299
H2- CTRIO High Speed Counter Card	$289
F2-02DA-2 Analog output card	$163
Signal conditioning	$100
Miscellaneous (machining, switches, proximity switches cables, belts etc)	$500
Optional tension sensor	$200
Lathe frame	$200
PLC software DS5	$350
automation encoder TRD-S1000-BD	$86
Total	$4,236

Overall cost of the machine is $4,236, which is an effective cost for a 2 axis filament winding machine. To add another axis in the existing prototype would require an additional motor and a motor control. This might raise the price by approximately $2,400 based on the price estimates of motors and motor controls, used in the prototype. The developed 2-axis winding machine in this project offers the following features:

- Angle control range of +/-33-89degress
- Accuracy of +/- 0.5 degrees`
- Fiber Tension of 0 to 8.8N
- Adjustable fiber winding pattern
- Adjustable fiber winding angle

- Mandrel speed of 10 to 40 RPM
- Flexible speed ratios available.
- A low cost durable PLC controller
- Supports mandrel diameter up to 100mm.

Chapter 7

CONTROL ALGORITHMS

This chapter deals with control mechanism as incorporated in the machine. The winder incorporates two closed loop controls viz. angle control and tension control respectively.

7.1 Angle Control

The winding angle is one the most important parameter in a filament winding machine. It sets the layout and orientation of the fibers in the mandrel. The winding angle governs the stress handling capacity of the produced composites as explained earlier section 4.2.1 in chapter 4.

7.1.1 Mathematical Model

The winding angle is proportional to the ratio of the mandrel angular velocity and the carrier head velocity.

$$\tan \alpha = \frac{2\pi R N_m}{60\, V_c} \tag{7.1}$$

where,

$\propto$ is the winding angle (Degrees)

N_m is the mandrel speed in RPM

V_c is the carier velocity (inches/sec)

R is the mandrel radius (inches)

V_c , is the linear motion. As the carrier is mounted on the screw V_c is related to angular velocity V_{RPM} (RPM) and the pitch T_p(threads per inch) of the screw, by the following; equation 7.2.

$$V_c = \frac{V_{RPM}}{T_p} \tag{7.2}$$

7.1.2 Control Schematic

Figure 7.1, below is a block diagram representation of the angle control schematic. The schematic also shows that the signal flow from the servo-drive to servomotor is bidirectional. Drive gives the output signal to the motor and receives position feedback from the motor. The PID controller is in the PLC.

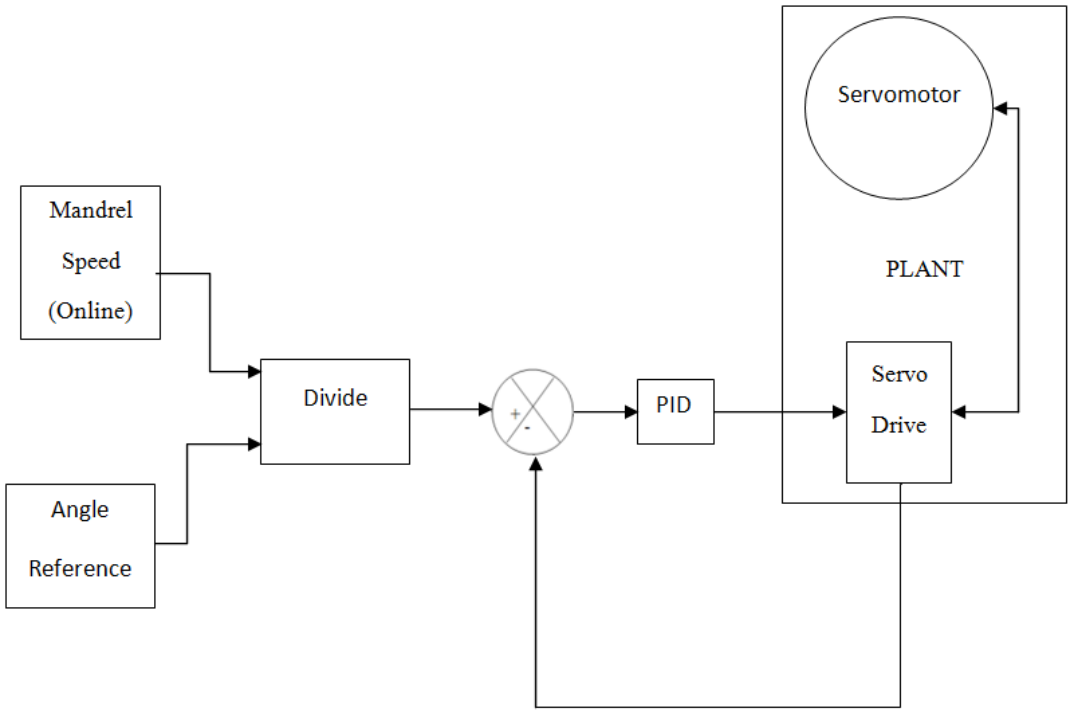

Figure 7.1: Control Schematic for angle control

7.1.3 Simulation

Figure 7.2, shows the simulation of the model. This simulation is for single movement of the horizontal slide in one direction. In the hardware and in practical setup this trend is to be repeated in each cycle twice, for forward and backward motions without initial disturbances. The initial disturbance in the plots is due to the time taken by the induction motor, driving the mandrel, to reach its set speed. This disturbance is onetime occurrence and doesn't repeat itself. In practical setup, the mandrel is started up and the angle control loop only comes to effect after the mandrel speed has steadied. Hence the disturbance, as observed in the initial part of the simulation results, in Figure 7.2 has no effect on the

angle control in practical winding operation. In general, the mandrel speed is kept steady for single winding operation.

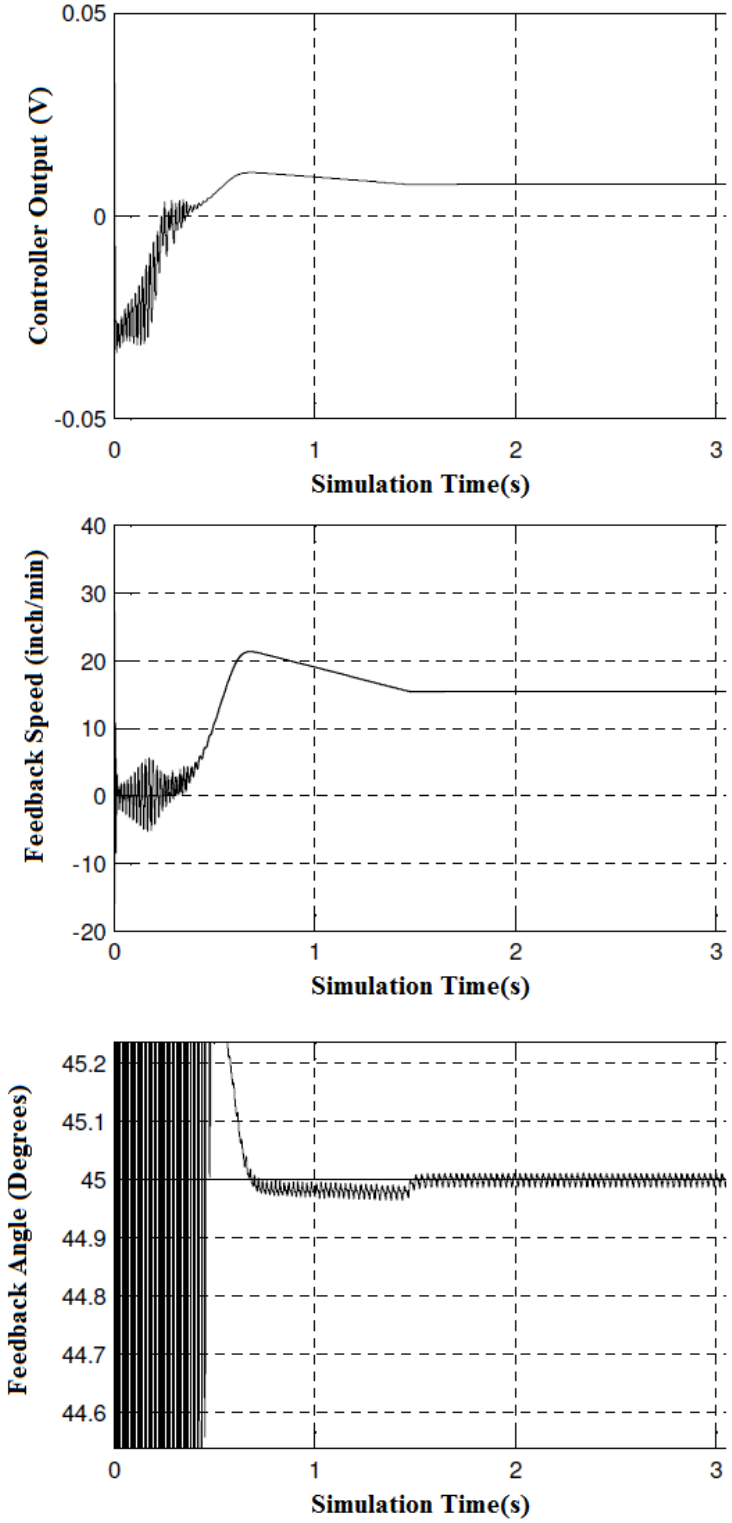

Figure 7.2: Simulation results of the angle control

7.2 Tension Control

Once the fiber orientation is achieved by controlling the winding angle, the next task is to control the winding tension in the fiber. The importance of the tension control is described in section 4.2.2 of chapter 4.

7.2.1 Mathematical Model

The motor rotates the mandrel with a gear ratio 'gr', when actuated; the actuator presses the fiber with a force F_a , which can be controlled by voltage V. The force F, results in generating a negative force opposing the motion of the fiber (viz.)μF_a. This force is the resisting force in the fiber-line. By this action of the actuator and the opposing motor pull, at the mandrel, a controllable tensile force in fiber is developed (see Figure 6.13)

When the actuator is not actuated, the tension in the system is steady, as there is no opposing force to that of the mandrel's motor. The scope of this design is to induce a controlled increase in the tension in fiber line by the actuator. For simplicity in understanding the change in tension due to the actuator would be referred as T (N), which is equivalent to $\mu\mu_0 \frac{N^2 I^2 A}{2g^2}$ (N).

7.2.1.1 System Feedback Model

The feedback is based on the power transmission and change in system's velocity, created due to the braking effect exerted by the actuator. When the actuator is activated, the load on the motor would increase. The increase in load would result in a change in the velocity of the system. To analyze the process, let the angular velocity of the motor be r_t , revolutions per minute and the power (output load of the motor) be p_t in watts, and t is the system time. Then the torque, $Tq_{motor\ (t)}$ in Newton-meters, generated by the motor due to load could be calculated by:

$$Tq_{motor(t)} = \frac{9.5493 p_t}{r_t} \qquad (7.3)$$

Since the mandrel is driven by the motor with a reduction gear and considering the gear ratio as "*gr*", the torque at the mandrel, $Tq_{mandrel(t)}$ in Newton-meters, can be expressed by:

$$Tq_{mandrel(t)} = \frac{9.5493\ gr\ p_t}{r_t} \tag{7.4}$$

If the radius of the mandrel is "R" meters, the tangential force, F_m, in Newton, generated at mandrel can be expressed as:

$$F_m = \frac{Tq_{mandrel}}{R} = \frac{9.5493\ gr\ p_t}{R\ r_t} \tag{7.5}$$

Now the tension in the system due to actuator will change the mandrel's pulling force F_m when the actuator is actuated. So the tension due to actuator, T, in Newton can be calculated by:

$$T = \frac{9.5493\ gr}{R}\left(\frac{p_t}{r_t} - \frac{p_{t0}}{r_{t0}}\right) \tag{7.6}$$

where t_o is the time at which the actuator is actuated, r_t is measured by an encoder at the motor and r_{t0} is measured by timing synchronization of the actuator actuation and the encoder output at that time. The above equation 7.6 is the feedback to the system.

Power output of the motor, p_t,, can be established in two ways. In the first approach utilizes the VFD output current and equivalent circuit values [50]; accordingly:

$$p_t = R_r \frac{1-S}{S}(I_S^2 - I_{S0}^2) - p_f - p_{stray} \tag{7.7}$$

where, R_r is rotor's resistance (Ω), S is the slip, I_s is the stator average RMS current(A), I_{s0} is the no load stator average RMS current(A), p_f is the power loss due to friction(W) and p_{stray} (W)is the stray power losses.

Realization of the above equation 7.7, is relatively very complicated and it increases the computational burden on PLC; moreover, it does not produce very accurate results.

The other approach for establishing the power is by curve fitting motor load's data. At any given frequency the motor RPM and motor loading would have a steady relationship. The relationship is not linear, but they fit well in a quadratic polynomial equation.

Table 7.1 tabulates the data as received from the motor manufacturer as a function of the RPM at 60 and 50 Hz, respectively, for load variation of 0 to 200% for the 0.5 HP 3 phase induction motor used in the setup. Since, the motor is going to run at a steady frequency in any given winding trial, the feedback polynomial equation can be modified for a given trial in concordance with the frequency.

Table 7.1: Motor load and speed data at 50 and 60Hz

Power in HP	Power in Watts	RPM at 60 Hz	RPM at 50 Hz
0.125	93.25	1785	1488
0.25	186.5	1773	1478
0.375	279.75	1760	1467
0.5	373	1745	1454
0.625	466.25	1730	1443
0.75	559.5	1713	1428
0.875	652.75	1690	1413
1	746	1671	1395

The following plots in Figure 7.3 and Figure 7.4, shows the fitting of the data in Table 7.1, at 50 Hz and 60 Hz respectively.

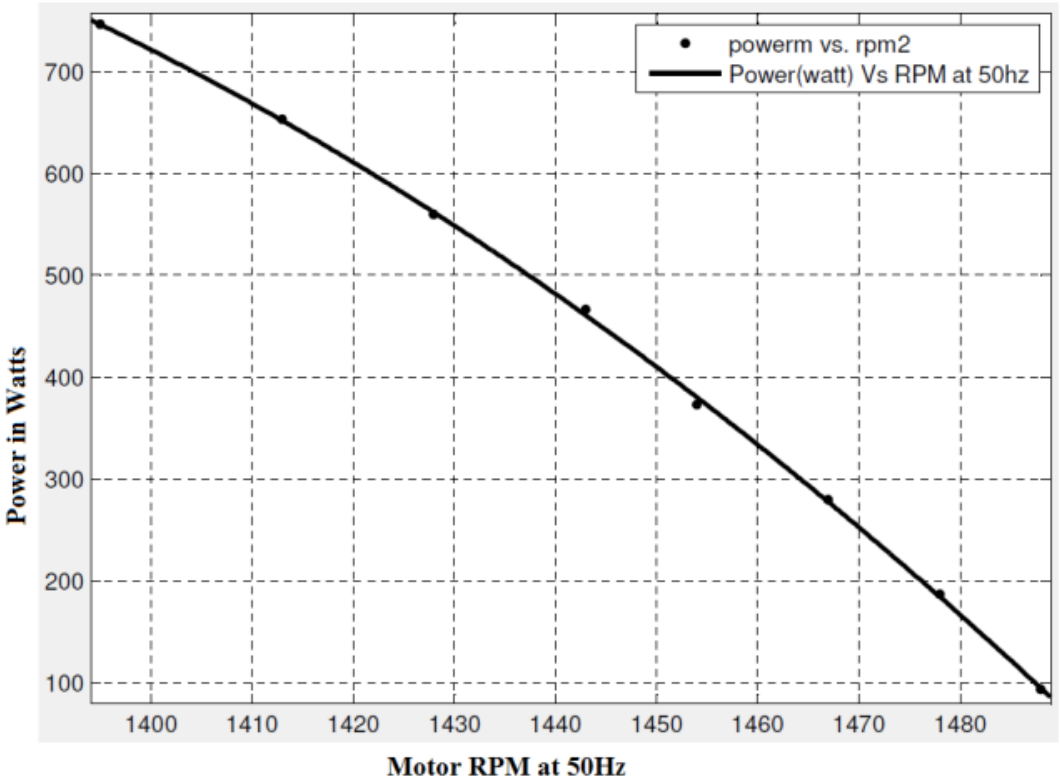

Figure 7.3: Motor load speed curve at 50Hz

As a result, the power model can be represented by the following quadratic equations, as a function motor's RPM for power values of 50 Hz and 60 Hz respectively:

$$p_t = -0.02352\, r_t^2 + 60.8 r_t - 3.83 \times 10^4 \tag{7.8}$$

$$p_t = -0.01772\, r_t^2 + 55.61 r_t - 4.269 \times 10^4 \tag{7.9}$$

The above equations; 7.8 and 7.9; provide the following statistical coefficients (with 99% confidence bounds): R^2=0.9996 (for the 50 Hz) and R^2=0.9992 (for the 60 Hz), respectively.

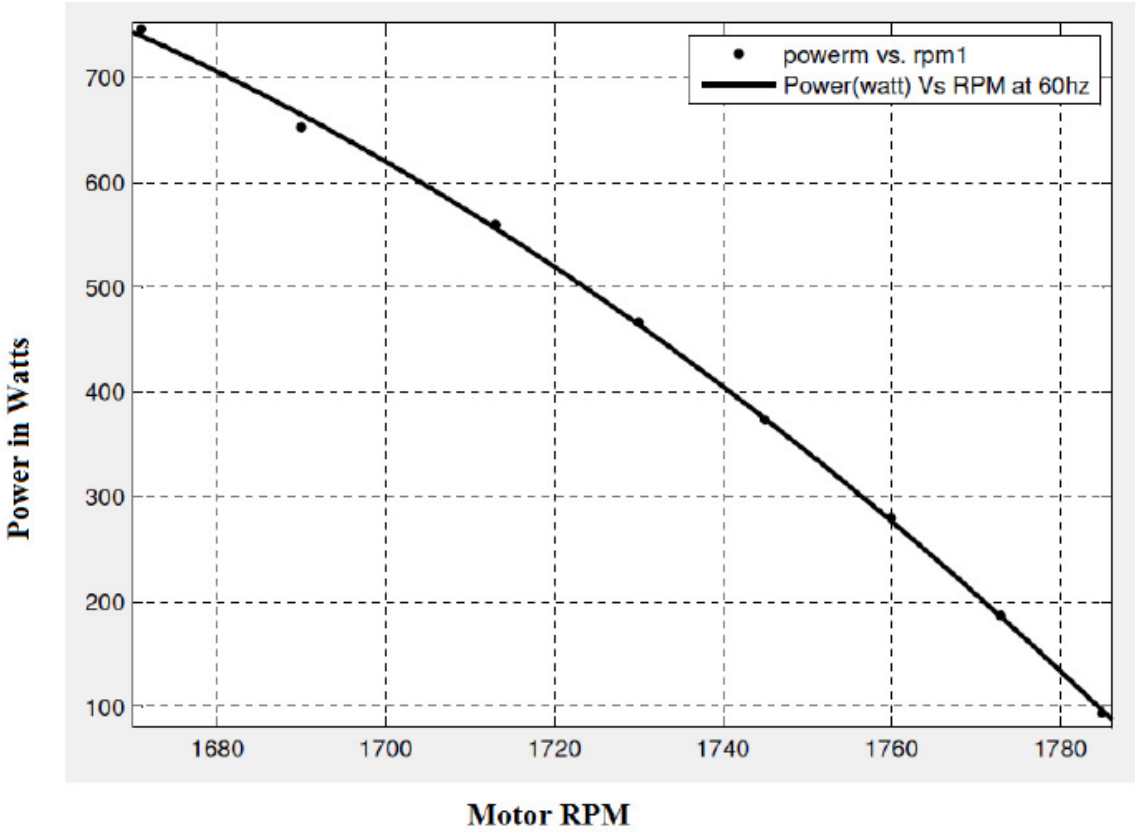

Figure 7.4: Motor load speed curve at 60Hz

The above equations 7.8 and 7.9; indicate that, the power could be estimated at each frequency and can be used in the feedback equation. With reference to equations 7.6, 7.8 and 7.9, the feedback equation can be expressed as:

$$T_{fb}(t) = \frac{9.5493gr}{R}\left(\left(\frac{ar_t^2+br_t+c}{r_t}\right) - \left(\frac{ar_{t0}^2+br_{t0}+c}{r_{t0}}\right)\right) \quad (7.10)$$

where, a, b and c are the coefficients in equations 7.8 and 7.9.

7.2.1.2 Machine Control Design

The mechanical equivalent of the system can be described as the following:

$$J\dot{r_t} + \frac{\mu}{Rgr}r_t = 0.41V^2 \quad (7.11)$$

J is the moment of inertia and r_t in, equation 7.11 is the change in mandrel RPM due to load increase by the actuator. The above equation is nonlinear, as the system is designed to control tension and the relationship of tension to RPM $r_t$is also a quadratic polynomial. As can be seen in Figure 7.8, the control of such a system by a PI or PID controller would be quite difficult. The only way, that the system could be controlled by a PI controller, is that it requires to be tuned online continuously. The values of the integral and proportional gain should be constantly updated. That can be done by gain scheduling [51].

To simplify the controller, a voltage controller is designed instead of a tension controller. The system equation of the controller would take the following form.

$$\dot{V} + V_{Fb} = V_o \tag{7.12}$$

where ;V_o is the actuator input voltage and V_{Fb} is the voltage feedback, using equation 7.19.

A PI controller is designed using the above system dynamics as in equation 7.12. Error dynamics involved in the equation is:

$$\ddot{e} + (1 + K_P)\dot{e} + K_i e = 0 \tag{7.13}$$

$$s^2 + (1 + K_P)s + K_i = 0 \tag{7.14}$$

Closed loop PI-based controller is designed, as shown in the following block diagram, in Figure 7.5.

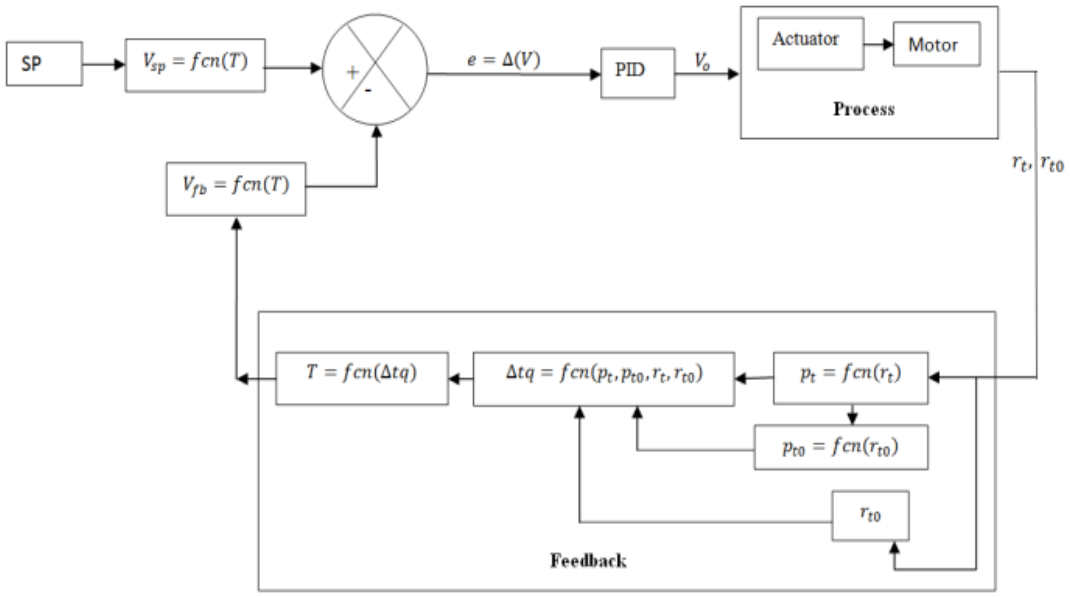

Figure 7.5: Closed loop block diagram

Since the variation of the Tension with Voltage is a known nonlinear relationship, the PI controller is designed as a voltage controller, which would indirectly control the tension. The variation of the actuator force to the actuator input voltage varies as in equation 6.5, as per vendor's data sheet (the same was also confirmed by fitting the data in the simulation). The graph in Figure 7.6, shows the fitting of the simulation curve.

As stated earlier, the force generated by the actuator in the direction, opposite to the fiber line of motion is represented by μF_a, where μ is the coefficient of friction. The voltage V, in terms of F_a can be expressed by equation 7.16 in concordance with equations 7.15 and 6.5.

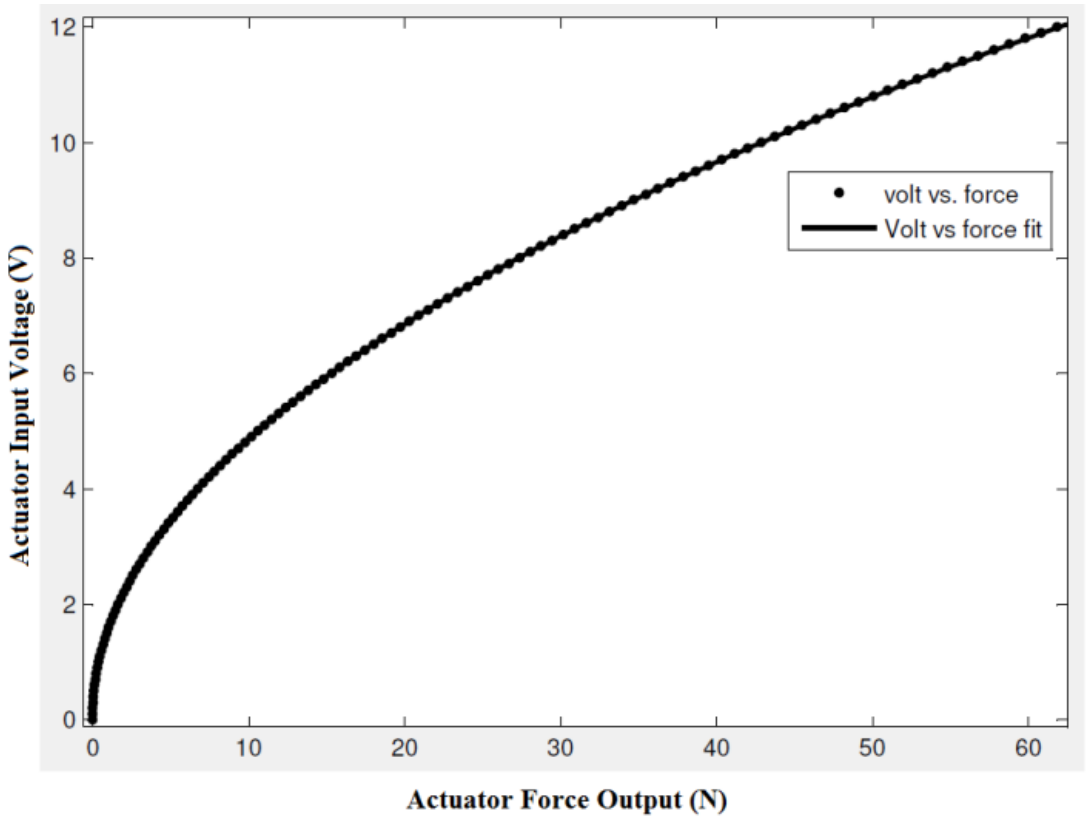

Figure 7.6: Voltage-force relationship

By fitting the curve in Figure 7.6 equation 7.15 is achieved.

$$f(x) = 1.555 * x^{\frac{1}{2}} \tag{7.15}$$

The above equations provide the following statistical coefficient (with 99% confidence bounds); R^2=1

$$V = 1.555\sqrt{\frac{F_a}{\mu}} \tag{7.16}$$

The error "e" in the system can be expressed by the following equation considering a voltage controller:

$$e = V_{sp} - V_{fb} \tag{7.17}$$

$$V_{sp} = 1.555\sqrt{\frac{SP}{\mu}} \tag{7.18}$$

$$V_{fb}(t) = 1.555\sqrt{\frac{T_{fb}(t)}{\mu}} \tag{7.19}$$

where; SP is the tension setpoint and $T_{fb}(t)$ is the tension feedback of the system.

The input to the actuator from the controller is voltage. Since the actuator is nonlinear, it is not possible for the PI controller to control the voltage input to the actuator by the tension-feedback directly. Therefore, it is necessary to condition the input or the output of the PI. In this case the input set point and feedback are conditioned by equations 7.18 and 7.19. In other words, the error of tension is converted to voltage demand, required to be fed to the actuator. Hence the controller works as a voltage controller instead of a tension controller but indirectly controls the tension.

After conditioning, both the input and the output would be in voltages form. This preconditioning removes the direct involvement of the nonlinearity of Tension with voltage via the PI. Designating the output of the PI controller as $V_0(t)$, and the feedback tension as $T_{fb}(t)$, it could be expressed as:

$$T_{fb} = \mu 0.41 V_o^2(t) \quad (7.20)$$

Using equation 7.19 $V_{fb}(t)$ can be expressed as:

$$V_{fb}(t) = 1.555\sqrt{\frac{\mu 0.41 V_0^2(t)}{\mu}} = 0.996 V_o(t) \quad (7.21)$$

So the error, *e,* can also be expressed as:

$$e = V_{sp} - V_o \quad (7.22)$$

Equation 7.22 is linear in terms of actuator input voltage. In a way, the PI acts as a voltage controller, but in this process it also indirectly reduces the error in the tension, since according to equation 7.19, $V_{fb}$is a function of(T_{fb}). So, as the value of $(V_{sp} - V_{fb})$ approaches zero, the resulting value of $(SP - T_{fb})$ would also approach zero. The same can be achieved if the output of the PI is squared and the PI becomes a direct tension controller; however, in that case the output of the PI has to be limited to the root of the maximum rated voltage of the actuator. This entire process could be referred as virtual linearization and this method is only possible for a known nonlinear process.

The PI equation for control would be presented as:

$$u(t) = k_p e(t) + k_i \int_0^t (e(\tau) d\tau) \tag{7.23}$$

7.2.2 Simulation

A PI controller is therefore designed accordingly. The values of proportional gain k_p and integral gain k_i are determined experimentally. Figure 7.7, shows the simulation result for the set point of tension, with variable step changes from 0 to 20N, 20N to 10N, 10N to 5N, with K_p as 0.1 and K_i as 5. The PI controller exhibits great controllability and there is literally no overshoots and the time to steady state is 0.5 second to 1 second. In this case, the controller starts action at 1.5 seconds and reaches steady state at approximately 2.0 seconds.

The Figure 7.8, shows that, the PI controller produces a very high overshoot; if the error in voltage instead of the error in tension is not preconditioned (i.e. the virtual linearization is not used). The overshot is nearly 50% the feedback (i.e., 29N) for the set point of 20N. This high overshoot and oscillation is not good for the system. The PI controller needs to be linearized to handle the transient state better.

The performance of the PI controller depends on the linearization and tuning of the system. The linearization by the above method would be possible only if the nonlinearity is known and is consistent.

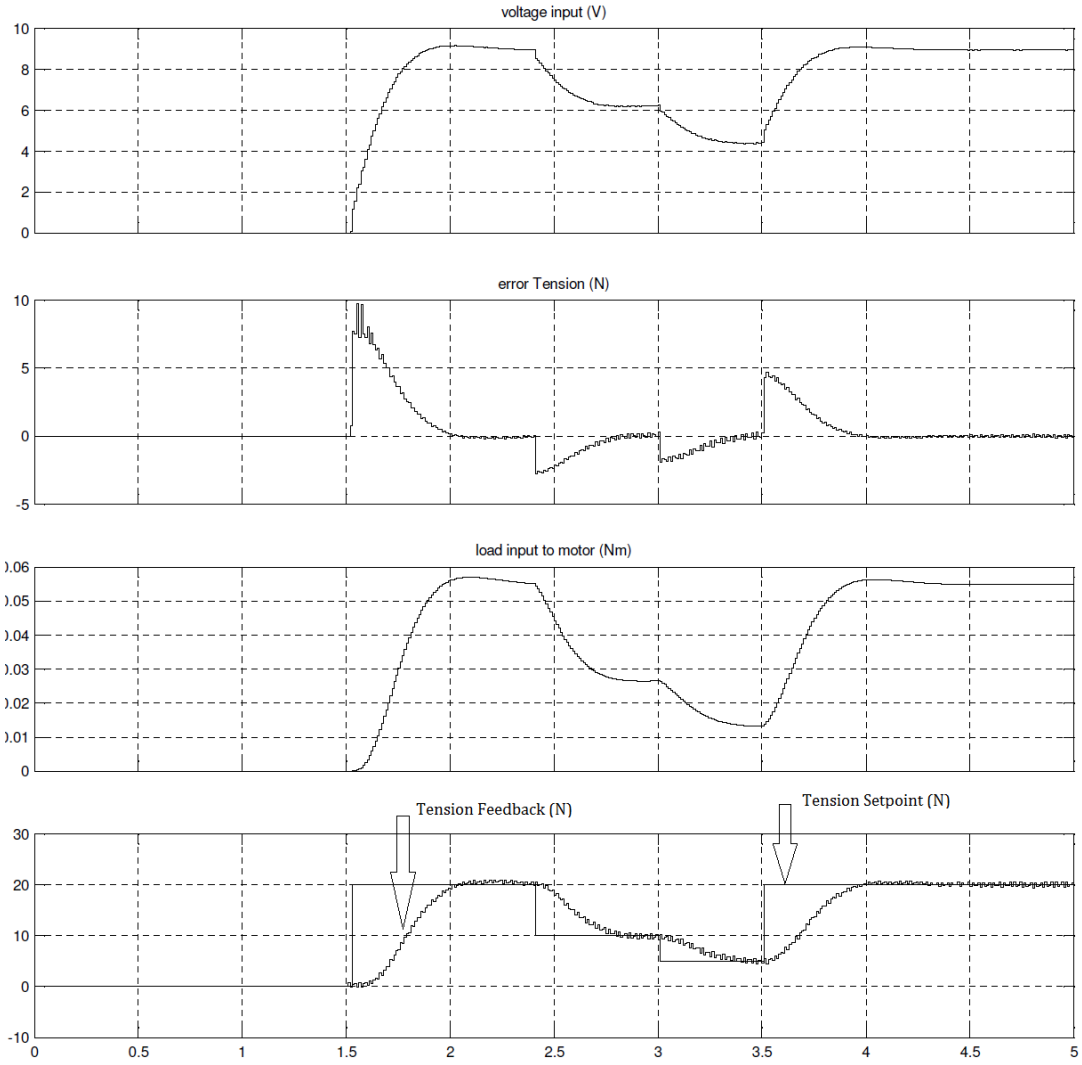

Figure 7.7: Tension feedback for a set point of a varying set point of 20 N, 10N, 5N using PI and virtual linearization

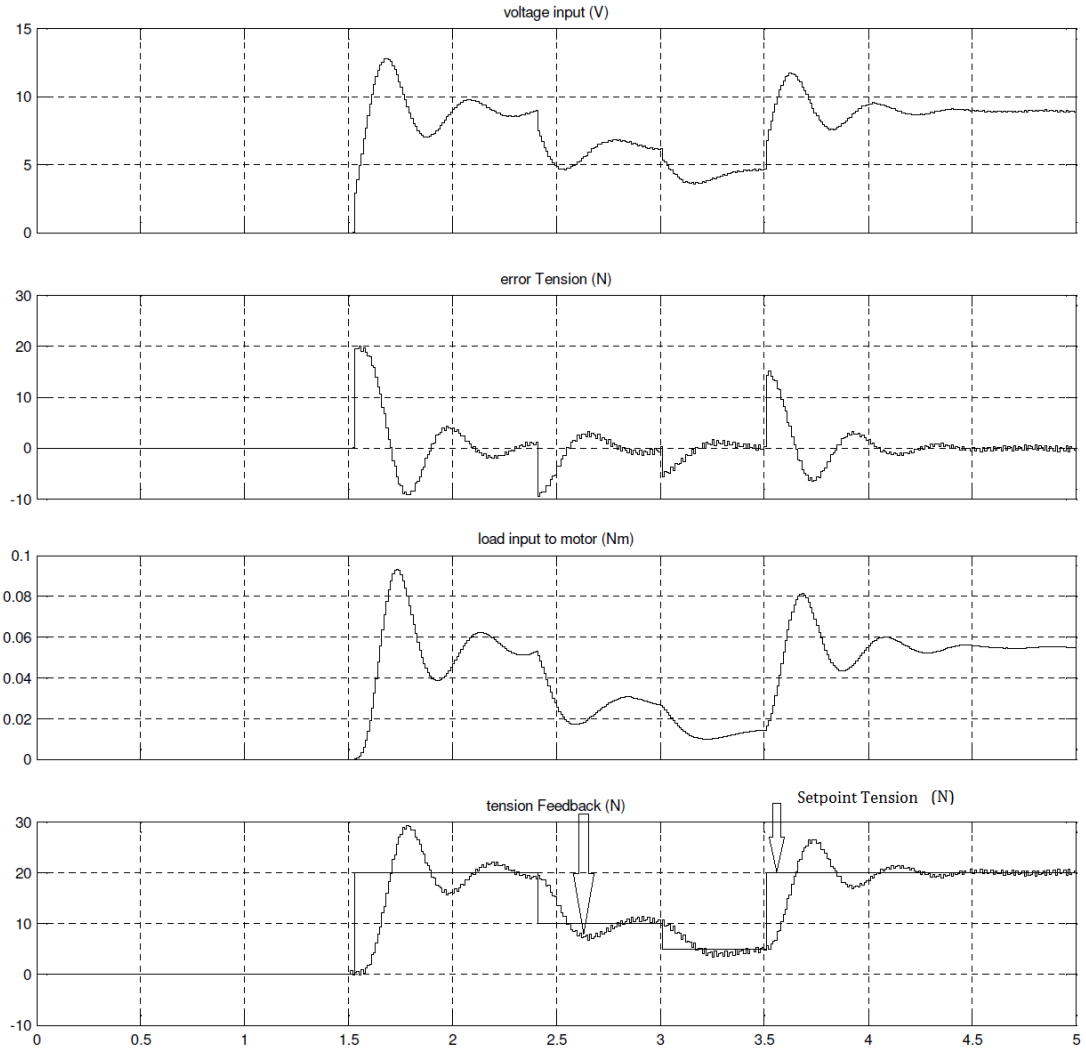

Figure 7.8: Tension feedback for a varying set point of 20 N, 10N, 5N using the designed PI controller as a tension controller, without error preconditioning.

If the nonlinearity is uncertain in such systems, then the best possible controller would be that based on a Fuzzy Logic Controller (FLC). The design and simulation of a proposed FLC for the scenario is described in chapter 10.

Chapter 8

PLC LOGIC AND FLOWCHART

In this chapter the logic, as implemented in the PLC is discussed and a flowchart representation of the logic is given.

8.1 PLC Logic

Before putting the PLC to run mode, the user has to enter the desired start point (Range 0-1016 mm), end point (Range 0-1016 mm), number of cycles, initial carrier speed (0-160 mm/s), mandrel diameter (in mm), tension setpoint (range 0 to 8.8 N) and timing cycle value (in one tenth of seconds). The timing cycle time is the time for which, the fiber positioner, on the horizontal slider would stop at end points in each direction.

After the PLC is put into run mode, the fiber positioner, starts moving backwards, until it touches the start limit switch, with the user entered speed value. After getting the signal from the start limit switch, the positioner moves to the start point, as specified by the user. At this point, the positioner waits till it receives the input signal from the user through a manual switch. Once the manual switch is turned on, the mandrel motor has to be started to start the winding. The speed signal from the mandrel speed encoder acts as a setpoint for the winding angle control, based on the equation 7.1.The final calculated setpoint would be referred to as set variable (SV), for this loop. The PID controller gives the output to the servomotor to control for the speed of the positioner. The process variable (PV) in this loop is the speed of the positioner. PV is internally calculated by the PLC through timers and position values. The SV also updates the bias (the concept of bias is detailed in section 9.3 of chapter 9), using the equation 9.5. The first term of the product, in equation 9.5, is SV. The loop can be put to auto or manual mode any time during the operation and if the loop is in auto mode, the positioner automatically stops when the mandrel motor is switched off. Otherwise it has to be stopped manually, using the machine switch.

The direction of the positioner is calculated by the PLC, based on the position feedback from the motor control drive and the user input values. At the point where the positioner changes direction, there is an adjustable timer to control the wait time of the positioner. This timing cycle can be used to modify or tune the winding circuit and pattern ratio.

Anytime during the operation, after the machine switch is turned on, tension control can be taken in auto or manual mode. In manual mode the user entered value of tension S.V is converted to voltage demand and output is feed to the actuator. In auto mode the mandrel speed change, acts as the PV for the system as calculated by the equation7.10, in section 7.2.1 of chapter 7.

When, the number of cycles are completed the machine stops automatically. The next run of PLC resets, the number of cycle counter counts for the next cycle. The PLC Ladder program is given in Appendix A.3

8.2 Flowchart

The flowchart of the logic, as implemented in the PLC, is illustrated in Figures 8.1, 8.2, 8.3 and 8.4. All the figures are in continuation. In Figure 8.1, the user feeds the desired start point, end point, number of cycles, initial carrier speed, mandrel diameter and the timing cycle value. The initialization of positioner movement is also done in this figure.

The position initialization is finalized in Figure 8.2. In this section of the flowchart, the logic sets the direction of the positioner. Figure 8.3, shows the section of the flowchart where, the PV and the SV of the PID loop, for winding angle control is configured.

Configuration of the fiber tension control is illustrated in Figure 8.4. This section of the flowchart, also deals with the adjustment of the timing cycle, TA. The logic nesting and flowchart termination is also exhibited in this section. The bias adjustment part is not shown in the flowcharts, as it is an internal operation of the PID loop.

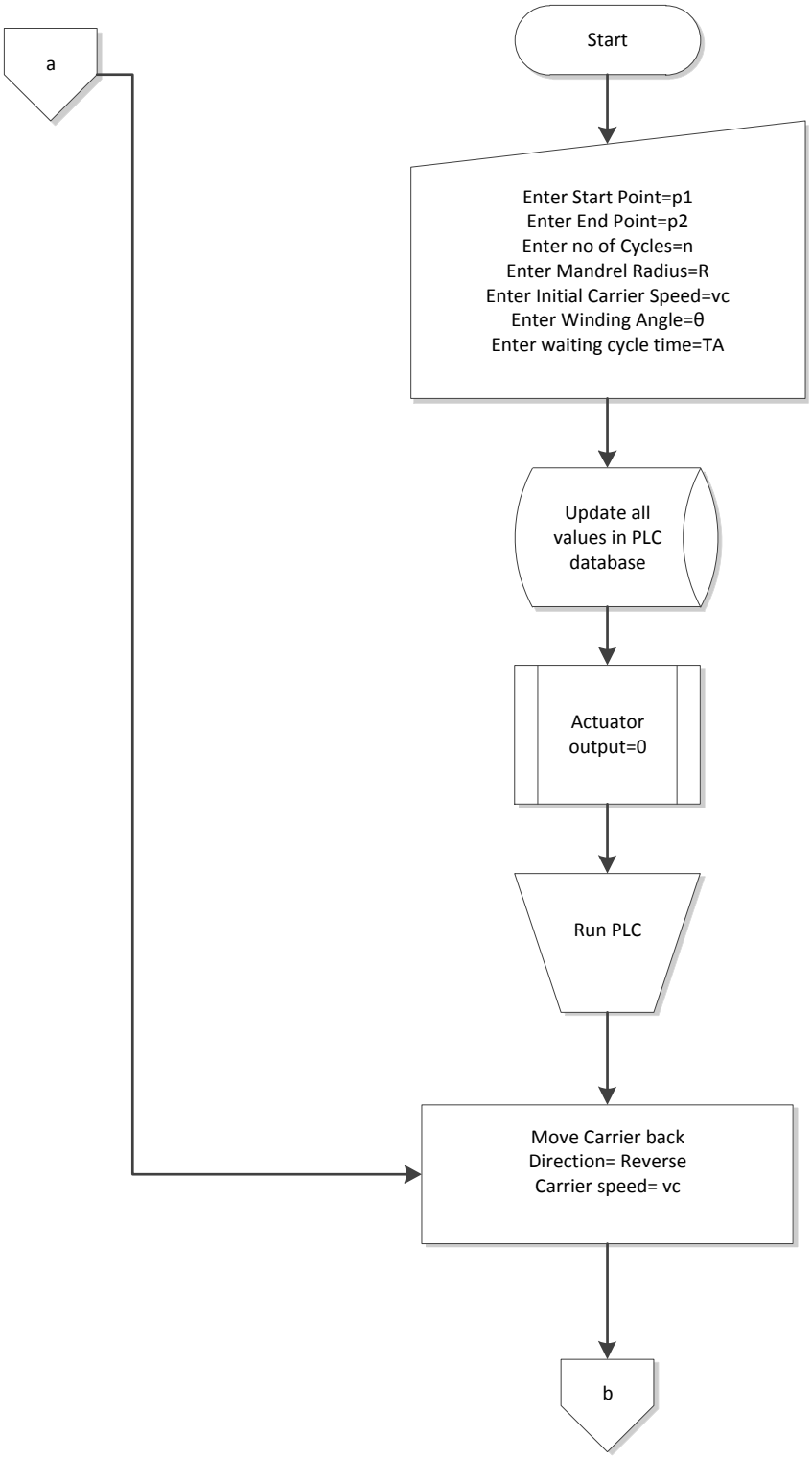

Figure 8.1: Flowchart of the logic implemented in the PLC

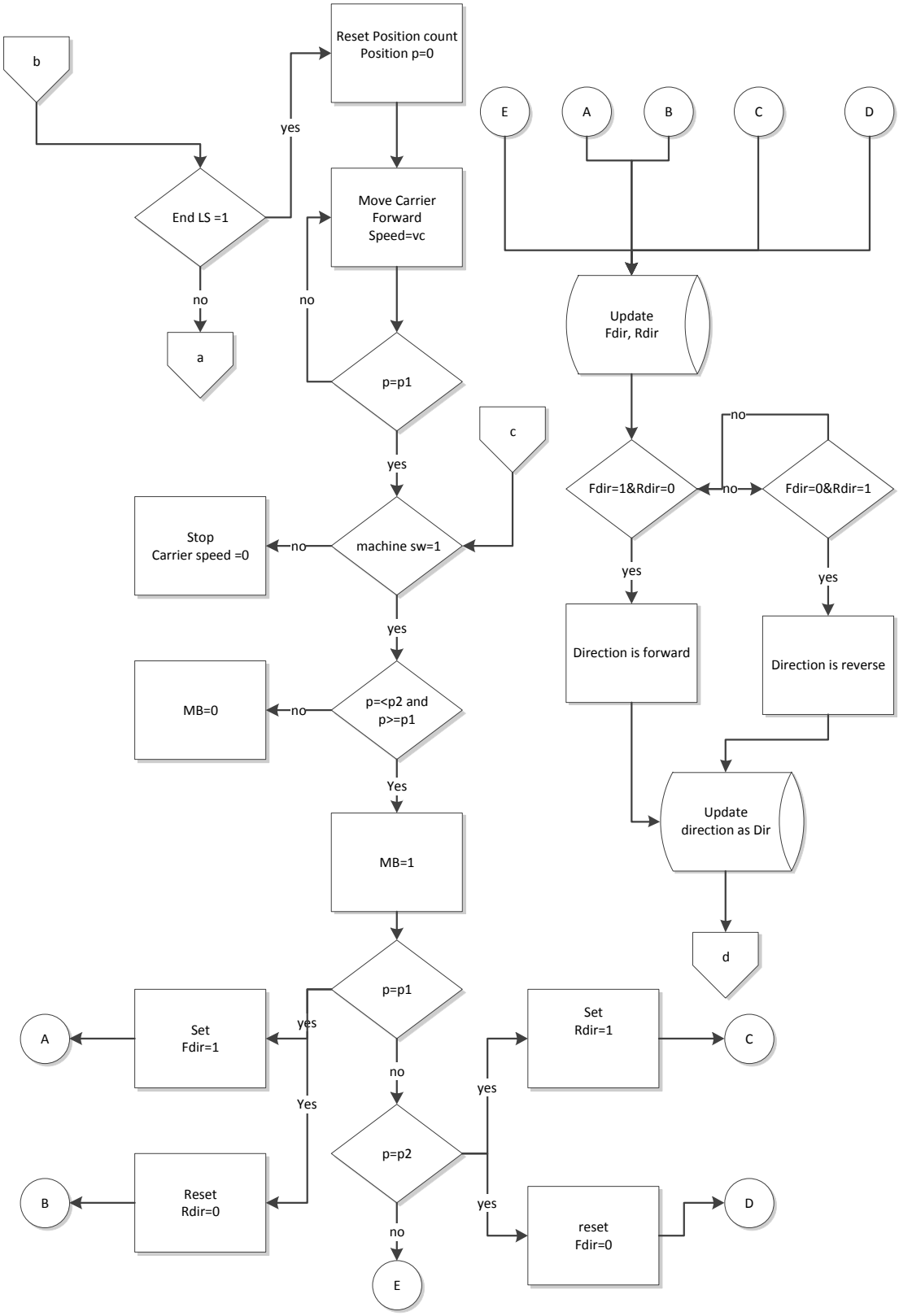

Figure 8.2: Flowchart of the logic implemented in the PLC (Continued).

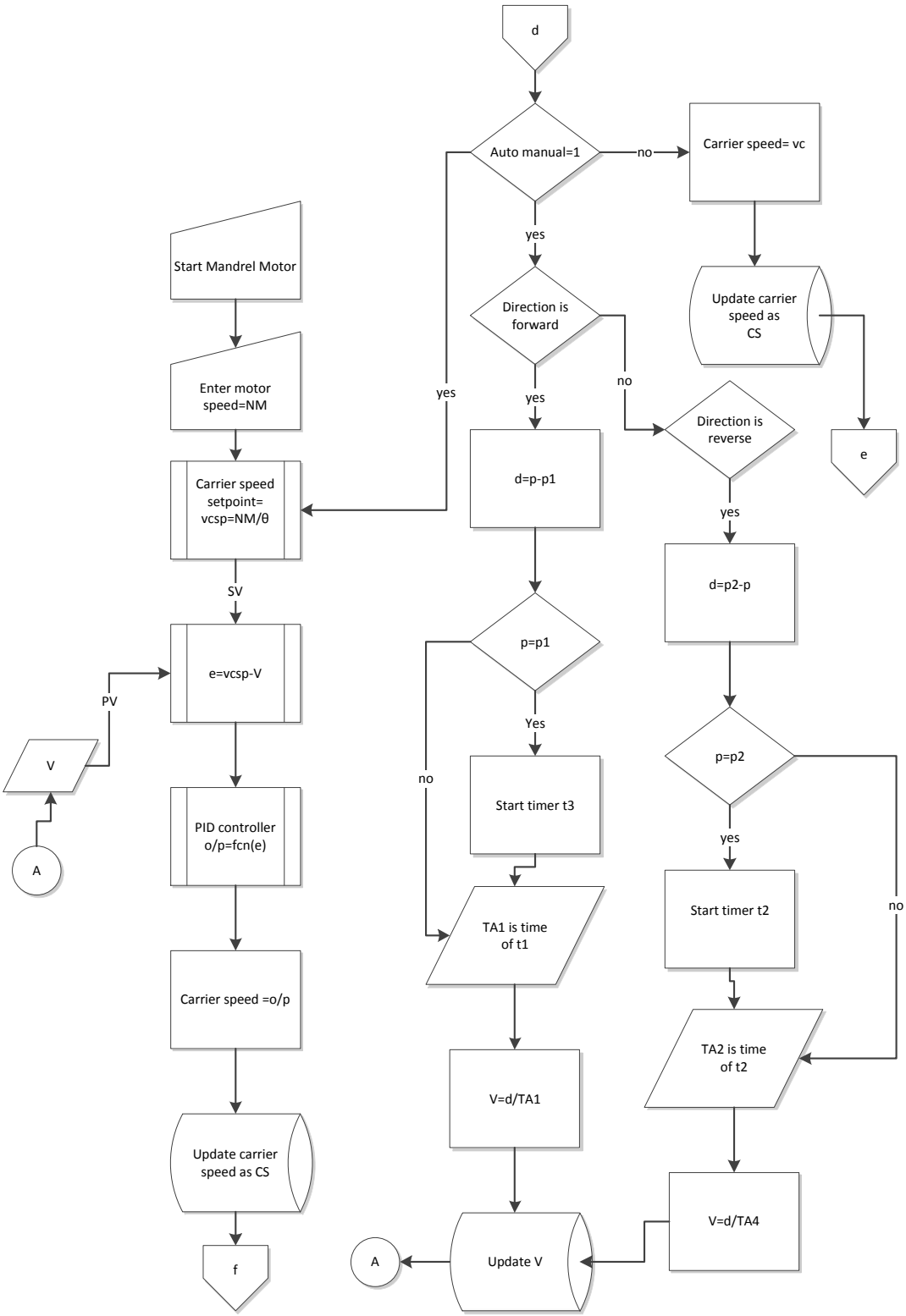

Figure 8.3: Flowchart of the logic implemented in the PLC (Continued).

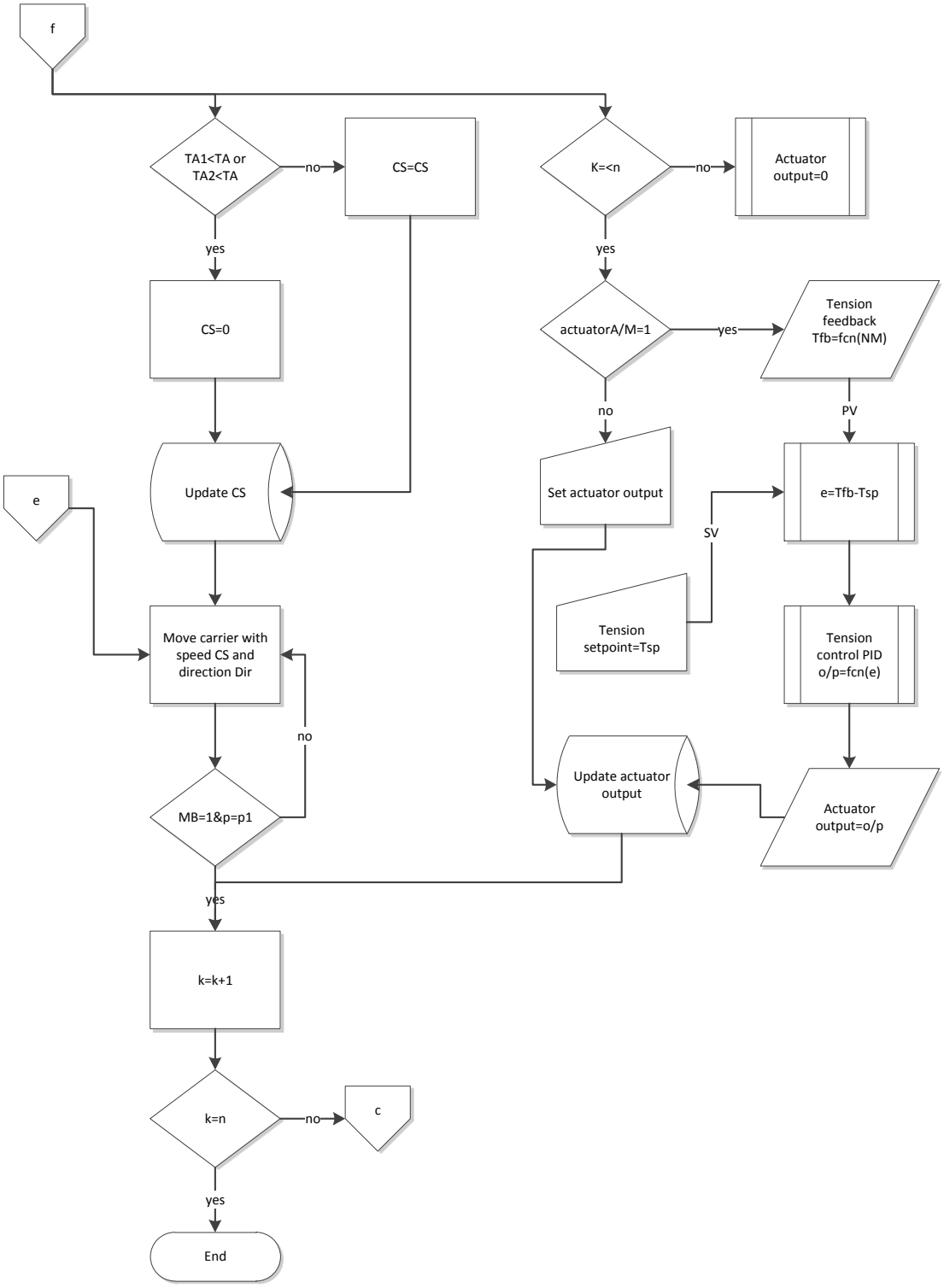

Figure 8.4: Flowchart of the logic implemented in the PLC (Continued).

Chapter 9

DEVELOPED EXPERIMENTAL SETUP AND RESULTS

In this chapter the online experimental results of tension control and angle control, in the prototype are listed. A novel concept of bias adjustment for practical implementation of the angle control is introduced to deal with the known disturbance in the system.

9.1 Tension Control

For the tension control, the experimental data is collected from the real setup and is fit in to a curve. The curve suggests the relationship of tension to voltage as:

$$V = 8.518 * \sqrt{T} \tag{9.1}$$

where, V is the actuator input voltage in volts and T is the system tension in lbf. The 0 to 12 volts to the actuator is 0 to 4095 counts in the PLC. Figure 9.1, shows the actual data plotting of the actuator tension as measured by a spring balance.

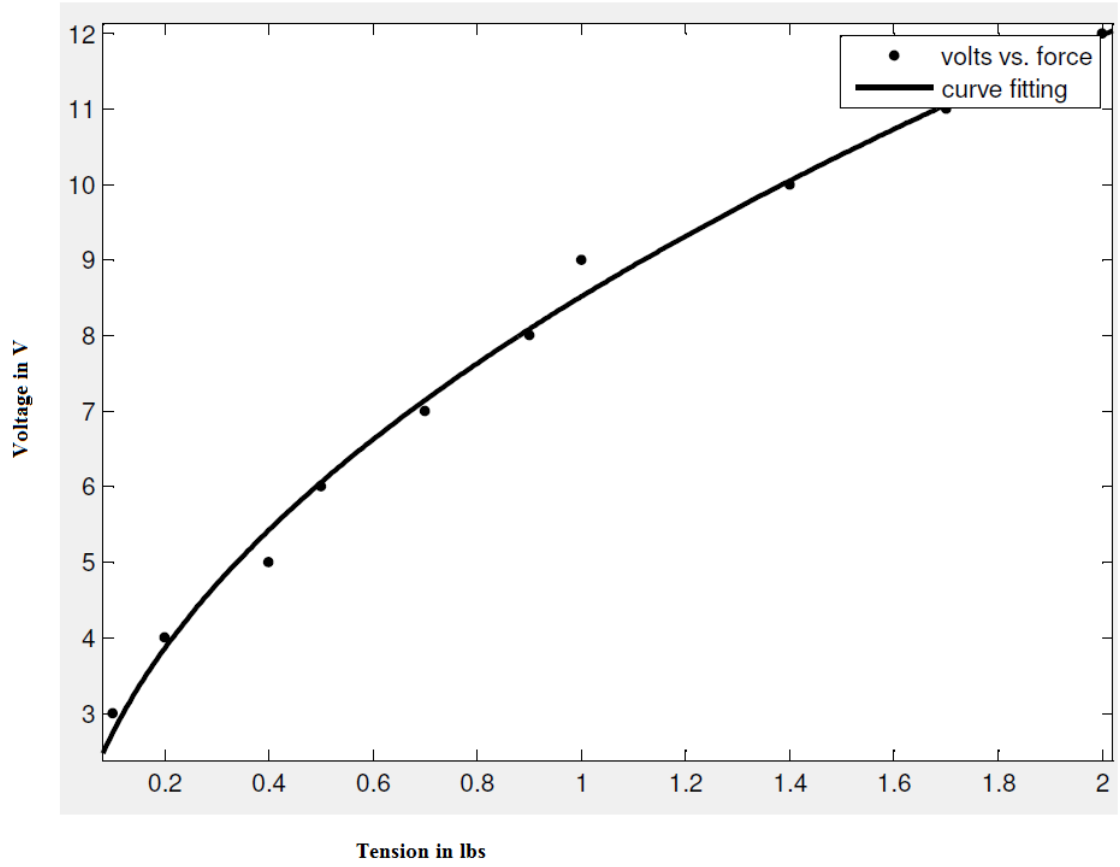

Figure 9.1: The measured Actuator force volt relationship

Table 9.1: Force and voltage data

Force (lbs)	0	0	0.1	0.2	0.4	0.5	0.7	0.9	1	1.4	1.7	2
Volts (V)	1	2	3	4	5	6	7	8	9	10	11	12

Figure 9.2, shows the response of the actuator over a step change in setpoints. The setpoints of 0 lbf to 1lbf is given in incremental step of 0.1lbf. The Figure 9.2, follows the pattern in Figure 9.1 and Figure 7.6, in chapter 7. Figure 9.3, shows the response of the voltage demand, for changing tension setpoint, with variation of 30 percent interval, for the maximum range of 0 to 2lbf. This Figure matches the inverse pattern of Figure 6.17, (i.e. simulated actuator response to a step change of input voltage from; 0V to 12V and

12V to 0V) in chapter 6. Figure 6.17; in chapter 6 is relationship of voltage to force and in the prototype force to volt relationship is used.

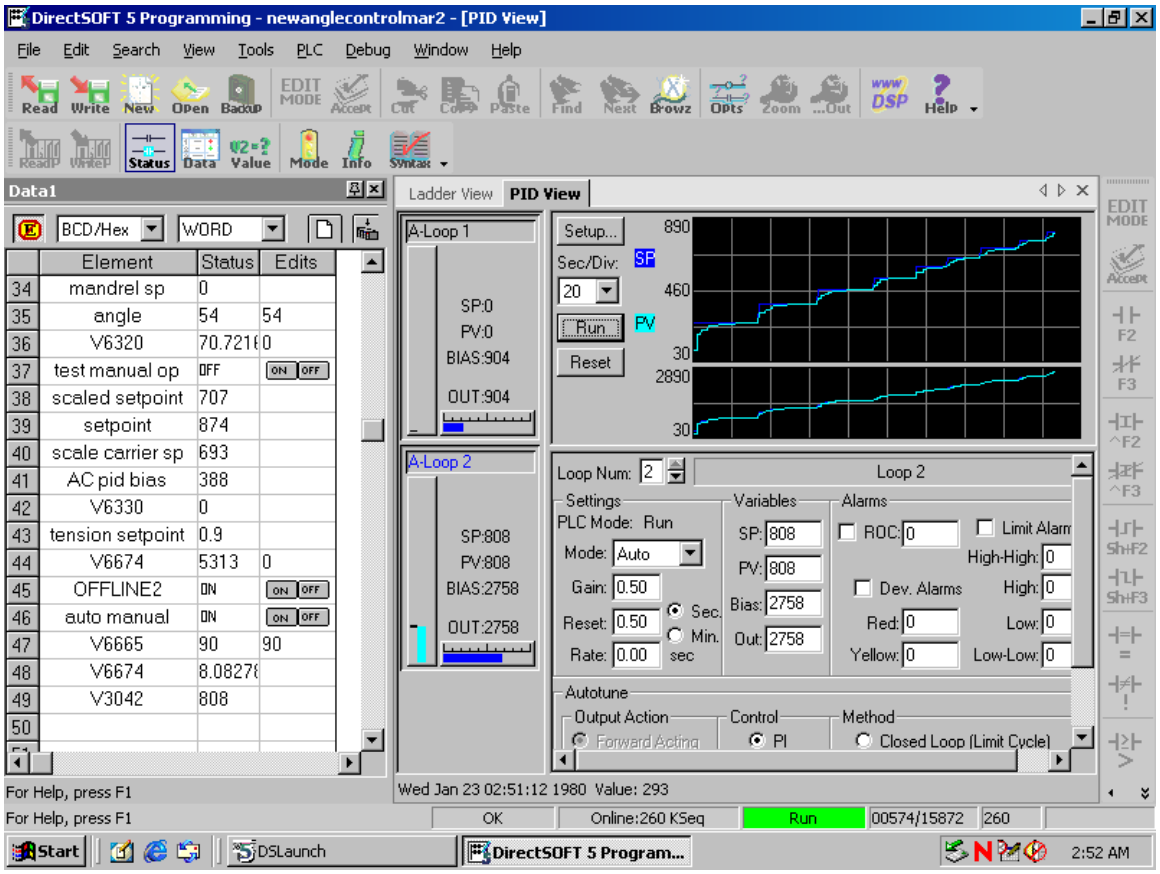

Figure 9.2: Actuator step response.

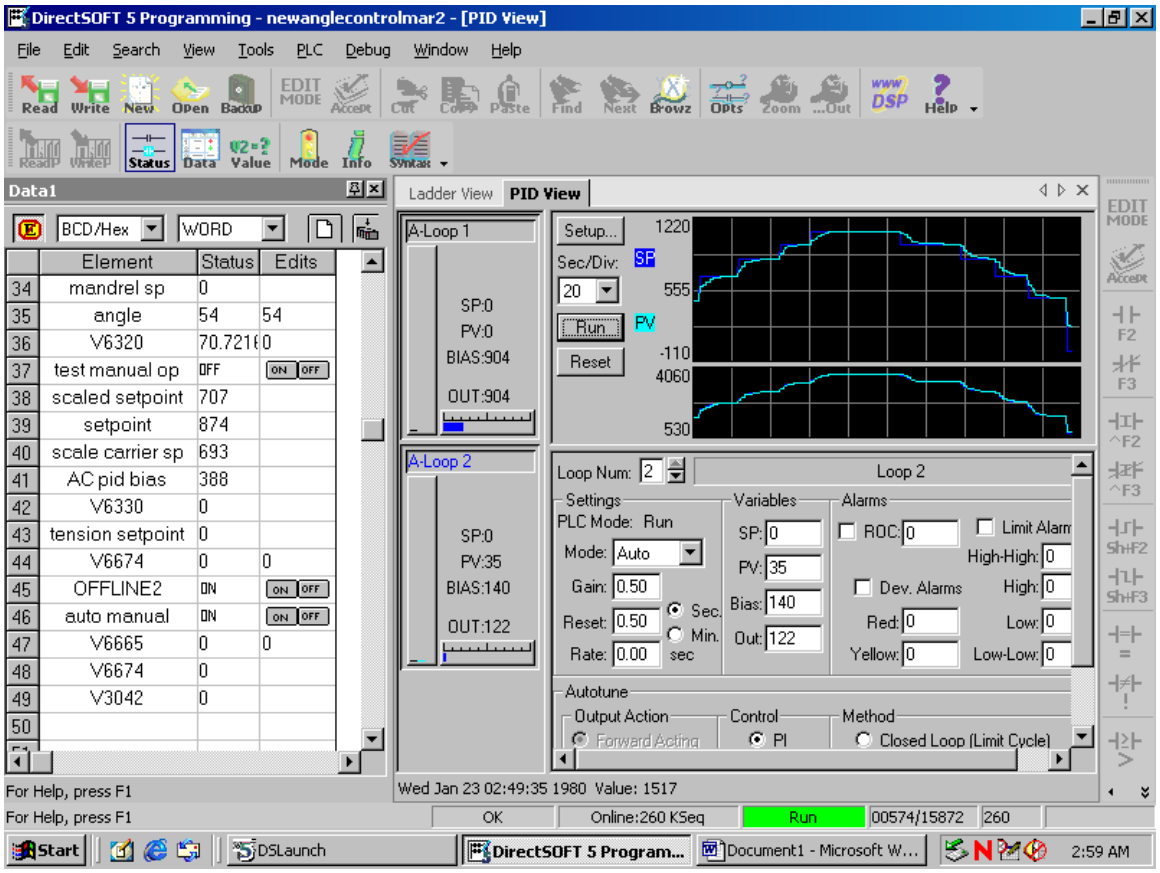

Figure 9.3: Actuator response over the entire range of 0 to 12 volts response.

On the prototype machine, the significant tension feedback could not be retrieved. The torque handling capacity of the machine increases with the high gear ratio and variation in mandrel speed becomes negligible with change in winding tension. Therefore the feedback as simulated in chapter 7 could not be realized on the hardware setup. The actuator response in voltage is non linear with the change in tension hence the set point pre-calculates the nonlinearity and varies the voltage accordingly to achieve the desired tension. Hence the virtual linearization has been achieved on a nonlinear system.

The response of the actuator is achieved by converting the tension demand in terms of voltage demand, as mentioned in chapter 7. The resolution of the system is up to 2 decimal points.

9.2 Angle Control

The angle control is done by controlling the speed of the horizontal slide with respect to the equation 4.1 in chapter 4. A maximum angle of 89^o and minimum of 33^o is possible with a 2 inch diameter pipe. The mandrel speed is the reference for the closed loop PID control. The Set-point of the loop is calculated by equation 9.2

$$V_{c_{ref}} = N_m \, \pi \, \frac{D}{60 \tan \alpha} \tag{9.2}$$

where $V_{c_{ref}}$ is the carrier linear velocity setpoint in mm/s, D is mandrel diameter in mm, N_m is the mandrel RPM and α is the user entered winding angle in degrees. Conventionally the speed control of the horizontal carrier is done by CNC machines. Numerical control gives higher accuracy. Even a slight variation in the speed would change the winding angle significantly. When the PID controller is used, at the beginning and at the end of every cycle the set point and the speed changes drastically. In normal PID configuration this change results in gradual increase of the output to achieve the desired speed. The normal PID configuration is not suitable for the angle control of a filament winding machine since PLC takes considerable period of time to minimize the error in the set point with some chances of overshoot, as can be seen in Figure 9.4.

In order to overcome this short coming, an adjustment in the bias of the PLC is done every time the positioner changes its direction. This activity basically creates a guiding action for the PLC and introduces a feed forward control to overcome the upcoming disturbances due to change in the direction and wait time at each change.

The bias is adjusted in accordance with the mandrel rotational speed using the above formulae and the output range. The bias is the combination of the integral and the initial output. The calculation of the bias is shown in the following equations 9.3 and 9.4.

$$Bx = K_i \, e_n + \, Bx_{n-1} \tag{9.3}$$

$$O_n = K_p\, e_n + K_d(PV_n - PV_{n-1}) + Bx_n \tag{9.4}$$

where Bx is the bias, O_n is the controller output at n^{th} controller step, K_p, K_i, K_d are proportional, integral and derivative gain respectively, e_n is the error at n^{th} controller step and PV is the process variable. In the winding process the set point change occurs twice in every cycle, and the set point goes down to zero. To stabilize the controller, the bias is frozen at the start of every change in the direction.

All these activities ensure that the controller takes minimum time to reach set point in each cycle. Figure 9.4, shows the response of a not adjusted bias controller and the Figure 9.5, shows the response when the bias is adjusted

The controller is programmed in such a way that at every change in direction of servomotor, the speed of the carrier is reduced to zero for a configurable time in order to ensure proper winding at the edges. The bias is reset to the required values as calculated by the equation 9.5, every time the direction changes. This aspect has been incorporated to ensure that the PID controller output consistently starts from the same value in the beginning of each cycle. Otherwise the output keeps gradually increasing for every cycle when a major setpoint change occurs (beginning of new direction), by the virtue of equation 9.3 and equation 9.4.

$$\mathrm{Bx} = \left(\mathrm{N_m}\, \pi \frac{\mathrm{D}}{60 \tan \alpha} \right) * \left(\frac{2045}{10(\mathrm{v_{max}} - \mathrm{v_{min}})} \right) \tag{9.5}$$

where the term, $\mathrm{v_{max}} - \mathrm{v_{min}}$ is the span of horizontal slides velocity in mm/sec. In the prototype this term is calculated to be 160 mm/s.

Figure 9.4; shows the response of the PID control without Bias control and Figure 9.5 shows the response with online bias tuning.

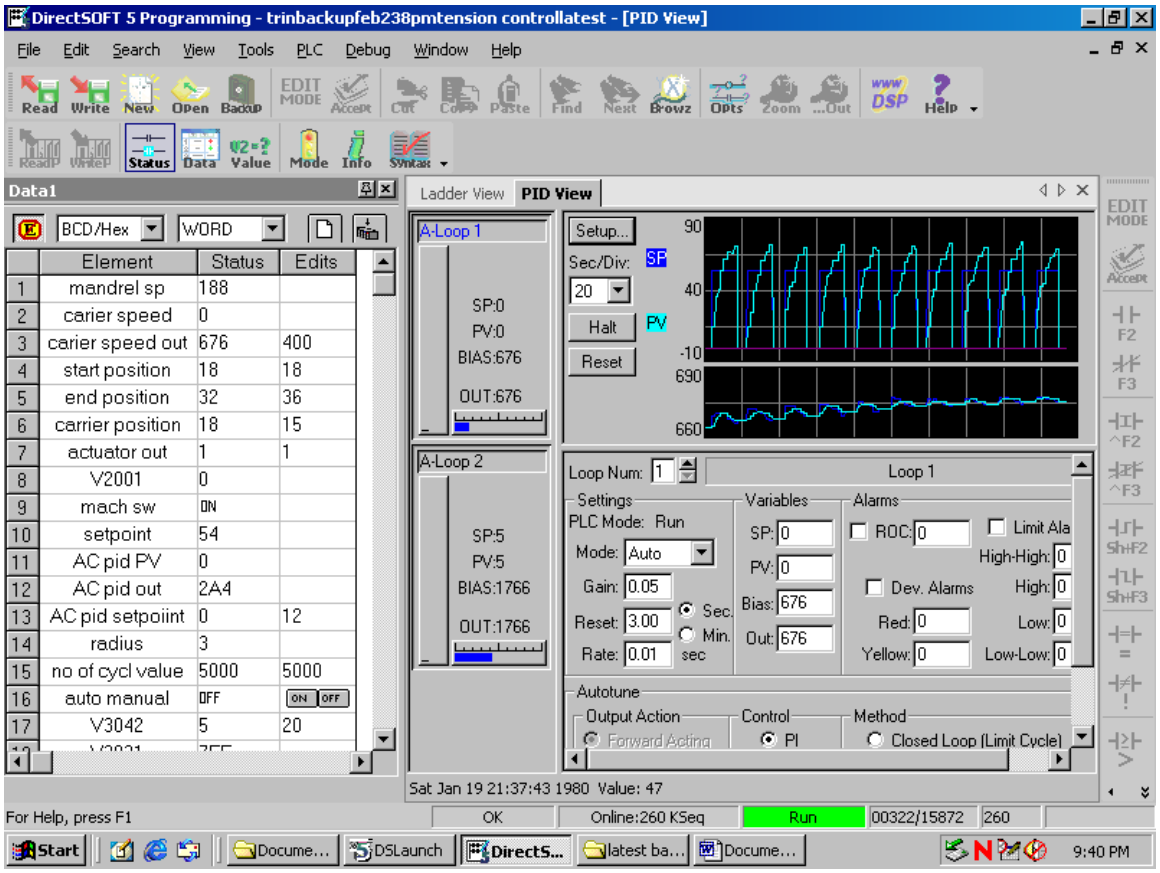

Figure 9.4: Angle control without bias guidance.

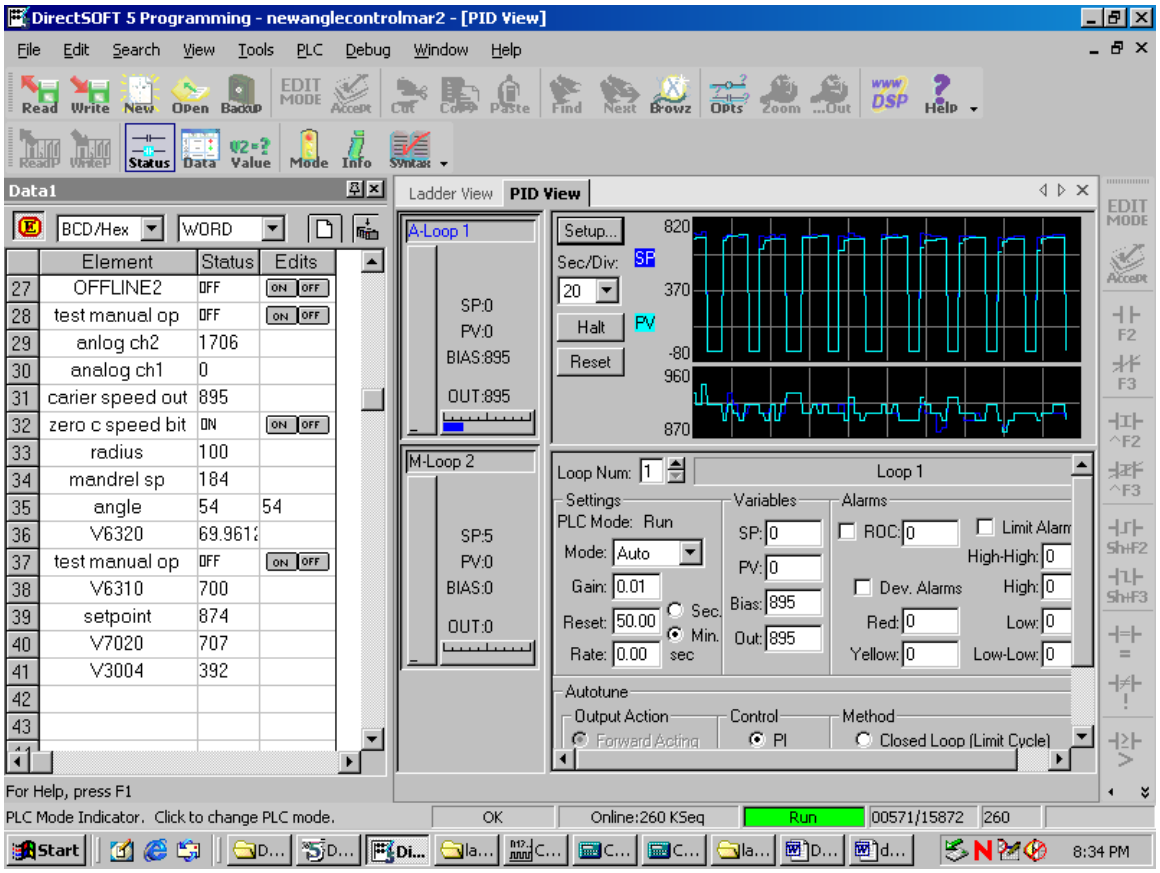

Figure 9.5: Angle control with bias control.

From the above Figures the following can be inferred

- A position control for the horizontal axis movement in filament winding controller can be achieved by implementation of a PID controller through PLC.
- But to make the control pattern consistent the bias of the controller has to be reset consistently during the start of forward and backward motion of each cycle. The response of the controller improves significantly by the implementation of this technique as conceived in the dissertation.

Chapter 10

A PROPOSED FUZZY TENSION CONTROLLER

The tension control as implemented in the prototype has been implemented as a voltage controller instead of tension controller using a concept of virtual linearization as discussed in section 7.2 in chapter 7. To make the control loop work directly, as tension control loop, a control algorithm which can handle system nonlinearity is required. With this thought process and as a part of current dissertation a Fuzzy Controller for the system has been conceived, designed and results are simulated.

10.1 Fuzzy Controller

The primary consideration that favors the fuzzy algorithm is that, such a system does not require linearization as required by PI controllers.

The Fuzzy controller designed herein is based on the Mamdani fuzzy inference system, with two inputs and one output. The two inputs are error e and change in error Δe, and output is incremental Voltage V.

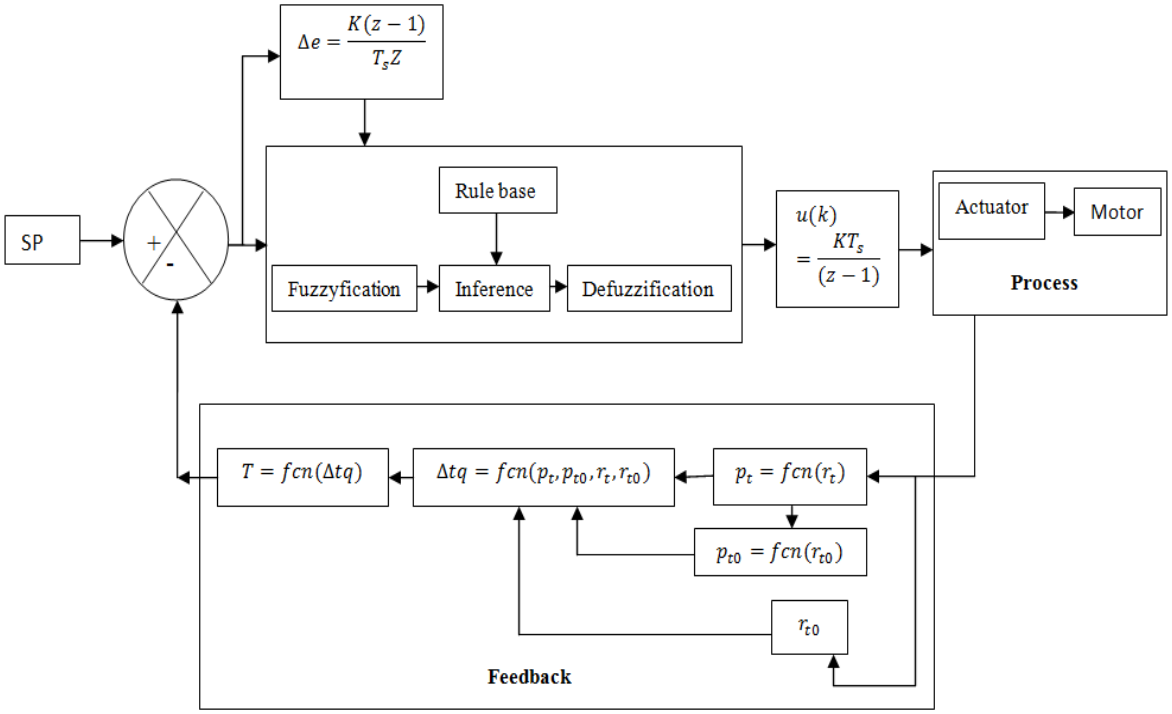

Figure 10.1: Schematic of the fuzzy controller

The controller implemented can be considered analogous to a classical PI controller [52] but it treats the system in a nonlinear way. The basic philosophy used is as follows:

$$u(k) = u(k-1) + \Delta u(k) \tag{10.1}$$

where u(k) is the current control action, u(k-1) is the previous control action, and $\Delta u(k)$ is the incremental control action, represented by:

$$\Delta u(k) = fn(e, \Delta e) \tag{10.2}$$

Similarly, for a PI controller one can state:

$$u(t) = K\left(e(t) + \frac{1}{T_i}\int e(t)dt\right) \tag{10.3}$$

$$u(k) = K\left(e(k) + \frac{1}{T_i}(e(k) + e(k-1) \ldots 0)\Delta T\right) \tag{10.4}$$

$$u(k-1) = K\left(e(k-1) + \frac{1}{T_i}(e(k-1) + e(k-2) \ldots)\Delta T\right) \tag{10.5}$$

Subtracting 10.5 from equation 10.4 we get

$$u(k) - u(k-1) = K\left(e(k) - e(k-1) + \frac{1}{T_i}\big(e(k)\big)\Delta T\right) \quad (10.6)$$

$$u(k) - u(k-1) = \Delta u(k) \quad (10.7)$$

So with reference to equation 10.6; the equation 10.7 can be rearranged as equation 10.8 where Δu(k) is the incremental control action.

$$\Delta u(k) = K\left\{(Change\ in\ error) - \frac{1}{T_i}\big(e(k)\big)\Delta T\right\} \quad (10.8)$$

Change in the error is the difference of two consecutive error samples and is analogous to the discrete derivative of the error "e" and can be expressed as:

$$\Delta e(z) = \frac{K(z-1)}{T_s Z} e(z) \quad (10.9)$$

where T_s is the sampling time and K is the change in error scaling coefficient; higher the value of K slower is the action, but lesser the over shoot.

Now considering, equation 10.1 it can be inferred that the current control action is the summation of all the incremental control action from k=0 to k. the same can be expressed by following equation, 10.10:

$$u(k) = \sum_0^k \Delta u(k) \quad (10.10)$$

Or in a discrete form, equation 10.10; can be expressed as the equation below considering *Δu(k)* being sampled every T_s sec.

$$u(z) = \frac{K_o T_s}{(z-1)} \Delta u(z) \quad (10.11)$$

where, k_o is the additive output scaling coefficient. Figure 10.1, shows the schematic of the FLC. The fuzzy model is designed such that it contains two dimensions' input and one dimension output. Inputs of the system are error and change in error. The output is incremental control action.

Table 10.1: Rule base for the fuzzy inference system.

		CHANGE IN ERROR				
	AND	NB	NS	Z	PS	PB
ERROR	NB	NB	NB	NS	Z	Z
	NS	NB	NS	NS	NS	Z
	Z	NB	NS	Z	PS	PB
	PS	NS	Z	PS	PS	PB
	PB	Z	PS	PS	PB	PB

Membership of the inputs and outputs are shown in Figures 10.2-10.4. The fuzzy linguistic terms of the inputs and output are used as negative big (NB), negative small (NS), zero (Z), positive small (PS) and positive big (PB). The discrete universe of input *e* is {-25,-12.5, 0, 12.5, 25}; for the input CE is {-1, -0.5, 0, 0.5, 1}, and for the output is {-12, 6, 0, 6, 12,}.

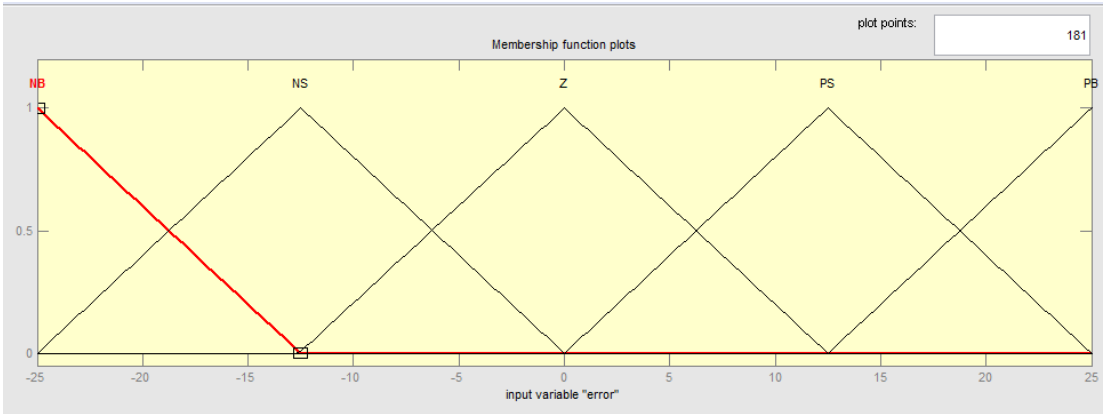

Figure 10.2: Membership function of error

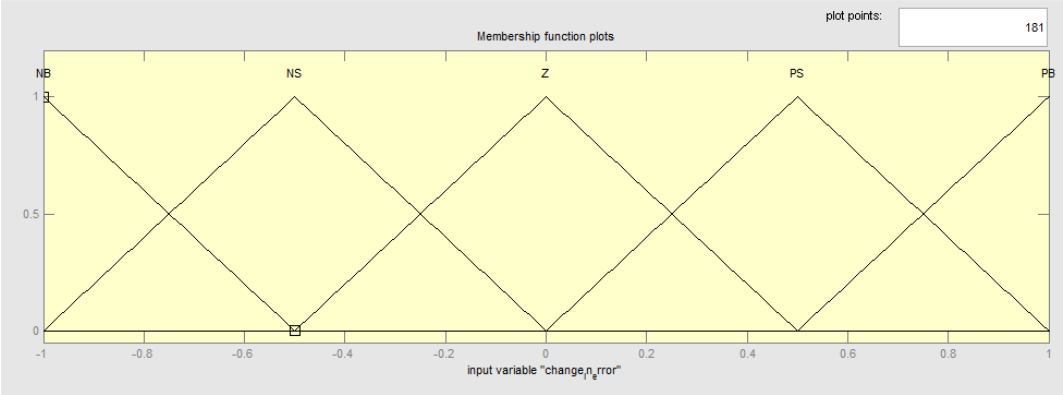

Figure 10.3: Membership function of change in error

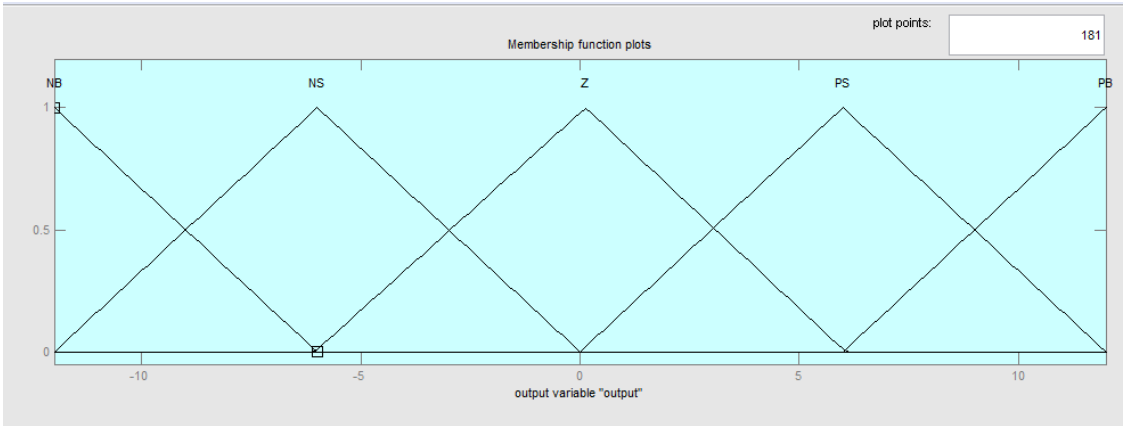

Figure 10.4: Membership function of incremental output

Rule bases are designed on the prior knowledge of system dynamics and using the primary rule forming method for feedback FLC as a PI controller, consisting of the "if then statements" logic operator being "And" [53]. Computations for all rules are done by minimum of the two memberships.

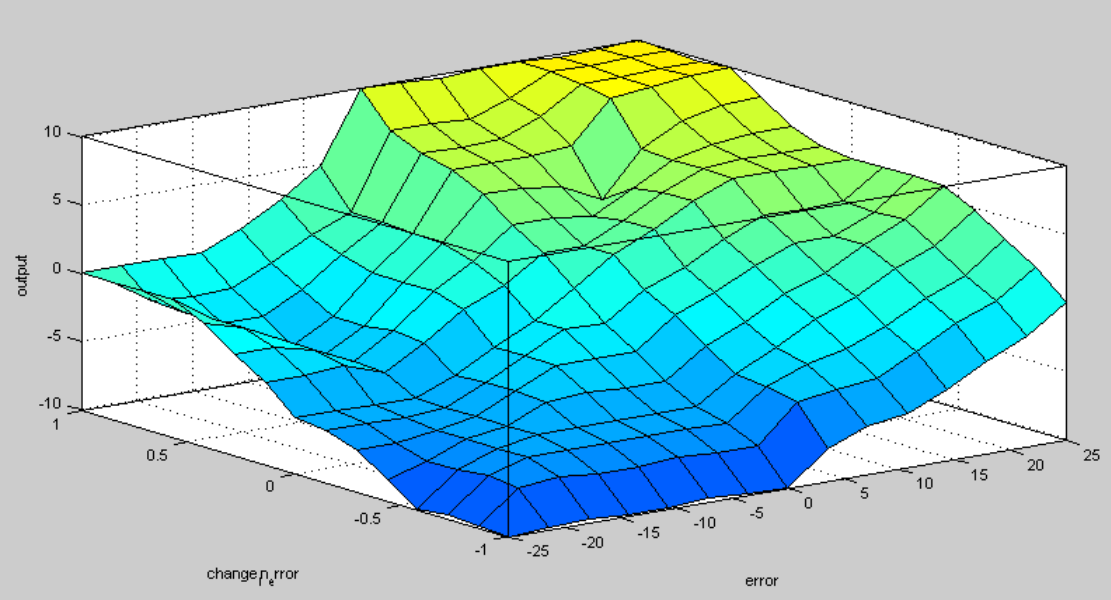

Figure 10.5: Surface mapping of the rules for the fuzzy inference system (FIS).

Defuzzification: The defuzzification is done by the Center of Gravity method, using the following formula to transform from fuzzy data to crisp data:

$$u^* = \frac{\int_{min}^{max} u\varphi(u)d_u}{\int_{min}^{max} \varphi(u)d_u} \tag{10.12}$$

where φ in equation 10.12, is the membership grade of the fuzzy set and u^* is the crisp value of fuzzy output u.

10.2 Simulation

Figure 10.6, below shows the simulation response of the FLC controller for the set point of tension, with variable step changes from 0 to 20N, 20N to 10N, 10N to 5N, to 20N. Input scaling for change in error is 0.1 and the output discrete integrator gain is 5.

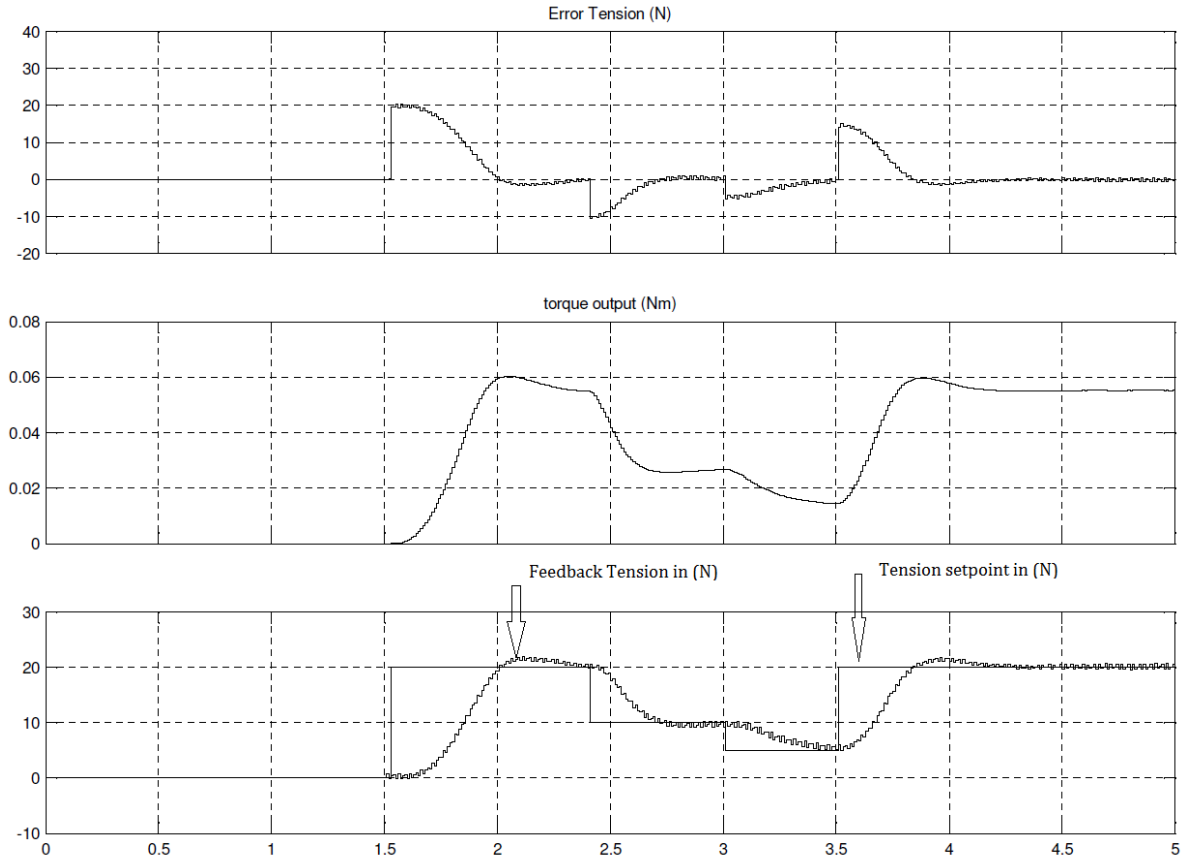

Figure 10.6: Response of the FLC as a PI controller.

The response has some overshoot but it is actually a tension controller not a voltage controller as is the PI controller.

To remove this slight overshoot the output of the FLC controller can be configured as below by equation 10.13:

$$u(z) = \frac{K_o T_s}{z(z-1)} \Delta u(z) + \Delta u(z) \tag{10.13}$$

where $\frac{K_o T_s}{z(z-1)} \Delta u(z)$ is the previous control action it is analogues to u(k-1) with reference to equation 10.10 and $\Delta u(z)$,is the incremental control action. With this response of the controller is shown below in Figure 10.7.

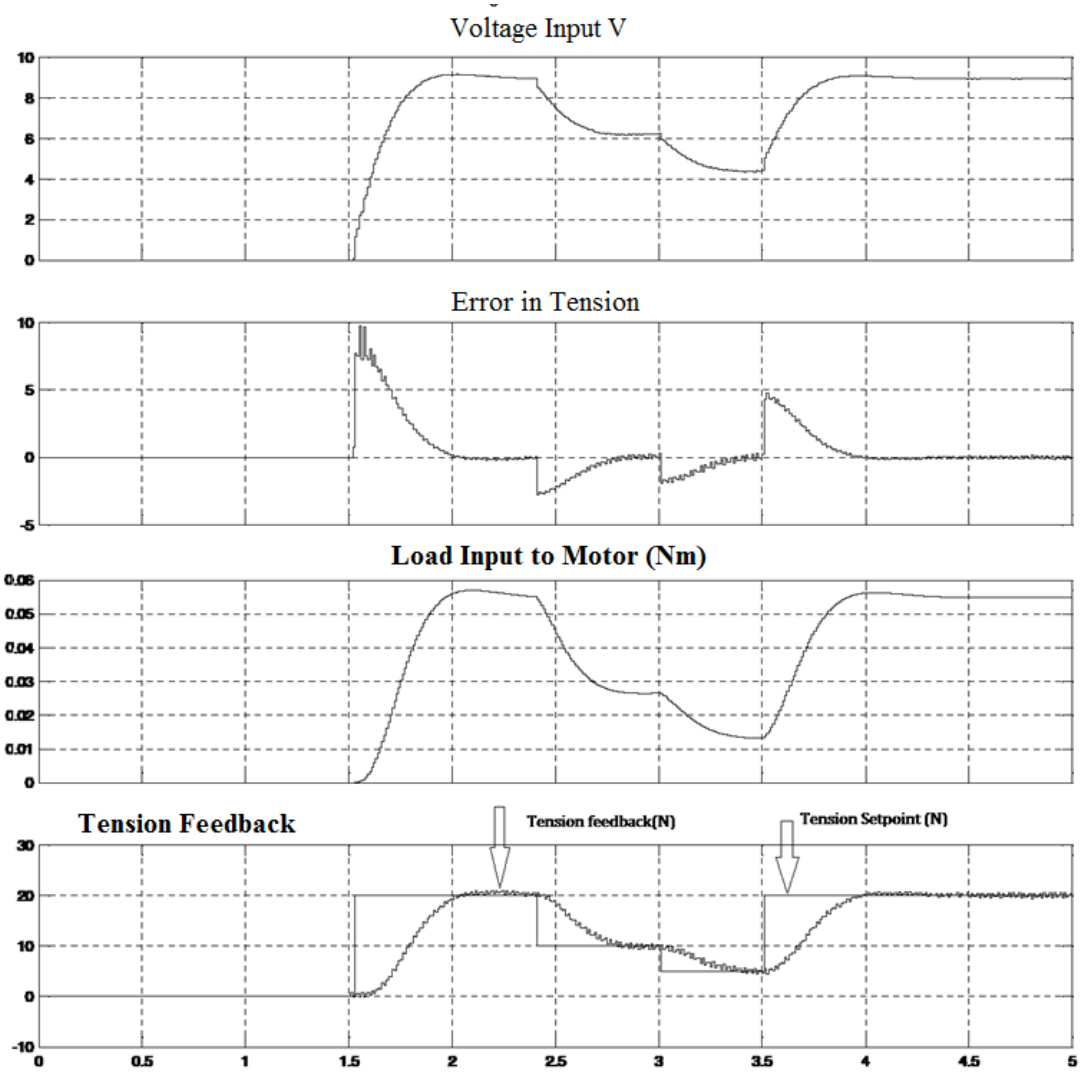

Figure 10.7: Response of FLC using equation 10.1.10

The response is similar to the PI controller. In fact it is more stable and again no preconditioning of the error is required here.

Chapter 11

CONCLUSION

The actuator developed for the prototype filament winding machine tension control, is different from the conventionally used tension actuation system. The conventional way of imparting tension in the machine is by use of an additional motor to operate fiber source creel, for example see [43], [47] and [46], also mentioned in section 5.2, of chapter 5. Additional motor increases the device price and demands additional motor control device. Therefore the designed actuator, as simulated and implemented in the prototype, is an innovative approach for controlling fibers' tension in a filament winding process. Moreover the implementation of a solenoid as force actuator, rather than position actuator is a challenge in itself.

The response of the actuator was modeled. Subsequently, a comparative analysis of more than one possible control techniques for the tension control was discussed and summarized. The tension control is a complicated process and with its nonlinearities, it is very challenging to achieve desired Tension. However, with proper linearization of the model and proper calibration of the system, the controllability can be achieved. Through simulations, it was observed that the conventional PI control can tackle this issue with proper tuning but not directly as a tension controller. The PI controller requires that nonlinearities in the system are consistent and known. The concept of virtual linearization for handling the known nonlinearities in the system, by a PI controller has been introduced.

To achieve fiber placement angle control, the numerical control of the conventional filament winding machine has been substituted by a PID control through PLC. In order to achieve, repeatability and consistency in the winding pattern through each moving path a feed forward bias updating has been implemented. Simulation response, shown in Figure 7.2, of chapter 7 is consistently repeated in each cycle in the prototype setup and can be

verified from Figure 9.5, of chapter 9. The winding angle is achieved by controlling the horizontal axis positioner speed in accordance to the mandrel rotational speed based on the speed reference given by equation 9.2 introduced in chapter 9. Based on the start and end position entered by the operator, the direction of movement of the horizontal positioner is sequentially controlled by the PLC. The concept of bias adjustment is a novelty for filament winding angle control. It makes the PID controller behave analogues to a numerical controller.

The shortcomings of the PI tension controller are that, the PI controller acts as voltage controller instead of being a tension controller. The same can be overcome by implementing a FLC. The fuzzy controller in literal sense breaks down the entire control action into small parts and as discussed in chapter 10, it calculates the output of the controller with inferred rules based on the 'change in error' and 'error'. Output of the FLC to the system is the incremental control action. The response time and the damping of the system can be formulated by adjusting the-change in error scaling coefficient k and the additive output scaling coefficient k_o. Higher, the value of k_o, the faster, the response and the greater, the oscillations in feedback. Conversely, higher the value of k, the lower the oscillations, thus the system is slower. The system can be tuned based on these two values.

The results of simulation suggested that the fuzzy controller could effectively handle the tension control problem, without any need of linearization as compared to the conventional PI controller. However, it was also demonstrated that the performance of the PI controller could be as effective as that of the Fuzzy controller when a virtual linearization scheme was applied to the PI controller.

Through this dissertation the following has been established

- An innovative tension actuator for the tension control of a prototype filament winding machine was successfully designed.

- An innovative fiber winding angle control system was designed using PID control, on a 2-axis prototype filament winding machine.
- The total price of the prototype was successfully kept low (i.e. under $5000).

11.1 Further Recommendations:

The prototype machine has the capacity to adjust a time interval or a gap between the movements in each direction. As discussed in section 4.2.1 of chapter 4 the winding pattern depends on the number of circuits. In the current winding machine it takes 14 circuits to build a pattern based on a dwelling angle of 180 degrees, winding at an angle of 54 degrees on mandrel of length of 680 mm and diameter of 50 mm. The winding with the above parameters yield an advance angle of 34.5 degrees. The timing cycle of the machine can be adjusted to adjust the dwelling angle. Further studies can be conducted to establish the relationship of the timing cycle with the dwell angle and reduce the circuit to pattern ratio and the advance angle. This will result in getting more layers in less winding cycles.

With increasing complexity in the industrial filament winding process, another forward path in this domain would be to conduct research on the ways to increase the degrees of freedom in the prototype without any significant increase in costing of the machine.

As stated, in chapter 10 implementation of the fuzzy control for the tension control could also be taken up in future research activities on the subject. The possible methods of implementing fuzzy control with PLC are

- Using a supervisory computer, the fuzzy control algorithm can update the PLC memory address through Modbus or OPC OLE client server configuration.
- A microcontroller can be designed to directly update PLC I/O mapping through physical hard wire.

The Designing of the feedback of the system could be modified and studies can be done to find out possible methods to measure tangential tension on a rotating surface.

REFERENCES

[1]. D. Rousseau, Perreux and N. Verdiere.*"The influence of winding patterns on the damage behaviour of filamentwound pipes".* Compos Sci Technol, 1999. vol.5, pp.1439-49.

[2]. M.Munro and C. Aleong *"Effect of Winding Tension and Cure Schedule on Residual Stresses in Radially-Thick Fiber Composite Rings".* 18, Ottawa : Polymer Engineering and Science, September 1991, Vol. 31.

[3]. *"Industry Segment Profile - Composites".* Columbus : EPRI Center for Materials Production, 2000.[Online] http://www.energy.ca.gov/process/pubs/composites.pdf. [Accessed: 1 Dec 2010].

[4]. *Composites Industry Statistics*: [Online] American Composites Manufacturers Association, http://www.acmanet.org/professionals/2006_composites_industryreport.pdf, May 2007. [Accessed: 5 Dec 2010].

[5]. www.archaeology.ws/archive. *World Archeology News.* [Online] May 14, 2004. http://www.archaeology.ws/2004-5-14.htm. [Accessed: 15 Jan 2011].

[6]. "Owens-Corning Fiberglas Corporation." *International Directory of Company Histories.* [Online] Encyclopedia.com, March 3, 2011. http://www.encyclopedia.com /doc/1G2-2840700243.html. [Accessed: 5 march 2011].

[7]. B Strong. *Fundamentals of composites manufacturing: materials, methods and applications.* Michigan : Society of Manufacturing Engineers, 2008 . 087263-854-5.

[8]. Continuous Filament Winding- used GRP Pipes. *www.dasanworld.com.* [Online] http://www.dasanworld.com/cn/pdf/CFWmachine-RV01.pdf. [Accessed: 15 Dec 2010].

[9]. Composites Basics: Composites Manufacturing. *www.mdacomposites.org.* [Online] American Composites Manufacturers Association, 2004. http://www.mdacomposites.org /mda/psgbridge_cb_mfg_process.html. [Accessed: 12 Nov 2010].

[10]. F. Taheri. *Lecture notes on* CIVL 6153.3 *Fiber reinforced Plastics*, Dalhousie University, Halifax : s.n., 1996.

[11]. How the Pultrusion Process Works. *The FRP Pultrusion Information Source.* [Online]PULTRUSIONS.org.http://www.pultrusions.org/articles/pultrusion_works.html. [Accessed: 21 Dec 2010].

[12]. products and process: process description. *Pultrusion Industry Council.* [Online] ACMA American Composite Manufacturers Association. http://www.acmanet.org /pic/products/description.htm. [Accessed: 22 Dec 2010].

[13]. Glossary of Laminating Methods. *Understanding Fiberglass.* [Online] Precisioneering. http://www.precisioneering.com/glossary_laminating_methods.htm. [Accessed: 1 feb 2011].

[14]. VARTM/RTM. *Manufacturing Process.* [Online] J and J Mechanic, 2003. http://www.jjmechanic.com/process/rtm.htm. [Accessed: 24 Dec 2010].

[15]. www.thaicomposites.com/technology. *www.thaicomposites.com.* [Online] Thai Composites Company Limited (TCC). [Accessed: 2 Dec 2010].

[16]. S, Beckwith. *"Composites Innovations and Advanced Technology synonymous with Pacific Rim in 06".* Arlington : Composite Manufacturing, 2006.

[17]. S. V. Hoa, *Principles of the manufacturing of composite materials.* Lancaster : DEStech Publications, Inc, 2009.

[18]. M. Munro.*"Review of Manufacturing of Fiber Composite Components by Filament Winding".* polymer Composites, october 1988, Vol. 9, pp. 352-359.

[19]. B Bora. *Design and Analysis of Filament Wound Composite Tubes.* Master of Applied Science Thesis, Department of Mechcanical Engineering, The Graduate School of Natural and Applied Sciences of Middle East University. 2004.

[20]. P. D. Soden, R. Kitching, P. C. Tse. *Experimental Failure Stresses For ±55° Filament Wound Glass Fibre Reinforced Plastic Tubes Under Biaxial Loads, Composites,.*. 2, Elsevier, March 1989, Compos Sci Technol, Vol. 20 , pp. 125-135 .

[21]. D. Cohen, *Influence of filament winding parameters on composite vessel quality and strength.* 1997, Elsevier Science Limited, pp. 1035-1037.

[22]. P. Mertiny, F. Ellyin. *Influence of the filament winding tension on physical and mechanical properties of reinforced composites.* 2002, Composites: Part A, vol 33, pp. 1615–1622.

[23]. P. D. Soden, R. Kitching, P. C. Tse, Y. Tsavalas.y. *Influence Of Winding Angle On The Stregth And Deformation Of Filament-Wound Composite Tubes Subjected To Uniaxial And Biaxial Loads,* Compos Sci Technol, Vol 46 (1993) pp. 363-378.

[24]. Tarnopollskii, M. Yu and A. I Bed. "Chapter 21, Filament Winding". [ed.] S T Peters. *Handbook of Composites.* Chapman And Hall, London, 1998.

[25]. G Lubin, *Handbook of Composites*, Van Nosterand Reinhold, New York, 1982.

[26]. S.T Peters, W.D Humphrey and R.F Foral, *Filament Winding Composite Structure Fabrication,* second priniting. SAMPE Covina, CA, 1991.

[27]. A Kelly, *Concise Encyclopedia of Composite Materials,* Oxford: Pergamon Press, London 1989.

[28]. D Rosato and C Grove. *Filament Winding: Its Development, Manufacture, Applications and Design.* John Wiley, New York 1964.

[29]. Mikrosam, Products, Filament winding machine. [Online] DirectIndustry , 2011. http://www.directindustry.com/prod/mikrosam/filament-winding-machines-21378-444252.html. [Accessed: 18 Dec 2010].

[30]. Overview of ATL/AFP, Filament Winding. *Composite World.* [Online] Gardner Publications, Inc, 2011. http://www.compositesworld.com/zones/atl-afp-filament-winding. [Accessed: 27 Dec 2010].

[31]. Filament Winding. *brochure.* [Online] http://www.entec.com/brochures/ filament.pdf. [Accessed: 21 Jan 2010].

[32]. A. K Allen, J. V. Andersen, and P. Carter, *The New L-O-T-U-S Filament-Winding Method for Composite Fabrication.* Proceedings: Global Advances in Materials and Process Engineerin. SAMPE Fall Technical Conference, Dallas, USA 2006.

[33]. San Diego Composites successfully manufactures toroidal tank fabricated using automated fiber winding technology. *News / Press Release.* [Online] San Diego Composites, Inc, 2009. http://www.sdcomposites.com/News/oct2009.html. [Accessed: 23 Dec 2010].

[34]. Michael Päßler, Ralf Schledjewski. *Filament winding with increased efficiency.* Institut für Verbundwerkstoffe GmbH . Kaiserslautern, Germany, 2002.

[35]. *Computer Control of Fiber Glass Filament Winding.* IEEE Transactions on Industry Applications Publication Society, 1985, Vol IA-21 Issue: 4, pp 1595-1604.

[36]. D. E Shaw, Stewart, *"Integrated Modwind Systems"*. first international on Automated Composites, the Plastics and Rubber Institute, Nottinghan, England 1986. Vol. 1. pp.8/1-8/14.

[37]. V. Middleton, M. J. Owen, D.G. Elliman and M. Shearing, *Developments in Non-Axisymetric Filament Winding*, Second International Automated Composites, The plastics and RubberInstitute, Noordwijkerhout, Netherlands, 1988. pp.10/1-10/15.

[38]. S K Chan, *Accuracy-speed relationships of a robotic filament winding cell,* Department of Mechanical and Aeronautical Engineering, Carleton University, Ottowa Canada, Master of Applied Science Thesis, 1994.

[39]. C A. Harper, *Handbook of plastics, elastomers, and composites,* McGraw Hill, Page 269, New York, 2002.

[40]. X Jiazhong, B You, D Jia and Z Li. *Research and Development on Control System of Winding Machine for FRP Sand-filling Pipes.* Proceedings of the 6th World Congress on Intelligent Control and Automation,, June 21 - 23, Dalian, China 2006.

[41]. S Wang, S Ning. *Research on Tension Control for Six-Axis Filament Winding Machine,* IEEE, International Conference on Apperceiving Computing and Intelligence Analysis , ICACIA , Chengdu, China, 2009.

[42]. Matrix, CADFIL® Software Systems Features and Price. July 2008. http://www.cadfil.com/product-info/Cadfil-option-chart-v4.pdf [online] [Accessed: 23 Jan 2011].

[43]. C Wang, Y Wang, R Yang, And H Lu. *Research On Precision Tension Control System Based On Neural Network.* IEEE Transactions On Industrial Electronics, Shanghai, China April 2004, Vol. 51, pp381-386.

[44]. J. Xu, B. You, D. Jia and D. Li, *Motion Synchronization System of Filament Winding Machine,* proceedings of 1st International conf. of Innovative computing ,Information and Control, Beijing, China, 2006. p. 105.

[45]. G. Wang, W. Ning. *Application of Fuzzy CMAC to Filament Tension Control,* Fourth International Conference on Fuzzy Systems and Knowledge Discovery, Haikou, Hainan, China 2007. Vol.4.

[46]. T Imamura, T Kuroiwa, K Terashima and H Takemoto. *Design and Tension Control of Filament Winding System.* Systems, Man, and Cybernetics, IEEE SMC Conference Proceedings, Tokyo, Japan, 1999.

[47]. W. Ji, F. Dai , Y. Luo. *A Novel Fuzzy Tension Controller Based On Adaptive Line Speed.* Sixth International Conference On Fuzzy Systems And Knowledge Discovery IEEE, 2009.

[48]. S. L. Ren, Y. N. Lai, Y. Z. Wang and L. Hua. *A New Fiber Winding Precisiong Tension,* International Conference on Automation and Logistics, ICAL '09. IEEE ,. Proceedings of the IEEE International Conference on Automation and Logistics. . Shenyang, China, 2009.

[49]. VFD article. *Kilowatt Classroom, LLC. Archives.* [Online] Kilowatt Classroom, LLC., 2003. http://www.kilowattclassroom.com/Archive/VFDarticle.pdf. [Accessed: 23 Oct 2010]

[50]. C. Kral, A. Haumer, and C. Grabner, *Consistent Induction Motor Parameters for the Calculation of Partial Load Efficiencies by Means of an Advanced Simulation Model.* Engineering Letters, February 2010. vol 18, issue1.

[51]. Y. Pan, M Yuan and S. Islam, *Electrostatic torsional micromirror: Its active control and applications in optical network.* IEEE International Conference on Automation Science and Engineering, Arlington, VA, 2008. pp 151 – 156.

[52]. E. H. Mamdani, *Application of Fuzzy Logic to Approximate Reasoning Using Linguistic Synthesis.* University of london, London, 1976.

[53]. C. Volosencu, *Pseudo-Equivalence of Fuzzy PI Controller.* 8th WSEAS International Conference on Signal Processing, Robotics and Automation. Timişoara, Romania, 2009, issue 4 Vol 4.

APPENDIX

A.1 Hardware Features, Datasheet and Specifications

This section of the appendix has information on the features, datasheet and specification of the hardware used in the prototype.

A.1.1 Motor datasheet

Model#: 56H17T5301 B **WINDING#:** ZT471 F 4

Table A.1.1: Typical motor performance data

HP	**KW**	**SYNC. RPM**	**F.L. RPM**	**FRAME**	**ENCLOSURE**	**KVA CODE**	**DESIGN**		
1/2	0.4	1800	1735	56C	TENV	L	B		
PH	**Hz**	**VOLTS**	**FL AMPS**	**START TYPE**	**DUTY**	**INSL**	**S.F**	**AMB**	**ELEVATION**
3	60	230/460	1.6/.8	INVERTER ONLY	CONTINUOUS	F3	1	40	3300

FULL LOAD EFF: 80	**3/4 LOAD EFF: 78.5**	**1/2 LOAD EFF: 75**	**GTD. EFF**	**ELEC. TYPE**	**NO LOAD AMPS**
FULL LOAD PF: 72	**3/4 LOAD PF: 63**	**1/2 LOAD PF: 50.5**	77.5	SQ CAGE INV DUTY	1 / .5
F.L. TORQUE	**LOCKED ROTOR AMPS**	**L.R. TORQUE**	**B.D. TORQUE**	**F.L. RISE**	
1.52 LB-FT	11.2 / 5.6	4.6 LB-FT 303	5.8 LB-FT 382	55	
SOUND PRESSURE @ 3 FT.	**SOUND POWER**	**ROTOR WK^2**	**MAX. WK^2**	**SAFE STALL TIME**	**APPROX. MOTOR WGT**
60 dBA	70 dBA	0.056 LB-FT^2	- LB-FT^2	- SEC.	25 LBS.

EQUIVALENT WYE CKT.PARAMETERS (OHMS PER PHASE)					
R1	**R2**	**X1**	**X2**	**XM**	
22.30668	17.028	24.123	18.1632	532.9764	
RM	**ZREF**	**XR**	**TD**	**TD0**	
20263.32	567.6	1.5	0.0054	0.885	
***** SUPPLEMENTAL INFORMATION *****					

DE BRACKET TYPE	ODE BRACKET TYPE	MOUNT TYPE	ORIENTATION	PAINT	
C-FACE	BRAKE OR ENCODER	BOLT-ON	HORIZONTAL	BLACK POWDER	
BEARINGS		**GREASE**	**SHAFT TYPE**	**SHAFT MATERIAL**	**FRAME MATERIAL**
DE	**OPE**				
BALL	BALL	STANDARD	STANDARD 56	STANDARD	ROLLED STEEL
203	203				

A.1.2 Solenoid datasheet

Solenoid is a Pontiac Coil - Arkansas Open Frame, Pull Type

Table A.1.2: Solenoid specification

Model Code	L-90PL012D-C
Part No.	F0461A
Voltage	12VDC
Duty Cycle	Continuous
Power (W)	13
Resistance (Ω)*	11
Current (A)	1.1

Table A.1.3: Solenoid force stroke data

Stroke (in.):	**Sealed**	**1/8**	**1/4**	**3/8**	**1/2**	**3/4**	**1**	**1-1/4**
Cont. Duty force	212 oz.	114 oz.	62 oz.	35 oz.	23 oz.	13 oz.	8 oz.	5 oz.

In the Prototype the stroke movement is negligible so the force varies with voltage.

A.1.3 Encoder technical specifications

Encoder Manufacturer: automation direct

Model: TRD-S1000-BD

The features of the encoder are:

- 38 mm diameter
- 30 mm depth
- 6 mm standard shaft
- 1000 pulses per revolution
- Open collector
- Up to 200 kHz response frequency
- Two-meter cable, tinned ends

Table A.1.4: Encoder specification

Electrical Specifications		
Model		**TRD-S1000-BD (open collector)**
	Operating Voltage	10.8 - 26.4VDC*
Power Supply	**Allowable Ripple**	3% max.
	Current Consumption	50 mA max.
Signal Waveform		Two-phase + home position
Max. Response Frequency		200kHz
Duty Ratio		50 ± 25%
Phase Difference Width		25 ± 12.5%
Signal Width at Home Position		100 ± 50%
	Rise/Fall Time	1μs max. (when cable
	Output Type	NPN open collector out- put, sinking

	Output Logic		Negative logic (active low)
	Output Current	**H**	-
	Output Voltage	**L**	0.4 V max.
	Influx Current		30mA max.
Output	**Load Power Voltage**		35 VDC max.
	Short-Circuit Protection		Between output and power supply
Mechanical Specifications			
Shaft			
Starting Torque	Max. 0.001 Nm (.00074 ft./lbs)		
Max. Allowable Shaft Load	Radial: 20N (4.5 lbs) Axial: 10N (2.25 lbs)		
Max. Allowable Speed	6000 rpm (highest speed that can support the mechanical integrity of encoder)		
Wire Size	AWG26		
Weight	Approx. 150g (5.3 oz) with 2m cable		
Environmental Specifications			
Ambient Temperature	10 to 70°C; 14 to 158°F		
Storage Temperature	-25 to 85°C; -13 to 185°F		
Operating Humidity	35-85% RH		
Voltage Withstand	500VAC (50/60Hz) for one minute		
Insulation Resistance	50M min.		
Vibration Resistance	Durable for one hour along three axes at 10 to 55 Hz with 0.75 amplitude		
Shock Resistance	11 ms with 490 m/s2 applied three times along three axes		
Protection	IP40: dust proof		

A.1.4 MicroFlex technical specifications (FMH2A06TR-EN23)

Table A.1.5: MicroFlex FMH2A06TR-EN23

24VDC control circuit supply input (X2)		
	Unit	
Nominal input voltage	**VDC**	24
Minimum input voltage		20
Maximum input voltage		30
Maximum ripple	**%**	±10
Maximum continuous current @24VDC	**A**	0.6
Power on surge current (typical)	**A**	
@24VDC, 100ms		4
Motor output power (X1)		
Nominal phase current	**ARMS**	6
Peak phase current for 3s	**ARMS**	12
Nominal output		
@ 230V, 3Φ	**VA**	2390
Output voltage range (line-line)		
@VDC-bus=320V	**VRMS**	0 - 230
Output frequency	**Hz**	0 -2000
Output dv/dt		
at		2
drive, phase-phase at drive, phase-ground		1.1
at motor (using 20m cable), phase-phase at motor (using 20m cable), phase-ground		1.9
	kV/µs	1.8
Nominal switching frequency	**kHz**	8
Minimum motor inductance (per winding)	**mH**	1
Efficiency	**%**	>95

Regeneration (X1)		
Nominal switching threshold (typical)	**VDC**	on: 388, off: 376
Nominal power	**kW**	0.25
(10% power cycle, R=57Ω)		
Peak power	**kW**	2.7
(10% power cycle, R=57Ω)		
Maximum regeneration switching current	**APK**	10
Minimum load resistance	**Ω**	39
Maximum load inductance	**µH**	100
Analog input (X3)		
	Unit	
Type		Differential
Common mode voltage range	**VDC**	±10
Common mode rejection	**dB**	>40
Input impedance	**kΩ**	>30
Input ADC resolution	**bits**	12
Equivalent resolution	**mV**	±4.9
Sampling interval	**µs**	125
Digital inputs - drive enable and general purpose (X3)		
	Unit	
Type		Opto-isolated inputs
Input voltage		
Nominal		24
Minimum Maximum		12
	VDC	30
Input current (@ Vin=24V)	**mA**	6.7
Sampling interval	**ms**	0.5
Maximum pulse input frequency	**MHz**	1
Minimum pulse width	**µs**	5

Step and Direction inputs (X3)		
	Unit	
Type		Non-isolated DC inputs
Input voltage	**VDC**	5
Input current (maximum, per input)	**µA**	20
Maximum step input frequency	**MHz**	1
Minimum pulse width	**ns**	250
Status output (X3)		
	Unit	
User supply (maximum)	**V**	30
Output current (max. continuous)	**mA**	100
Fuse		
Approximate trip current	**mA**	200
Reset time	**s**	<20
Update interval	**ms**	0.5
Incremental encoder feedback option (X8) this is used in the prototype		
	Unit	
Encoder input		A/B Differential, Z index
Maximum input frequency	**MHz**	8
(quadrature)		
Hall inputs		Single ended, 5V logic
Output power supply to encoder		5V (±7%), 200mA max.
Maximum recommended cable length		30.5m (100ft)

Encoder output (simulated) (X7)		
Signal		RS422
with encoder input on X8		Output is a copy of the input on X8.
Serial RS232/RS485 interface (X6)		
Signal		RS232, non-isolated CTS/RTS
		or
		RS485, non-isolated
		(model dependent)
Bit rate	**baud**	9600, 19200, 38400,
		57600 (default)
Environmental		
	Unit	
Operating temperature range*		0-45
Storage temperature range*		-40 to +85
Humidity (maximum)*	**%**	93
Forced air cooling flow	**m/s**	1
(vertical, from bottom to top)		
Maximum installation altitude	**m**	1000
Shock*		10G
Vibration*		1G, 10-150Hz
IP rating		IP20

A.1.5 Servo motor datasheet

Table A.1.6: Servo motor datasheet

Catalog Number	**Unit**	BSM80B-233AF
Continuous Stall Torque	lb-in	19.4
	N-m	2.2
Continuous Current	amps	6.74
Peak Torque	lb-in	68.15
	N-m	7.7
Peak Current	amps	20
Mechanical Time Constant	msec	4.4
Electrical Time Constant	msec	3.9
Rated Speed	rpm	6000
Rated Voltage	volts	200
Torque Constant	lb-in/amp	3.39
	N-m/amp	0.384
Voltage Constant	Vpk/krpm	32.8
	Vrms/krpm	23.24
Resistance	ohms	1
Inductance	mH	3.91
Inertia	lb-in-s2	0.005
	Kg-cm2	5.649
Maximum Speed	rpm	7000
Number of Motor Poles		4
Resolver Speed		1
Weight	lbs/Kg	14/6.4

A.1.6 Servo Drive VS1ST technical specifications.

Table A.1.7: VS1ST VFD specifications

Voltage	115V
Voltage Range	99-126V
Phase	Single Phase
Frequency	50/60Hz ±5%
Impedance	1% minimum from main connection
Horsepower Rating	1/2-1.5 HP 115VAC, 1 PH
	1/2-3 HP 230VAC, 1PH
	2-3 HP 230VAC, 3PH
	1-10 HP 460VAC, 3PH
Overload	
Capacity	150% for 1 minute; 175% for 2 seconds
Frequency	0-500Hz
Voltage	0 to maximum input voltage (RMS)
Trip	Missing control power, over current, over voltage, under voltage, over temperature (motor or control), output shorted or grounded, motor overload
Stall Prevention	Over voltage suppression, over current suppression
External Output	LED trip condition indicators, 4 assignable logic outputs, 2 assignable analog outputs
Short Circuit	Phase to phase, phase to ground
Overload	-10 to 50°C De-rate 3% per degree C

	above 50 to 55°C maximum surrounding temperature
Temperature	0.5hp Natural; 1-10hp Forced air
Cooling	NEMA 12, NEMA 4X
Enclosure	Sea level to 3300 Feet (1000 Meters)
	De-rate 2% per 1000 Feet (303 Meters)
Altitude	above 3300 Feet
	10 to 90% RH Non-Condensing
Humidity	1G
Shock	0.5G at 10Hz to 60Hz
Vibration	
Storage	-20 to +65°C
Temperature	1
Duty Cycle	V/Hz inverter, Sensorless vector
Control Method	Adjustable 8, 16 or 32kHz
PWM Frequency	0-10 VDC, 0-20 mA; digital (keypad)
Speed Setting	0-3000 seconds
Accel/Decel	
Velocity Loop	Adjustable to 180 Hz (Control only)
Bandwidth	
Current Loop	Adjustable to 1200 Hz (Control only)
Bandwidth	0-10VDC, 10mA (1k ohm)
Analog Output	30VDC@5A, 250VAC@5A

A.1.7 PLC CPU D2-260 specifications

Table A.1.8: DL 205 D2 260 CPU Specifications

System Capacity	
Total memory available (words)	30.4
Ladder memory (words)	15872 Flash
V-memory (words)	14592
Battery Back up	Yes
Total CPU memory I/O pts. available (actual I/O pts. depend on I/O configuration method selected)	8192 (1024 X + 1024 Y +2048 CR + 2048 GX + 2048 GY)
Local I/O (pts.)	256
Local Expansion I/O (pts.)	1280 (4 exp. bases max.) (Including local I/O)
Serial Remote I/O (pts.)	8192 max. (Including local and exp. I/O)
Remote I/O channels	8 (7+1 CPU port)
I/O per remote channel	2048
Ethernet Remote I/O	Yes
Discrete I/O pts.	8192 (Including local and exp.I/O)
Analog I/O channels Remote I/O channels	Map into V-memory Limited by power budget
I/O per remote channel	16,384 (16 fully expanded
Performance	
Contact execution (Boolean) Typical scan (1K Boolean)	0.61µs
	1.9ms

Programming and Diagnostics	
RLL Ladder	Yes
RLLPLUS/Flowchart Style (Stages)	Yes/1024
Run time editing	Yes
Supports Overrides	Yes
Variable/fixed scan	Variable
Instructions	231
Control relays	2048
Timers	256
Counters	256
Immediate I/O	Yes
Subroutines	Yes
For/Next loops	Yes
Timed Interrupt	Yes
Integer Math	Yes
Floating-point Math	Yes
Trigonometric functions	Yes
Table Instructions	Yes
PID	Yes, 16 loops
Drum Sequencers	Yes
Bit of Word	Yes
ASCII Print	Yes
Real-time clock/calendar	Yes
Internal diagnostics	Yes
Password security	Multi-level
System and user error log	Yes

Communications	
Built-in ports	Port 1 RS-232 and Port 2 RS-232/422/485)
K-sequence (proprietary protocol)	Yes
NET™	Yes
Modbus RTU master/slave	Yes
ASCII communications	IN/OUT
Maximum baud rate	38.4K port 2

A.1.8 H2 CTRIO High speed counter technical specifications

The CTRIO functions, features, genral counter applications and the specification is listed in this section.

A.1.8.1 CTRIO Functions and features

- The CTRIO module supports five primary input functions: Counter, Quad Counter, Pulse
- Catch, Edge Timer, and Dual Edge Timer.
- Three secondary input functions are also supported. These functions, Reset, Capture, and Inhibit, each modify the primary input functions in some way.
- The CTRIO module supports three primary output functions: Pulse train output for servo/stepper motor control, configurable for CW/CCW or step and direction, discrete output functions assigned to Counter/Timer input functions, and raw output control directly from the CPU interface program.

A.1.8.2 Typical Counter Applications

- High-speed cut to length operations using encoder input
- Pick-and-place or indexing functions controlling a stepper drive
- Dynamic registration for web material control
- Accurate frequency counting for speed control with onboard scaling
- Positioning (e.g. flying punch)
- PLS - programmable limit switch functions for packaging, gluing or labeling
- Stepper motor drive control
- Valve control
- Rate monitoring for speed and/or flow

A.1.8.3 Specifications

Table A.1.9: H2 CTRIO high speed counter technical specifications

General	
Module Type	Intelligent
Modules Per Base	Limited only by power consumption
I/O Points Used	None, I/O map directly in PLC V-memory or PC control access
Field Wiring Connector	Standard removable terminal block
Internal Power Consumption	400mA Max at +5V from Base Power Supply (H2, H4, T1H-CTRIO) 250mA at +5V from Base Power Supply (H0-CTRIO) (All I/O in ON State at Max Voltage/Current)
Operating Environment	32°F to 140°F (0°C to 60°C), Humidity (non-condensing) 5% to 95%
Manufacturer	Host Automation Products, LLC
Isolation	2500V I/O to Logic, 1000V among Input Channels and All Outputs
CTRIO Input Specifications	
Inputs (H2, H4, T1H-CTRIO)	8 pts. sink/source 100K Hz Max
Inputs (H0-CTRIO)	4 pts. sink/source 100K Hz Max
Minimum Pulse Width	5 µsec
Input Voltage Range	9-30VDC
Maximum Voltage	30VDC
Input Voltage Protection	Zener Clamped at 33VDC

Rated Input Current	8mA typical 12mA maximum
Minimum ON Voltage	9.0VDC
Maximum OFF Voltage	2.0VDC
Minimum ON Current	5.0mA (9VDC required to guarantee ON state)
Maximum OFF Current	2.0mA
OFF to ON Response	Less than 3 µsec
ON to OFF Response	Less than 3 µsec
CTRIO Input Resources	
Counter/Timer (H2, H4, T1H-CTRIO)	4, (2 per each 4 input channel group); supports 2 quadrature counters max.
Counter/Timer (H0-CTRIO)	2, (2 per single channel, 4 input channel); supports 1 quadrature counter max.
Resource Options	1X, 2X, or 4X Quadrature, Up or Down Counter, Edge Timer, Dual Edge Timer, Input Pulse Catch, Reset, Inhibit, Capture
Timer Range/ Resolution	4.2 billion (32 bits); 1 µsec
Counter Range	2.1 billion (32 bits or 31 bits + sign bit)
CTRIO Output Specifications	
Outputs (H2, H4, T1H-CTRIO)	4 pts, independently isolated, current sourcing or sinking FET Outputs: open drain and source with floating gate drive
	2 pts, isolated, either both current sourcing or both current sourcing

Outputs (H2-CTRIO)	FET Outputs: open drain and source with floating gate drive
Voltage range	5VDC - 36VDC
Maximum voltage	36VDC
Output clamp voltage	60VDC
Maximum load current	1.0A
Maximum load voltage	36VDC
Maximum leakage current	100µA
Inrush current	5A for 20ms
OFF to ON response	less than 3µsec
ON to OFF response	less than 3µsec
ON state V drop	0.3V
External power supply	for loop power only, not required for internal module function*
Over current protection	15A max
Thermal shutdown	Tjunction = 150°C
Over temperature reset	Tjunction = 130°C
Duty cycle range	1% to 99% in 1% increments (default = 50%)
Configurable Presets a) single	a) each output can be assigned one preset, or

b)multiple	b) each output can be assigned one table of presets, one table can contain max. 128 presets, max. predefined tables = 255
CTRIO Output Resources	
Pulse output / Discrete outputs (H2, H4, T1H-CTRIO)	Pulse outputs: 2 channels (2 outputs per each channel) Discrete outputs: 4 pts.
Pulse output / Discrete outputs (H0-CTRIO)	Pulse outputs: 1 channel (2 outputs per single channel) Discrete outputs: 2 pts.
Resource Options	Pulse outputs: pulse/direction or cw/ccw; Profiles:Trapezoid, S-Curve, Symmetrical S-Curve, Dynamic Position, Dynamic Velocity, Home Search, Velocity Mode, Run to Limit Mode, Run to Position Mode Discrete outputs: configurable for set, reset, pulse on, pulse off, toggle, reset count functions (assigned to respond to Timer/Count input functions). Raw mode: Direct access to discrete outputs from user application program
Target Position Range	2.1 billion (32 bits or 31 bits + sign bit)

A.1.9 Analog output card datasheet

F2-02DA-2 is Voltage output card it has 2 channels on channel is configured as 0V to 5V for tension actuator in the prototype and the other channel is configured as -10V to +10V for the horizontal positioned.

A.1.9.1 F2-02DA-2 Features

- Analog outputs are optically isolated from the PLC logic.
- The module has a removable terminal block, so the module can be easily removed or changed without disconnecting the wiring.
- With a DL240, DL250–1 or DL260 CPU, it is possible to update both channels in one scan.
- Low-power CMOS design requires less than 60mA from an external 18–30 VDC power supply.
- Outputs can be independently configured for any of these four ranges:

    1. 0 to 5 VDC
    2. 0 to 10 VDC
    3. - 5 t o +5 VDC
    4. -10 to +10 VDC

A.1.9.2 F2-02DA-2 Specifications

Table A.1.10: Specifications of F2-02DA-2

Number of Channels	2
Output Ranges	0 to 5V, 0 to 10V, +/-5V, +/-10V
Resolution	12 bit (1 in 4096)
Output Type	Single ended, 1 common
Peak Output Voltage	15VDC (clamped by transient voltage suppressor)
Load Impedance	2000Ω minimum
Load Capacitance	.01µF maximum
Linearity Error (end to end)	+/-1 count (+/-0.025% of full scale) maximum
Conversion Settling Time	5 µs maximum (full scale change)
Full-Scale Calibration Error (offset error included)	+/-12 counts max. unipolar @ 25_C (77_F) +/-16 counts max. bipolar @ 25_C (77_F)
Offset Calibration Error	+/-3 counts maximum @ 25^{O}C (77^{O}F) unipolar +/-8 counts maximum @ 25^{O}C (77^{O}F) bipolar
Accuracy vs. Temperature	+/-50 ppm/_C full scale calibration change (including maximum offset change of 2 counts)
Maximum Inaccuracy	Unipolar ranges +/-0.3% @ 25^{O}C (77^{O}F) +/-0.45 0–60^{O}C (32–140^{O}F) Bipolar ranges +/-0.4% @ 25^{O}C (77^{O}F) +/-0.55% 0–60C (32–140^{O}F)
PLC Update Rate	1 channel per scan maximum (D2–230 CPU) 2 channels per scan maximum (D2–240/250–1/ 260 CPU)
Digital Outputs Output Points Required	1 binary data bits, 2 channel ID bi s, 1 sign bit 16 point (Y) output module
Power Budget Requirement	40 mA @ 5 VDC (supplied by base)

External Power Supply	F2−02DA−2: 18-30 VDC, 60 mA (outputs fully loaded) F2−02DA−2L: 10-15 VDC, 70 mA (outputs fully loaded)
Operating Temperature	0−60^{O}C (32−140^{O}F)
Storage Temperature	−20 to 70^{O} C (−4 to 158^{O} F)
Relative Humidity	5 to 95% (non-condensing)
Environmental Air	No corrosive gases permitted
Vibration	MIL STD 810C 514.2
Shock	MIL STD 810C 516.2
Noise Immunity	NEMA ICS3−304

A.2 CTRIO Workbench

CTRIO configuration is done via a software utility, eliminating the need for ladder programming to configure the module. The software utility is called CTRIO Workbench. After successfully configuring the module enables the user, toggle the CTRIO module between Program Mode and Run Mode and enter the Monitor I/O dialog. Configuration changes can be done in either Run Mode or Program Mode, but to saving the configuration to the module, requires clicking "Write Module" which is only active in Program Mode. In the lower left corner of the main Workbench dialog, is the Config Status indicator. If the current configuration is different from the CTRIO and different from any saved files, the Config Status indicator will display the word "Changed" in red. If the current configuration has been written to the module or a file, the indicator will show "Same as Module," in green.

Address mapping of inputs and outputs of CTRIO to the PLC address memory location is also done by the workbench. In Workbench configuration the starting address as required by the programmer is entered. The software automatically maps the I/O of the CTRIO to the PLC address location. Given below is the I/O Map created for the Prototype:

Given below are the memory locations of the card as configured in the Prototype:

Ch1/Fn1 - Quad Counter (horizontal slide Position Feedback)

V2000-2001 = Scaled Units, C1F1_ScldUnit
V2002-2003 = Raw Value, C1F1_RawValue
V2020.1 = At Reset Value, C1F1_AtRstVal

V2054.1 = Reset, C1F1_Reset

Ch2/Fn1 - Quad Counter (Mandrel RPM)

V2010-2011 = Scaled Units, C2F1_ScldUnit

V2012-2013 = Raw Value, C2F1_RawValue

V2021.1 = At Reset Value, C2F1_AtRstVal

V2055.1 = Reset, C2F1_Reset

Output 0 - Raw

V2022.0 = Output Enabled, Out0_OutEnbld

V2056.0 = Enable Output, Out0_EnablOut

Output 1 - Raw

V2022.8 = Output Enabled, Out1_OutEnbld

V2056.8 = Enable Output, Out1_EnablOut

Output 2 - Raw

V2023.0 = Output Enabled, Out2_OutEnbld

V2057.0 = Enable Output, Out2_EnablOut

Output 3 - Raw

V2023.8 = Output Enabled, Out3_OutEnbld

V2057.8 = Enable Output, Out3_EnablOut

System Functions(Read only)

V2024.6 = SysCmd Error, SysCmdError
V2024.7 = SysCmd Complete, SysCmdComplet
V2025.0 = Ch1 A, Ch1A
V2025.1 = Ch1 B, Ch1B
V2025.2 = Ch1 C, Ch1C
V2025.3 = Ch1 D, Ch1D
V2025.4 = Ch2 A, Ch2A
V2025.5 = Ch2 B, Ch2B
V2025.6 = Ch2 C, Ch2C
V2025.7 = Ch2 D, Ch2D
V2025.8 = Out 0 Active, Out0_Active
V2025.9 = Out 0 Mode, Out0_Mode
V2025.10 = Out 1 Active, Out1_Active
V2025.11 = Out 1 Mode, Out1_Mode
V2025.12 = Out 2 Active, Out2_Active
V2025.13 = Out 2 Mode, Out2_Mode
V2025.14 = Out 3 Active, Out3_Active
V2025.15 = Out 3 Mode, Out3_Mode

V2060.7 = Process SysCmd, ProcSysCmd

In Run mode the CTRIO Workbench utility also allows the user to monitor and verify the proper operation of inputs and outputs. The count change, scaled, raw values ,reset, etc. using the Monitor I/O dialog. Monitor I/O is very useful for debugging and commissioning of a new system.

When using Direct LOGIC CPU the CTRIO mode follows the CPU mode. If the CPU is placed in Run Mode, the CTRIO module will also enter Run Mode. If the CPU is placed in STOP or PROGRAM Mode, the CTRIO will enter Program Mode. The CTRIO also responds to mode changes made in Workbench and can be placed in Run Mode while the CPU is in Stop or Program Mode. The CTRIO module responds to the most recent change whether performed in Workbench or from the CPU.

A.2.1 Configure IO Dialog Overview

The Configure IO dialog is the location where input and output functions are assigned to the module. The choice of input and output functions determines which options are available.

The input and output function boxes prompt the user with selections for supported functions. The Workbench software disallows any unsupported configurations. In the Config I/O window, the input options are listed by function. Four boxes labeled A, B, C, and D correspond to the input terminals on the face of the module (1A-1D or 2A-2D) based, on the channel. The Config I/O window has a tab for each input Channel. The Output functions are listed as 0, 1, 2, and 3. These numbers correspond to the markings beside the module's output terminals (Y0-Y3)

Not performing Write Module operation (or a Write File operation) after a configuration change, will result in loss of all the changes upon quitting Workbench. This applies to all changes to the module configuration.

The module supports five primary input functions:

- Counter
- Quadrature Counter
- Pulse Catch
- Edge Timer
- Dual Edge Timer

Each of the primary functions uses one or two input terminals for making connections to field devices (plus a common). Combinations of the listed functions are possible.

Three secondary input functions are also supported

- Reset
- Capture
- Inhibit

Each secondary input modifies the primary input functions in some way and uses one input terminal
Additionally the any of the inputs can be configured as a normal digital input accepting 0V for on state and 9-36 V for off state.

Since in the prototype all the inputs are configured as either quadrature counter or normal digital inputs, in this appendix only quadrature counter is described.

The CTRIO module supports quadrature counting using quadrature encoders as inputs. The inputs A and B on either channel can be configured as quadrature counter. A second quadrature encoder can be connected to the other channel. The C and D inputs are available to control the quadrature input counting. The C and D inputs can be used for Reset, Inhibit, or Capture.

If for example inputs to terminal 1A and 1B are to be configured as quadrature counter, then the user needs to select the Channel 1 tab near the top of this window and click “Quad Counter” in box A. Since a quadrature counter uses two slots together input 1B is automatically slaved to input 1A.

Once a Channel has been configured as a quadrature counter the following three possible decision options exist:

A multiplier can be applied to the quadrature input to increase its resolution by selecting "1x", "2x", or "4x." options. [1X = pulses processed on leading edge of input A, 2X = pulses are processed on both edges of input A, 4X = pulses processed on both edges of input A and both edges of input B.]

The "Reset Value" can be assigned by clicking in the data input field and typing in a value. When the count is reset, using any of the reset methods, the count value returns to the Reset Value.

The last remaining decision to be made is about scaling. Clicking the button with the ruler symbol starts the Scaling Wizard. The Scaling Wizard is intelligent in that it offers only those scaling options that are appropriate for the input selected.

A.2.2 Scaling Wizard

Scaling raw signals to engineering units is accomplished using the Scaling Wizard. The Scaling Wizard is started by clicking the ruler button on the Configure IO dialog. This button appears only after a Counter or Timer functions is selected.

The Scaling Wizard options are different for the Counter functions as compared with the Timer functions. "Position" and "Rate" scaling are available the user selects a Counter function. If Timer function is selected then "Interval" scaling is available.

Since in the prototype, only quadrature counter is used, so in this appendix only Counter Scaling wizard is described.

Scaling Wizard:

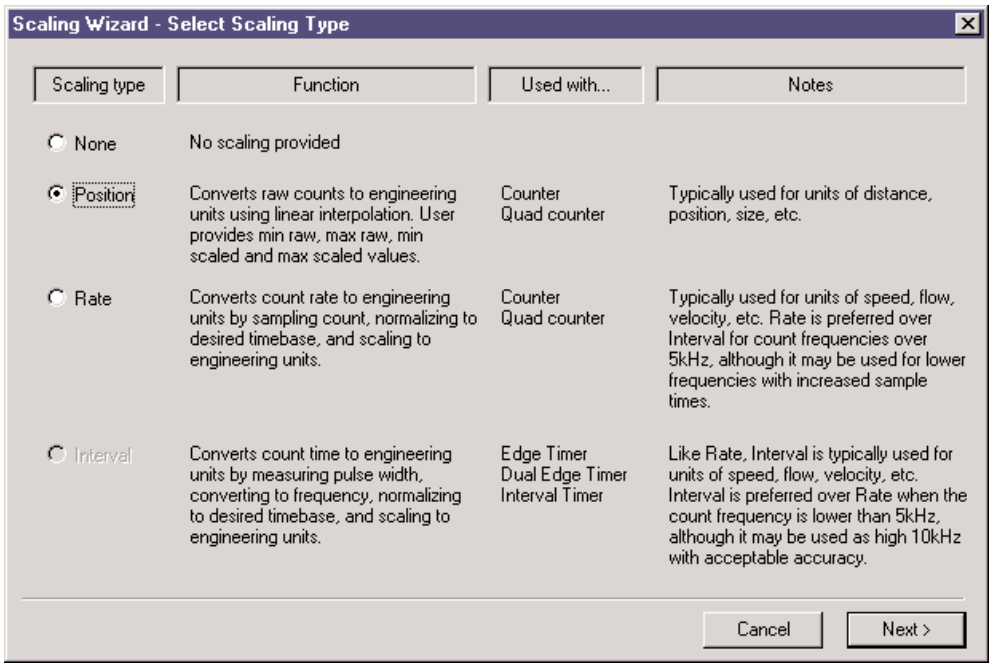

Figure A.2.1: Counter scaling wizard.

On the counter Scaling Wizard, one can select None, Position, or Rate. No scaling is accomplished if the "None" button is selected. Position scaling is appropriate for measuring distance, position, or size. Rate scaling is appropriate for velocity, RPM, flow, or similar rate based measurements.

A.2.2.1 Position Scaling (Counter)

When on the scaling wizard window "position" option is selected and return key is pressed the "Output Settings" dialog appears. In this dialog the field for engineering units has to be filled and data type for the scaled value to be written in the PLC memory V address has to be specified. Seven data types are available including BCD (to make values more easily used by Direct LOGIC PLCs). As shown in Figure A.2.2a.

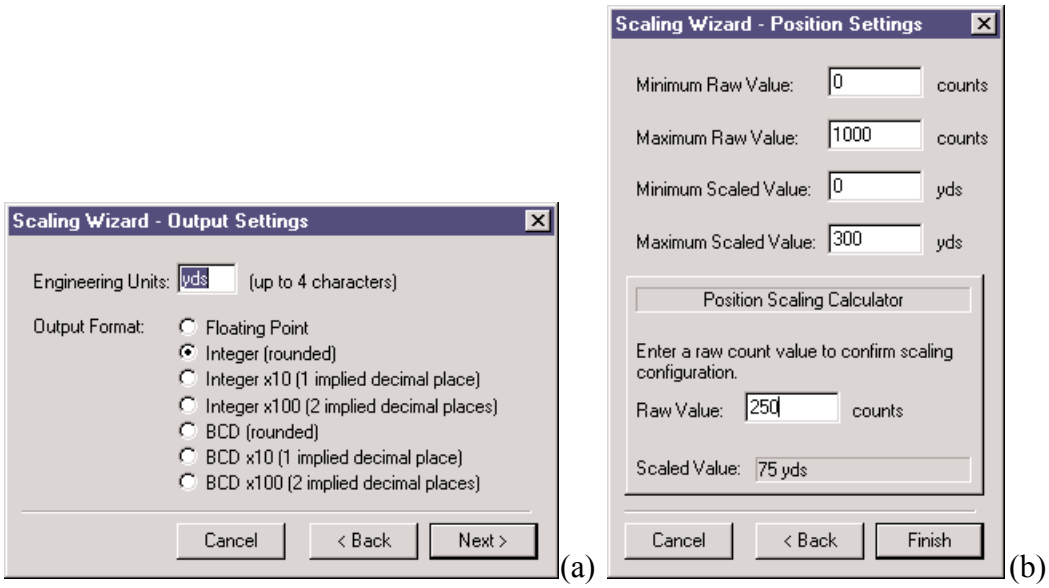

Figure A.2.2: (a) Output setting dialog (b) Position setting dialog

Then entering the next window Figure A.2.2b, the raw counts and corresponding engineering scaled values are entered.

A.2.2.2 Rate Scaling (Counter)

When Rate option is selected, in "select scaling type" dialogue in Figure A2.1.1, first the output setting dialog opens which is same as in position scaling, pressing next that opens "Rate Settings" dialog shown in Figure A.2.3. Here the counts per unit of time and the time base are entered. A scale offset is also provided to adjust the result by a constant amount.

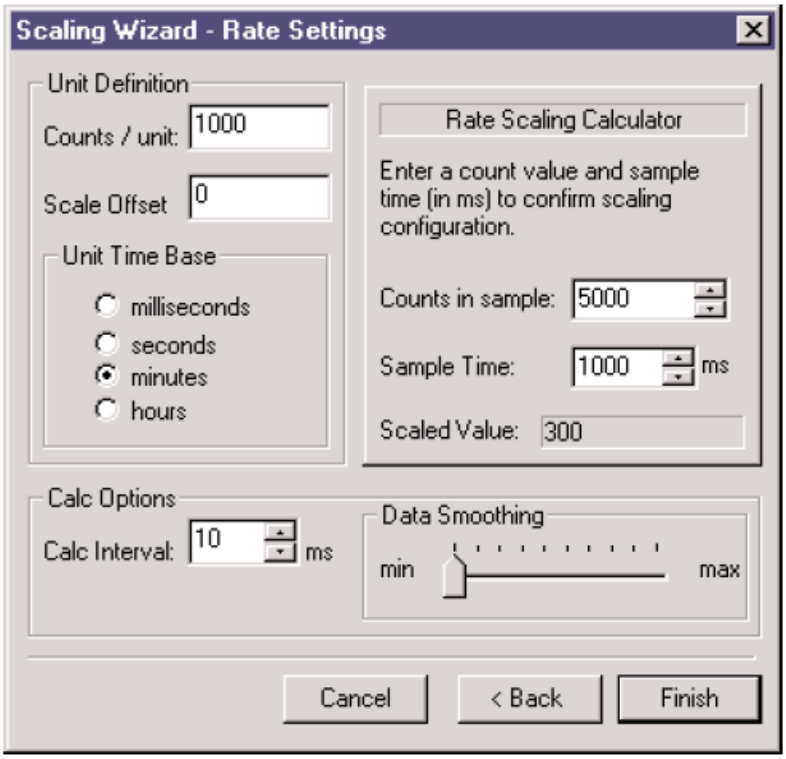

Figure A.2.3: Rate setting dialog

.

In this Appendix only few selected concepts of CTRIO Workbench are stated as excerpts from the CTRIO operation manual, the complete information of the CTRIO card can be found out at : http://www.automationdirect.com/static/manuals/hxctriom/hxctriom.html

A.3 PLC Program

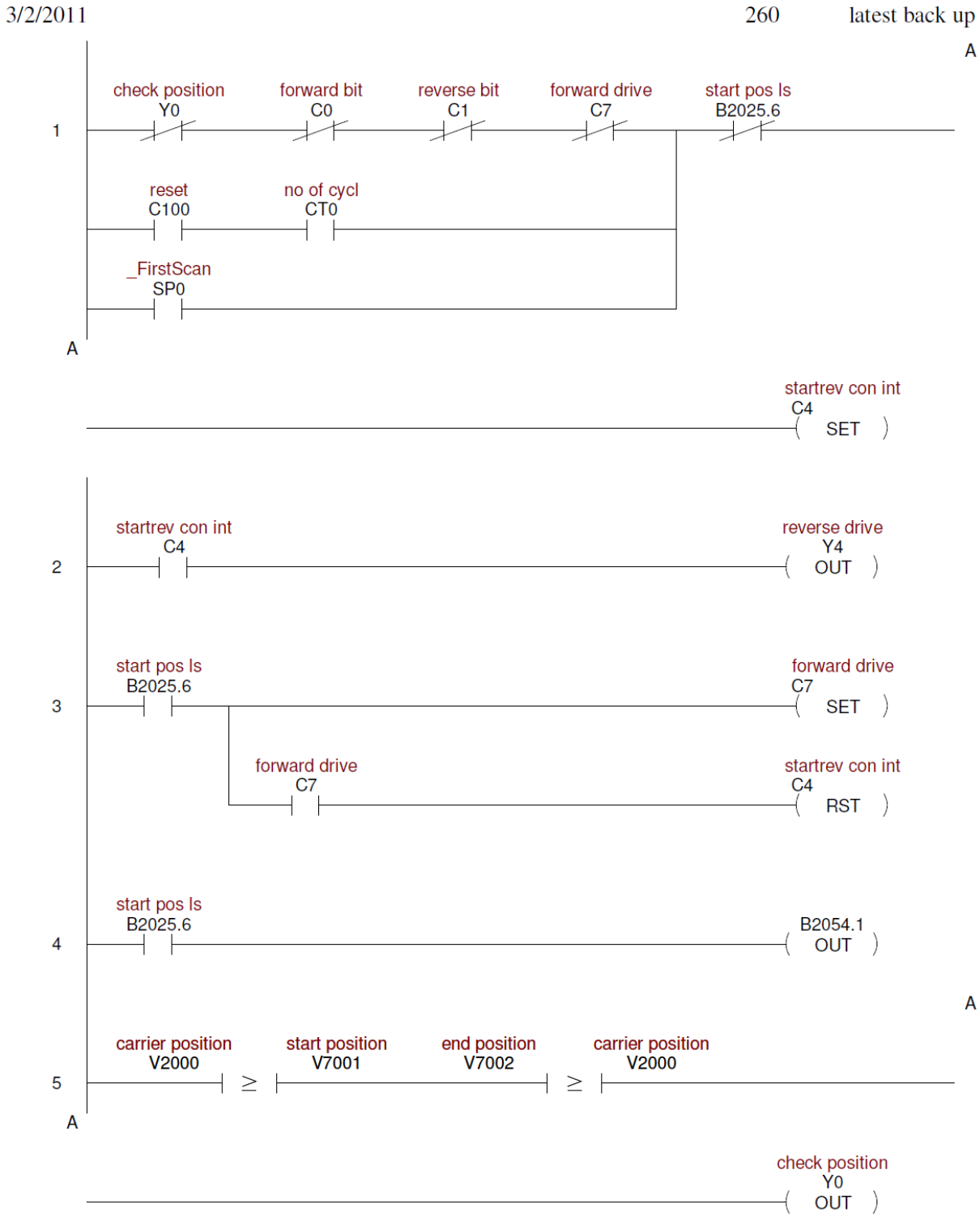

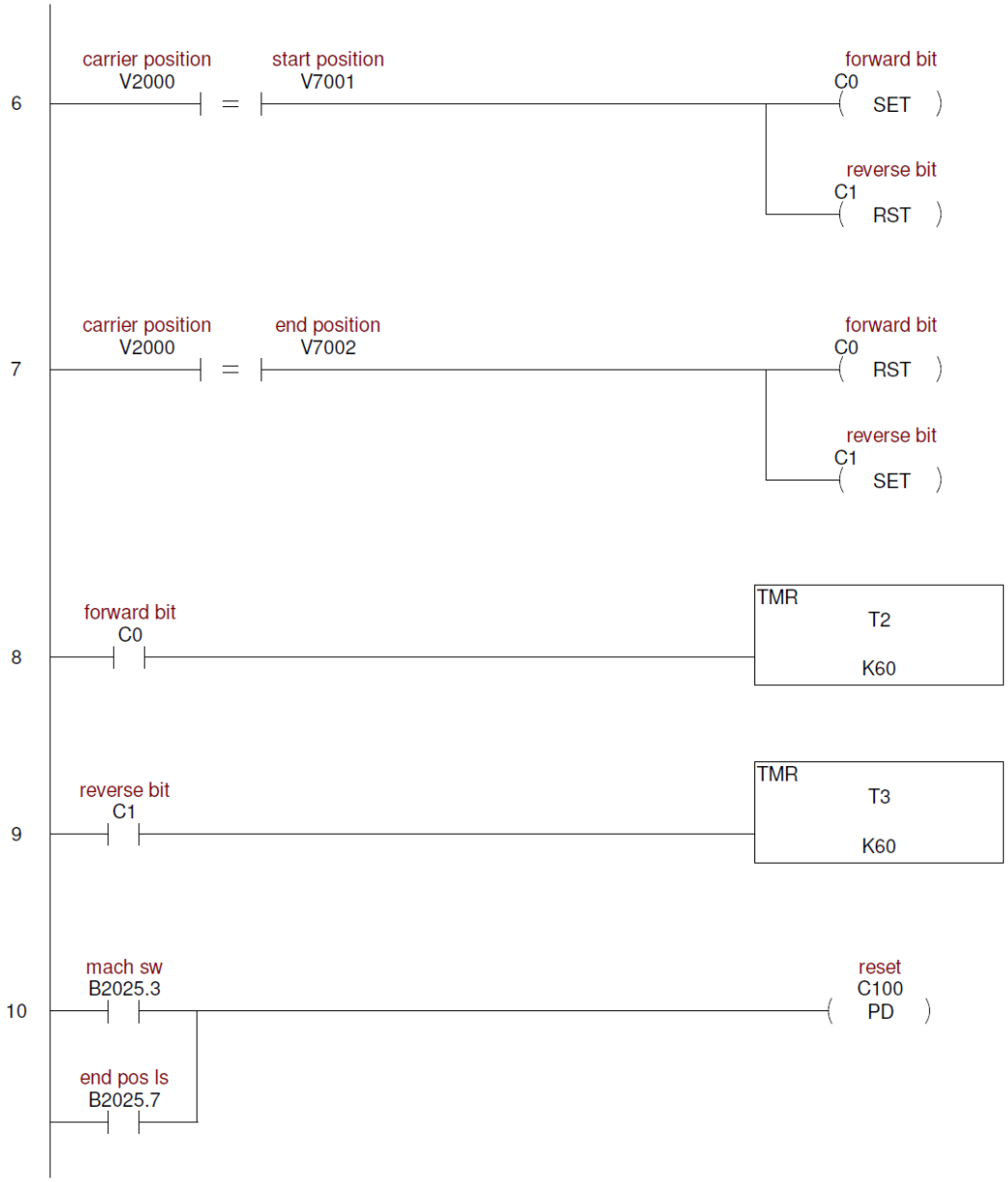
6
carrier position
V2000
=
start position
V7001
forward bit
C0
SET
reverse bit
C1
RST
7
carrier position
V2000
=
end position
V7002
forward bit
C0
RST
reverse bit
C1
SET
8
forward bit
C0
TMR
T2
K60
9
reverse bit
C1
TMR
T3
K60
10
mach sw
B2025.3
end pos ls
B2025.7
reset
C100
PD

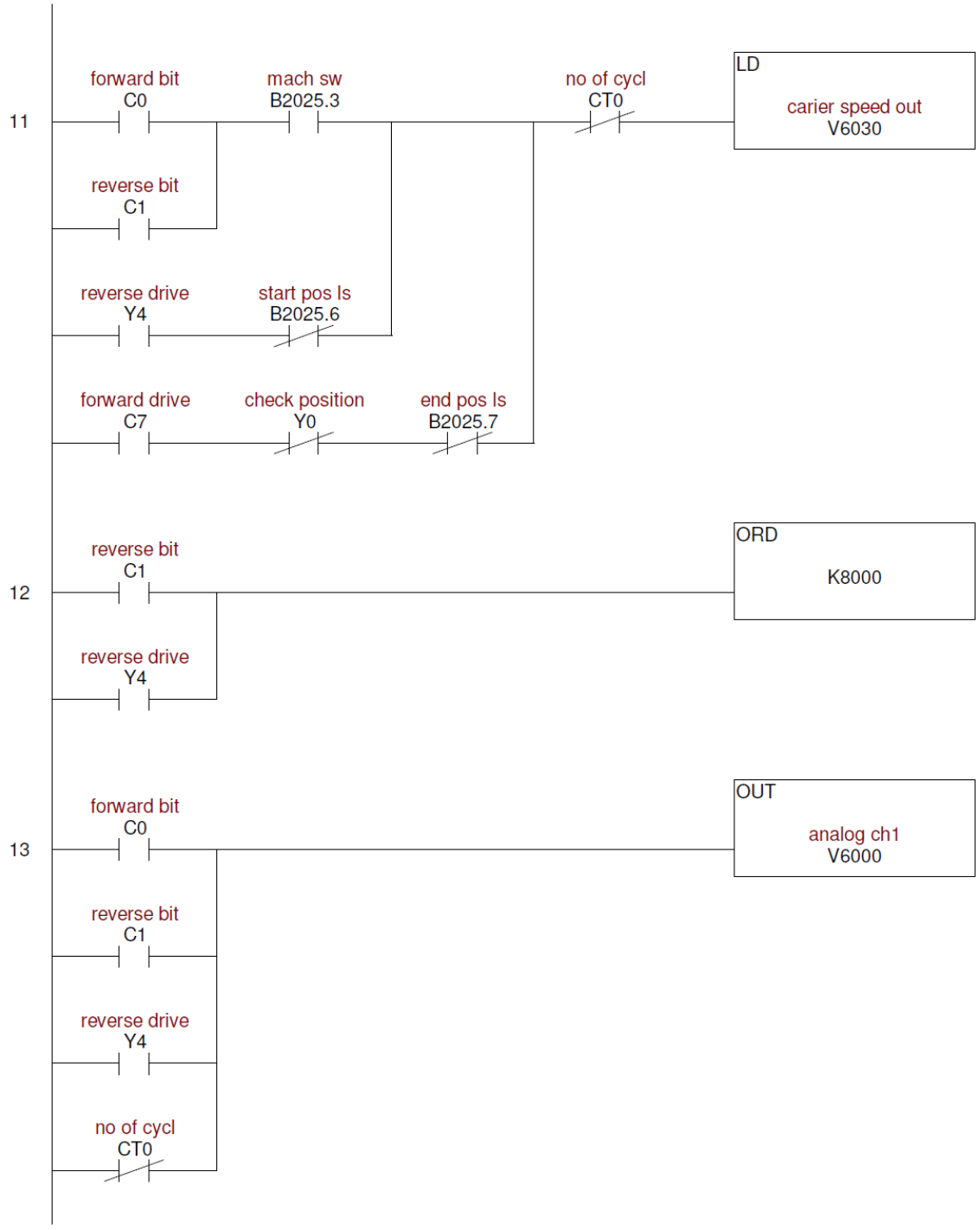
11
forward bit
C0
mach sw
B2025.3
no of cycl
CT0
LD
carier speed out
V6030
reverse bit
C1
reverse drive
Y4
start pos ls
B2025.6
forward drive
C7
check position
Y0
end pos ls
B2025.7
12
reverse bit
C1
ORD
K8000
reverse drive
Y4
13
forward bit
C0
OUT
analog ch1
V6000
reverse bit
C1
reverse drive
Y4
no of cycl
CT0

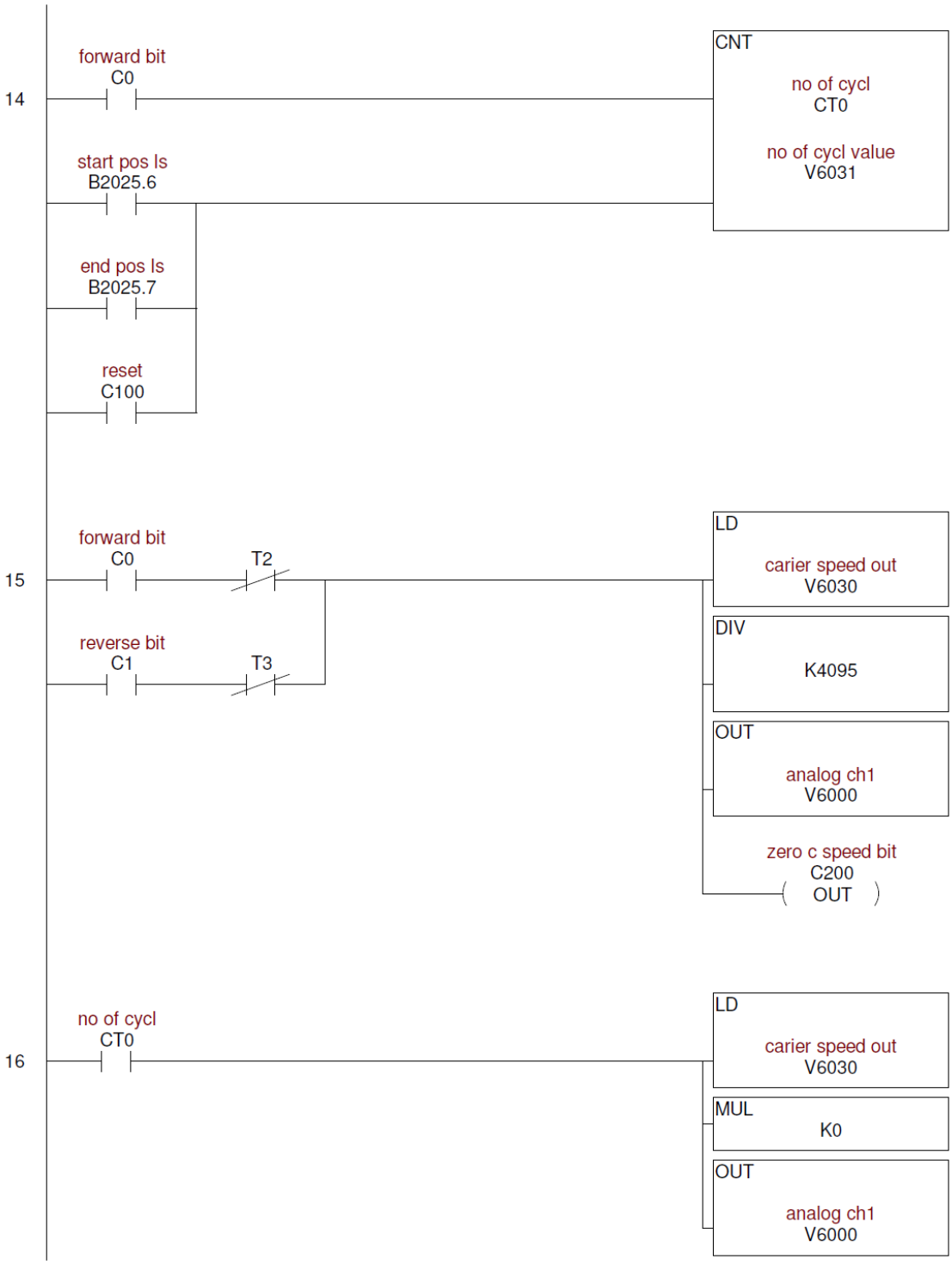
14
forward bit
C0
start pos ls
B2025.6
end pos ls
B2025.7
reset
C100
CNT
no of cycl
CT0
no of cycl value
V6031
15
forward bit
C0
T2
reverse bit
C1
T3
LD
carier speed out
V6030
DIV
K4095
OUT
analog ch1
V6000
zero c speed bit
C200
OUT
16
no of cycl
CT0
LD
carier speed out
V6030
MUL
K0
OUT
analog ch1
V6000

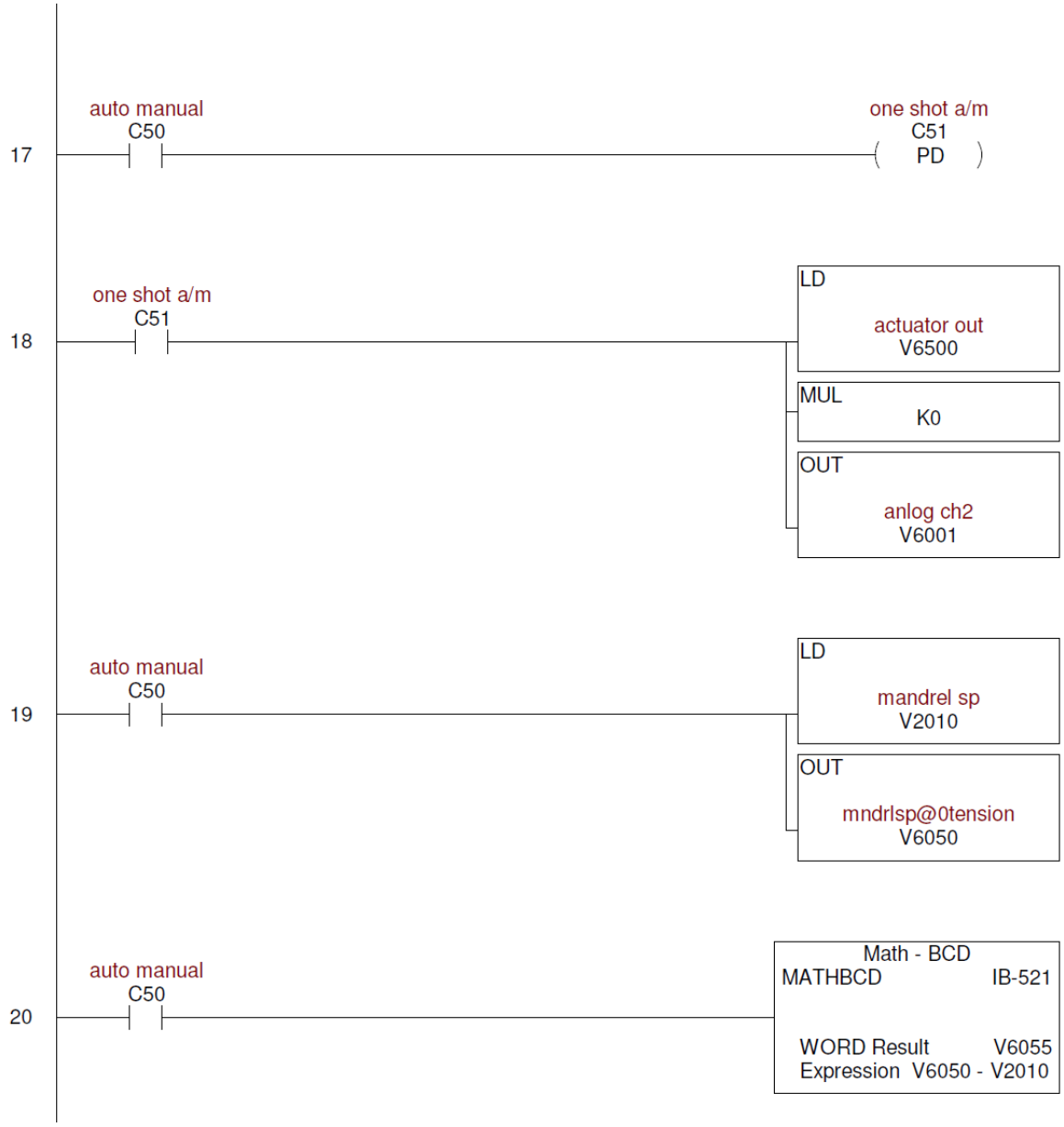
17
auto manual
C50
one shot a/m
C51
PD
18
one shot a/m
C51
LD
actuator out
V6500
MUL
K0
OUT
anlog ch2
V6001
19
auto manual
C50
LD
mandrel sp
V2010
OUT
mndrlsp@0tension
V6050
20
auto manual
C50
Math - BCD
MATHBCD
IB-521
WORD Result
V6055
Expression
V6050 - V2010

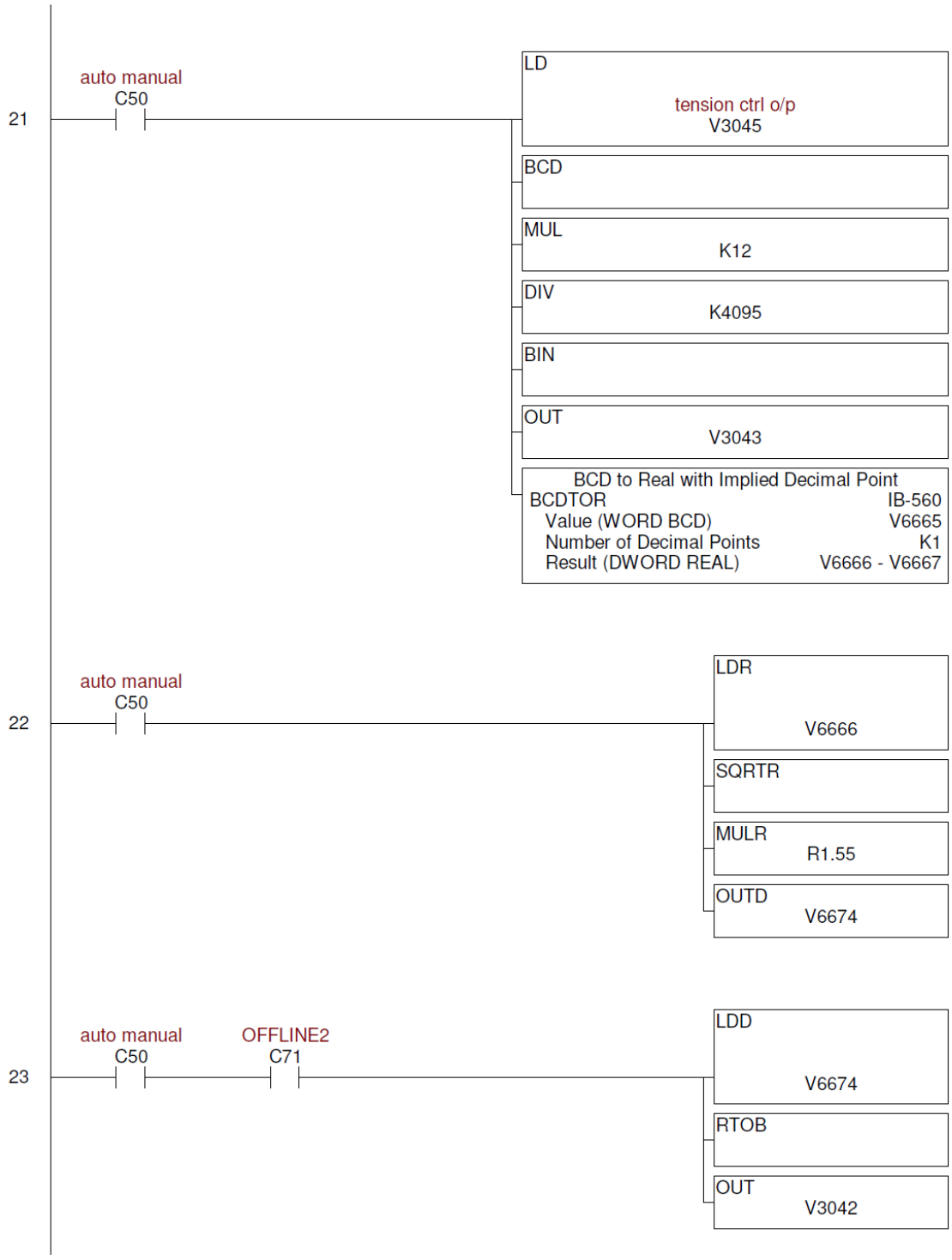
21
auto manual
C50
LD
tension ctrl o/p
V3045
BCD
MUL
K12
DIV
K4095
BIN
OUT
V3043
BCD to Real with Implied Decimal Point
BCDTOR IB-560
Value (WORD BCD) V6665
Number of Decimal Points K1
Result (DWORD REAL) V6666 - V6667
22
auto manual
C50
LDR
V6666
SQRTR
MULR
R1.55
OUTD
V6674
23
auto manual
C50
OFFLINE2
C71
LDD
V6674
RTOB
OUT
V3042

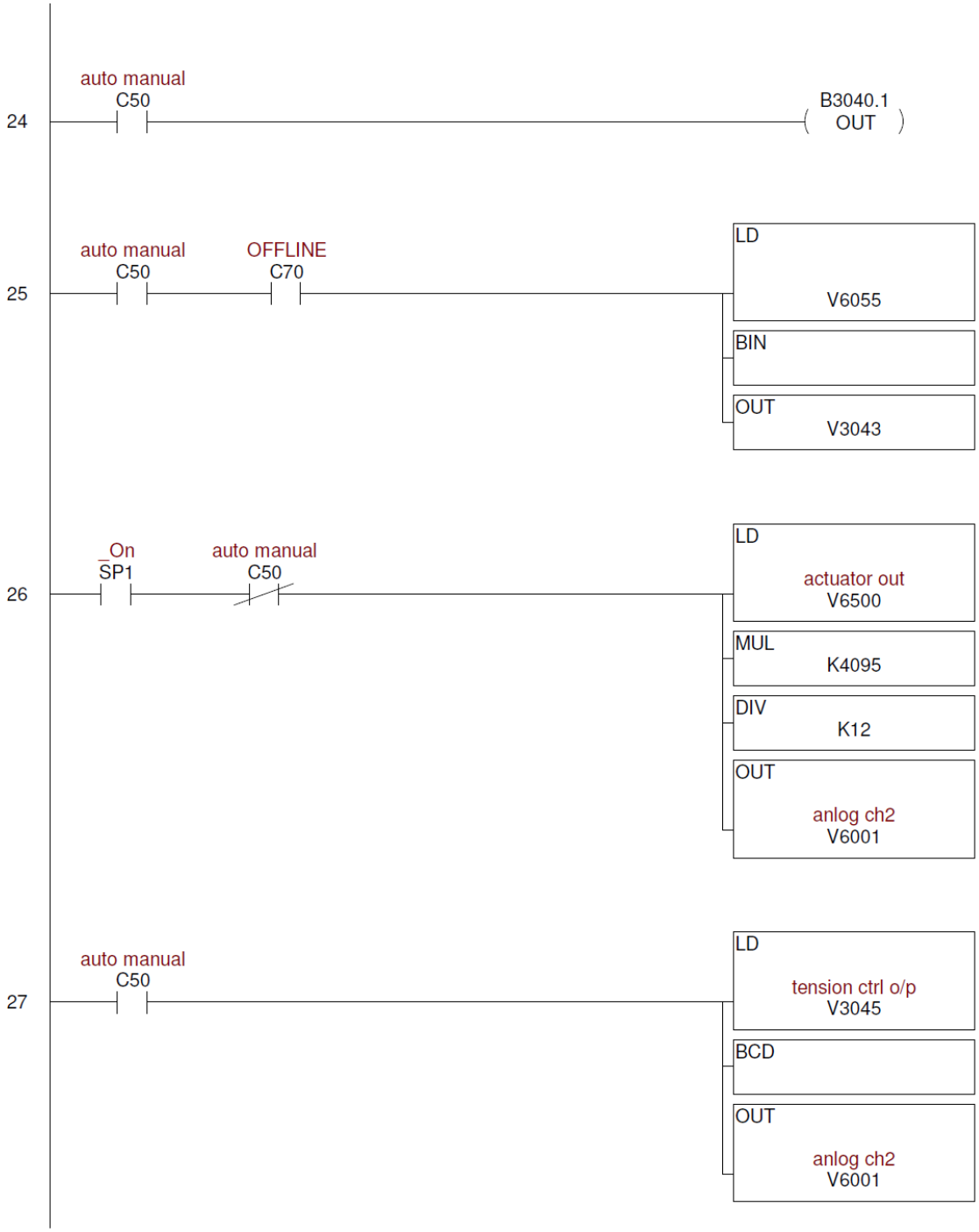
24
auto manual
C50
B3040.1
OUT
25
auto manual
C50
OFFLINE
C70
LD
V6055
BIN
OUT
V3043
26
_On
SP1
auto manual
C50
LD
actuator out
V6500
MUL
K4095
DIV
K12
OUT
anlog ch2
V6001
27
auto manual
C50
LD
tension ctrl o/p
V3045
BCD
OUT
anlog ch2
V6001

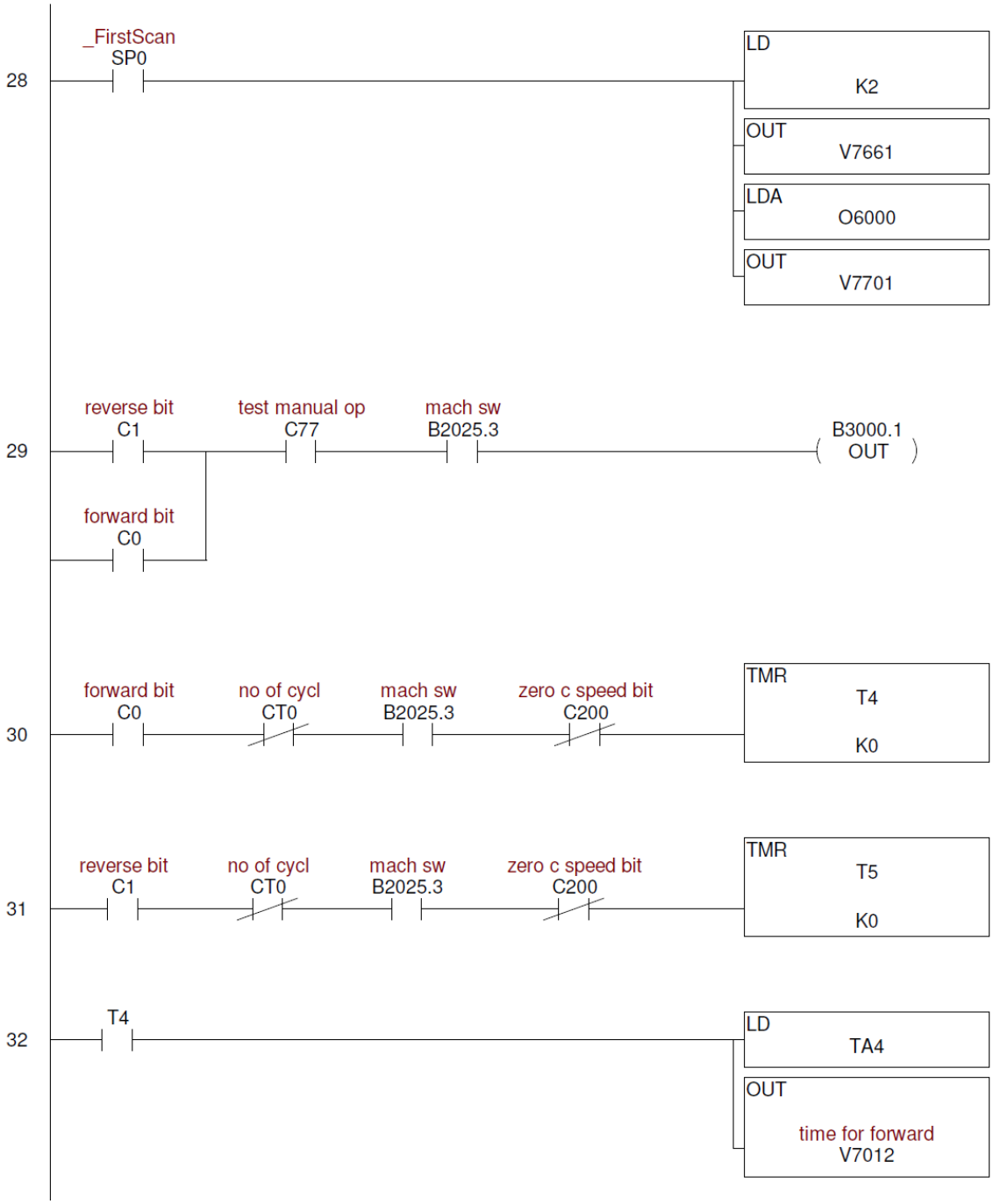
28
_FirstScan
SP0
LD
K2
OUT
V7661
LDA
O6000
OUT
V7701
29
reverse bit
C1
test manual op
C77
mach sw
B2025.3
B3000.1
OUT
forward bit
C0
30
forward bit
C0
no of cycl
CT0
mach sw
B2025.3
zero c speed bit
C200
TMR
T4
K0
31
reverse bit
C1
no of cycl
CT0
mach sw
B2025.3
zero c speed bit
C200
TMR
T5
K0
32
T4
LD
TA4
OUT
time for forward
V7012

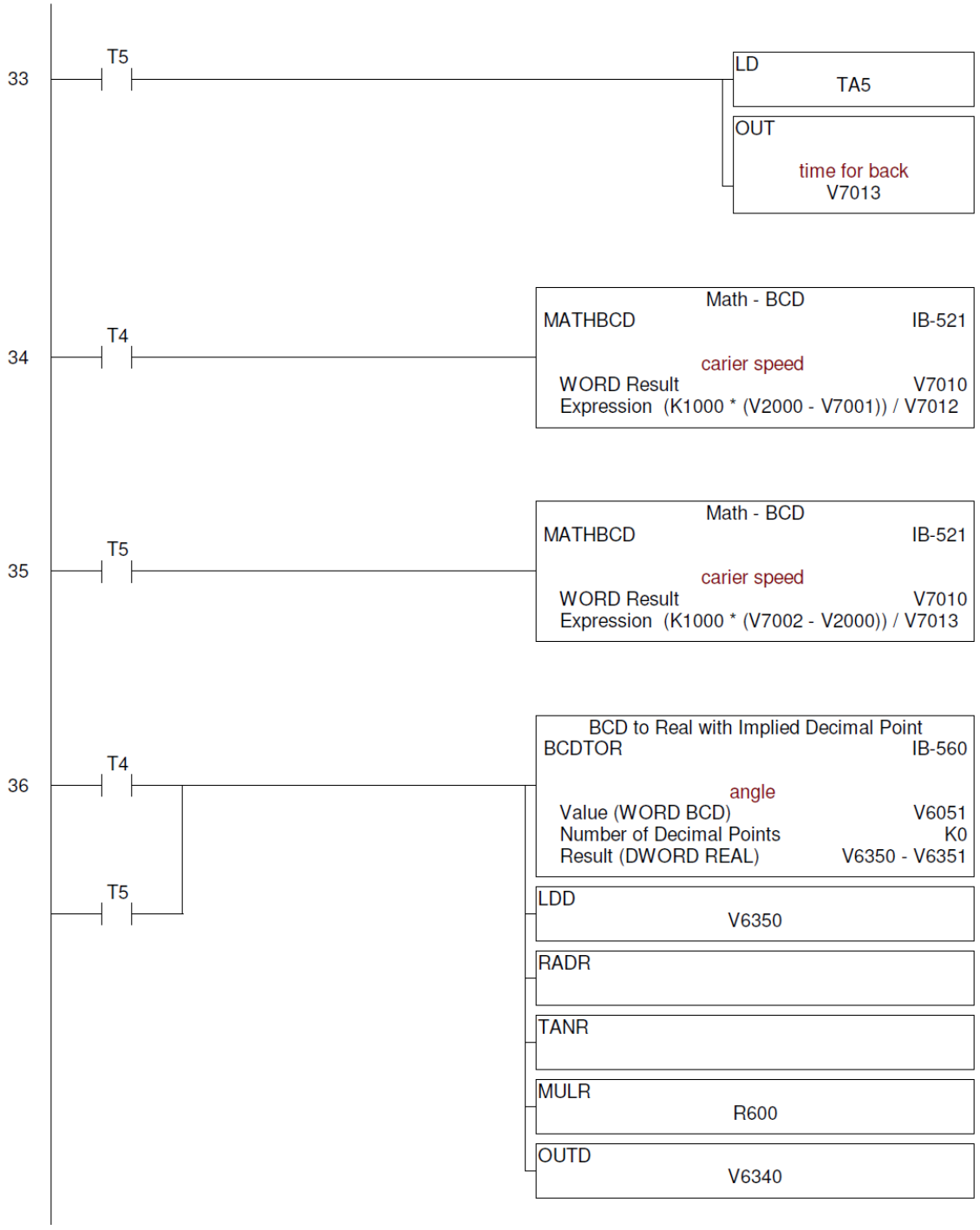
33
T5
LD
TA5
OUT
time for back
V7013
34
T4
Math - BCD
MATHBCD
IB-521
carier speed
WORD Result
V7010
Expression (K1000 * (V2000 - V7001)) / V7012
35
T5
Math - BCD
MATHBCD
IB-521
carier speed
WORD Result
V7010
Expression (K1000 * (V7002 - V2000)) / V7013
36
T4
T5
BCD to Real with Implied Decimal Point
BCDTOR
IB-560
angle
Value (WORD BCD)
V6051
Number of Decimal Points
K0
Result (DWORD REAL)
V6350 - V6351
LDD
V6350
RADR
TANR
MULR
R600
OUTD
V6340

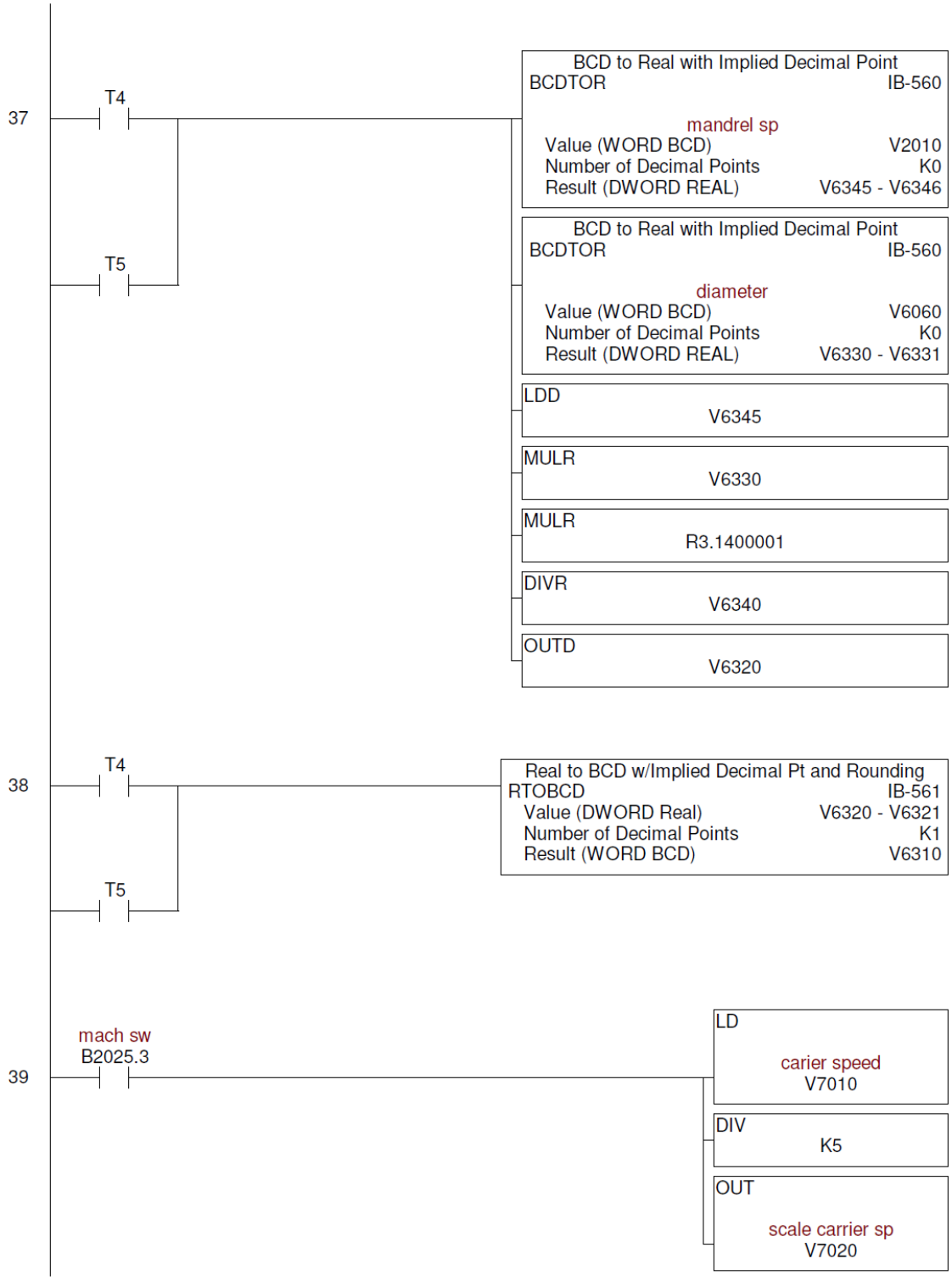
37
T4
T5
BCD to Real with Implied Decimal Point
BCDTOR IB-560
mandrel sp
Value (WORD BCD) V2010
Number of Decimal Points K0
Result (DWORD REAL) V6345 - V6346
BCD to Real with Implied Decimal Point
BCDTOR IB-560
diameter
Value (WORD BCD) V6060
Number of Decimal Points K0
Result (DWORD REAL) V6330 - V6331
LDD
V6345
MULR
V6330
MULR
R3.1400001
DIVR
V6340
OUTD
V6320
38
T4
T5
Real to BCD w/Implied Decimal Pt and Rounding
RTOBCD IB-561
Value (DWORD Real) V6320 - V6321
Number of Decimal Points K1
Result (WORD BCD) V6310
39
mach sw
B2025.3
LD
carier speed
V7010
DIV
K5
OUT
scale carrier sp
V7020

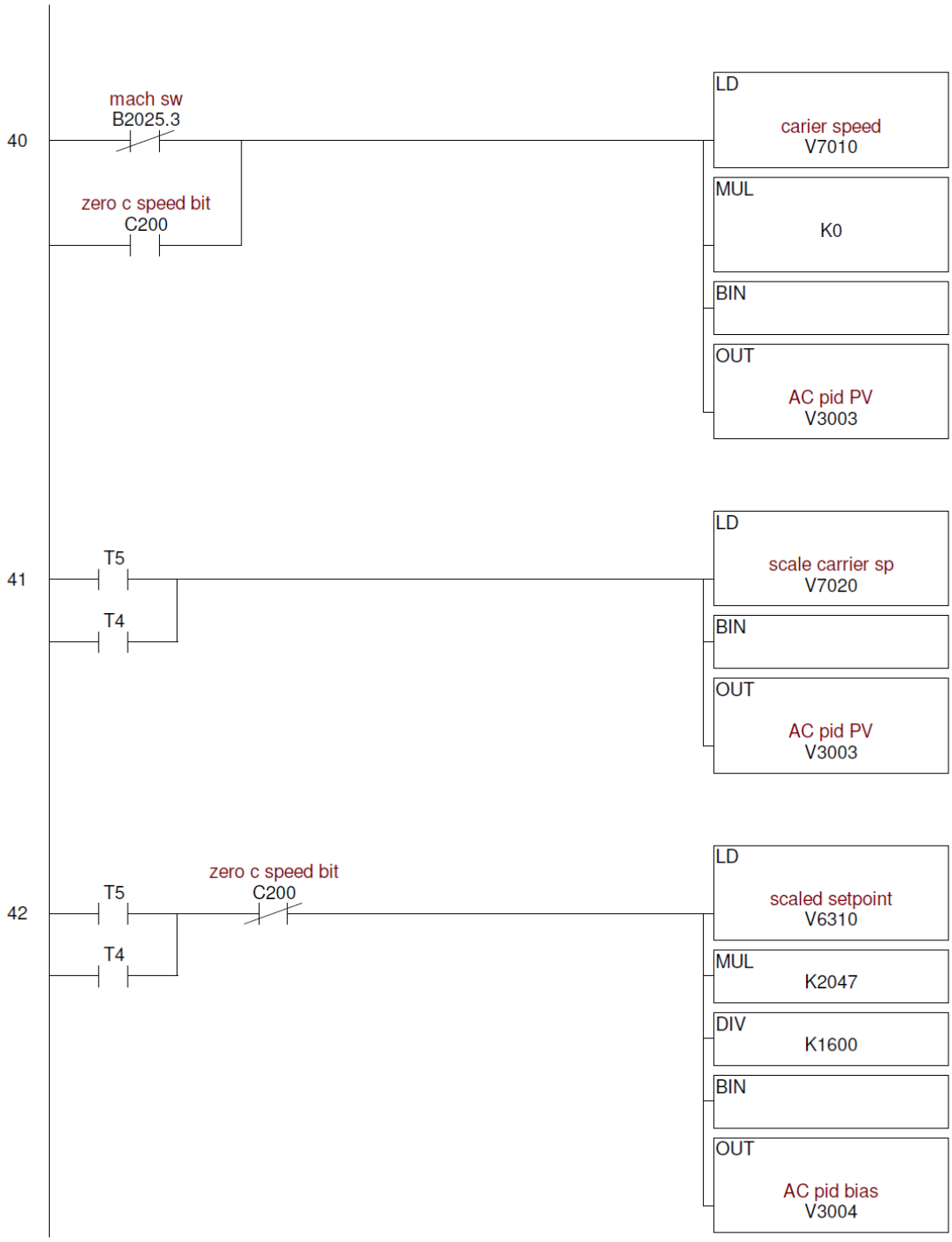
40
mach sw
B2025.3
zero c speed bit
C200
LD
carier speed
V7010
MUL
K0
BIN
OUT
AC pid PV
V3003
41
T5
T4
LD
scale carrier sp
V7020
BIN
OUT
AC pid PV
V3003
42
T5
T4
zero c speed bit
C200
LD
scaled setpoint
V6310
MUL
K2047
DIV
K1600
BIN
OUT
AC pid bias
V3004

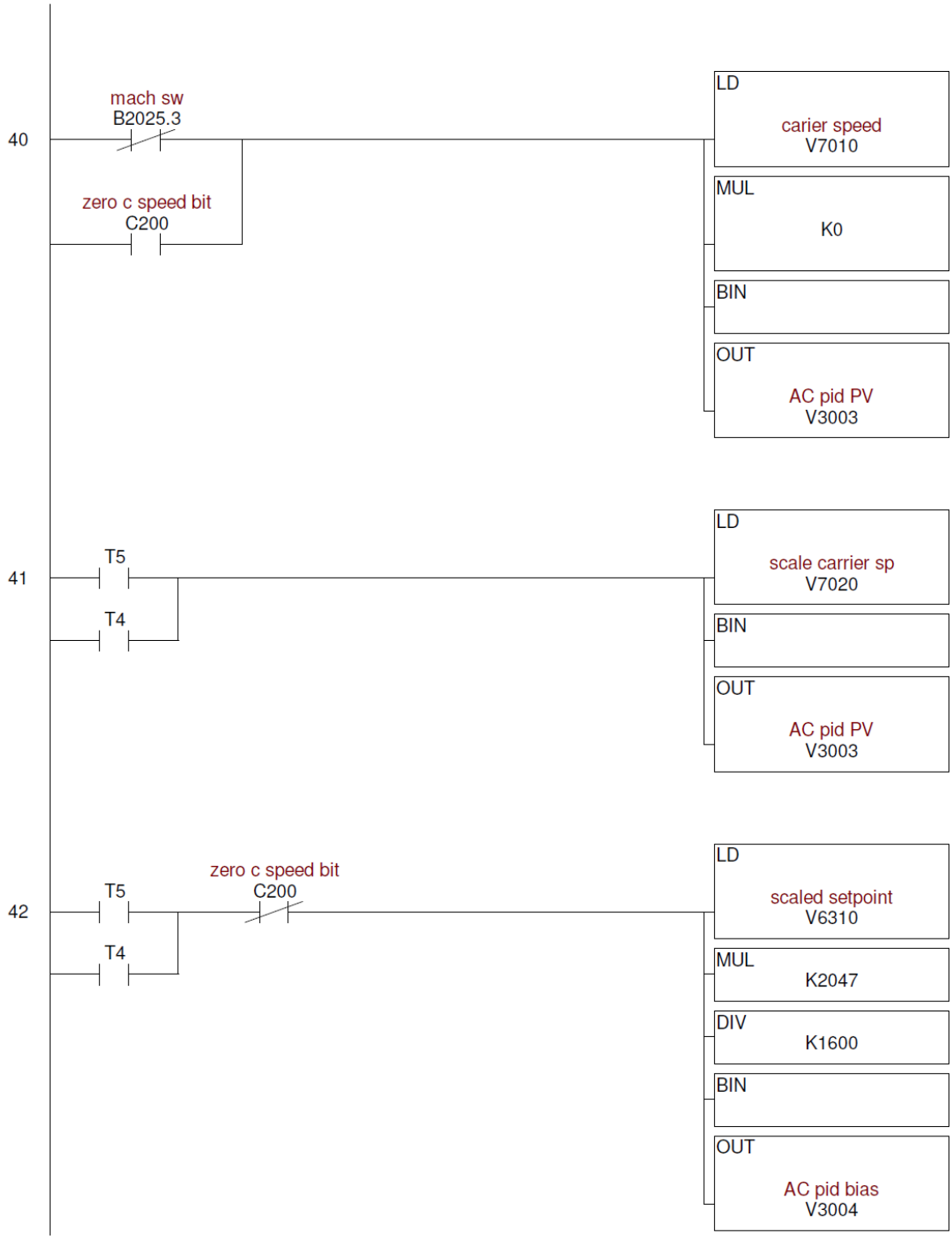
40
mach sw
B2025.3
zero c speed bit
C200
LD
carier speed
V7010
MUL
K0
BIN
OUT
AC pid PV
V3003
41
T5
T4
LD
scale carrier sp
V7020
BIN
OUT
AC pid PV
V3003
42
T5
T4
zero c speed bit
C200
LD
scaled setpoint
V6310
MUL
K2047
DIV
K1600
BIN
OUT
AC pid bias
V3004

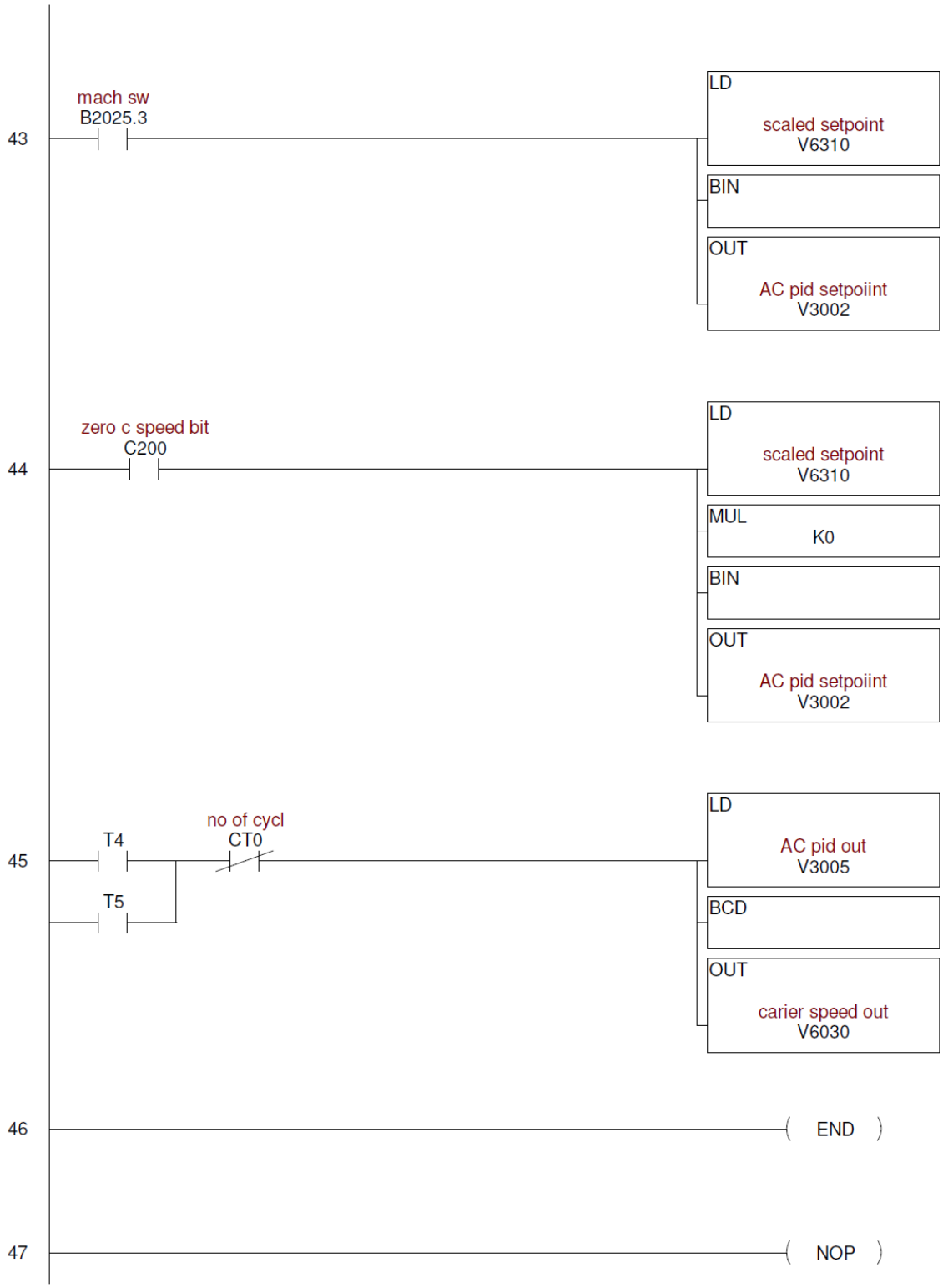
43
mach sw
B2025.3
LD
scaled setpoint
V6310
BIN
OUT
AC pid setpoiint
V3002
44
zero c speed bit
C200
LD
scaled setpoint
V6310
MUL
K0
BIN
OUT
AC pid setpoiint
V3002
45
T4
T5
no of cycl
CT0
LD
AC pid out
V3005
BCD
OUT
carier speed out
V6030
46
END
47
NOP